SPACE DIVISION

CRYSTAL GROWTH IN FUSED SOLVENT SYSTEMS

D. R. Ulrich, M. J. Noone, K. E. Spear,
W. B. White and E. C. Henry

CASE FILE COPY

FINAL REPORT

June 1973

Contract NAS 8-28114
Control Number DCN-1-1-50-13670 (1F)

Prepared for the

National Aeronautics and Space Administration
Marshall Space Flight Center
Huntsville, Alabama 35812

Prepared by

General Electric Company
Space Division
Space Sciences Laboratory
P. O. Box 8555
Philadelphia, Pennsylvania 19101

GENERAL ⊛ ELECTRIC

CRYSTAL GROWTH IN FUSED SOLVENT SYSTEMS

D. R. Ulrich, M. J. Noone, K. E. Spear,
W. B. White and E. C. Henry

FINAL REPORT

June 1973

This report was prepared by the Space Sciences

Laboratory of the General Electric Company

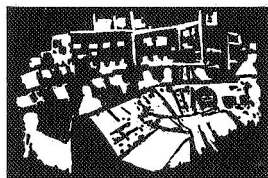under Contract NAS 8-28114, "Study of Crystal

Growth in Fused Solvent Systems," for the

George C. Marshall Space Flight Center of the

National Aeronautics and Space Administration.

TABLE OF CONTENTS

TABLE OF CONTENTS (cont'd)

TABLE OF CONTENTS (cont'd)

LIST OF FIGURES

LIST OF TABLES

FOREWORD

This report was prepared by a team of General Electric Space Sciences Laboratory and Pennsylvania State University Materials Research Laboratory staff personnel. The research was carried out under the supervision of Mr. R. Ruff, Contract Monitor, of the Materials Division, Astronautics Laboratory, George C. Marshall Space Flight Center of the National Aeronautics and Space Administration and Dr. Donald R. Ulrich, Principal Investigator, of the General Electric Company Space Sciences Laboratory, Valley Forge Space Technology Center.

The authors are respectively:

Dr. Donald R. Ulrich, Group Leader, Electronic Materials, General Electric Company, Space Sciences Laboratory

Dr. Michael J. Noone, Ceramist, General Electric Company, Space Sciences Laboratory

Dr. William B. White, Professor of Geochemistry, Materials Research Laboratory, Pennsylvania State University

Dr. Karl E. Spear, Assistant Professor of Solid State Science, Materials Research Laboratory, Pennsylvania State University.

Dr. E. C. Henry, Corporate Consultant, General Electric Company.

SUMMARY

Under Contract NAS 8-28114, "Study of Crystal Growth in Fused Solvent Systems," work was undertaken on the growth of electronic ceramic crystals from solution as a feasibility study for the future growth of crystals in a microgravity environment.

OBJECTIVES

The objectives of the study were:

1. To study the technique of crystal growth from a fused solvent system for application in the environment of space.

2. To identify materials that can benefit by production with this technique in space.

3. To develop an optimum method for growing electronic ceramic single crystals from a fused solvent in space.

PROGRESS AND CONCLUSIONS

Progress was made in several areas which include:

1. The identification of several technologically important crystals whose size and perfection are limitations to their current use and performance;

2. The identification of gravity-dependent growth problems with these crystals;

3. The preliminary definition and design of a space experiment for the growth of triglycine sulfate from an aqueous solution.

4. The development of fused solvent systems for the seeded growth of lithium niobate and lead germanate;

5. The understanding of the growth of lithium niobate from a fused solvent system.

6. The understanding of the growth of lead germanate and bismuth germanate from the melt for comparison with the seeded glass solvent growth of these crystals;

7. The characterization of triglycine sulfate.

Several ceramic crystals have been identified as the basis for many of the emerging and advanced electronic technologies and devices of the 1980's. There are six areas of advanced applications where systems performance is directly dependent on the quality of the ceramic oxide crystals used. These are in computer memories, optical communications, optoelectronics, pyroelectric detection, surface acoustics, and ultrasonics. While some of the crystals can be grown in useable sizes in a terrestrial environment, they generally fall short of their theoretical figures of merit due to the imperfections introduced during growth. Others are limited by size and surface perfection. All of the crystals are grown by melt or solution growth techniques. Experimental evidence indicates that the primary sources of the imperfections are due to convection and sedimentation in the growth solution.

Gravity dependent growth problems have been associated with the ceramic crystal used for each of the aforementioned technologies. Rare earth garnets and rare earth gallium garnets grown from a fluxed melt are the bases for magnetic bubble memories. However, growth bands control bubble size and facets control the uniaxial strain regions. High quality piezoelectric ceramic crystals with electrooptic properties covering a wide range of compositions are required as light modulators in optical communication systems; surface wave acoustic delay lines in radar, navigation, and communication systems; pyroelectric detectors in infrared thermal imaging systems, optical storage media and page composers in holographic memories, and ultrasonic filters in the communications industry.

These include crystals of lithium niobate, bismuth germanate, lead germanate, lithium tantalate, triglycine sulfate and lithium iodate. Lithium niobate can be grown to a large size; however, growth striations and compositional non-uniformity cause electrooptic variations and holographic distortions. Growth striations in lead germanate control the optical rotary switching power. Haze, occlusions, and growth striations distort the electrooptic properties of lithium iodate. Flaws and solvent inclusions reduce the infrared detectivity of triglycine sulfate. Imperfections and ridges distort the sonic propagation along the surfaces of bismuth germanate.

Based on these considerations crystal materials grown by low and high temperature solution growth were selected for further study. These included triglycine sulfate (TGS) grown from aqueous solution, lithium and potassium sodium niobate grown from seeded glass solvents, and lead germanate and bismuth germanate grown from the melt and glass solvents.

Work was conducted on the seeded growth of lithium niobate from glass solvents, notably 40 w/o lithium niobate and 60 w/o lithium disilicate ($Li_2O \cdot 2SiO_2$). The procedures used were to insert a seed crystal into the glass solution and then to either cool the solution or hold at constant temperature for several hours. For the experimental conditions investigated there was little growth on the seed crystals even in melts where coarse dendritic structures were formed in the bulk glass surrounding the seed. However, a seed introduced at 1000°C and held at 1000°C for 64 hours resulted in no growth of the seed and no dendritic growth in the melt. Further work was not pursued under NAS 8-28114; the results indicated that growth experiments should be performed at 990°C but that the rate of growth would be very slow.

Crystals of lead germanate ($Pb_5Ge_3O_{11}$) and bismuth germanate ($Bi_{12}GeO_{20}$) were grown by the slow cooling of a seeded melt. A cooled tip was utilized in some experiments in place of the crystal seed. Crystals with faces up to 2 cm long were grown with the seeded melt technique. These crystals were particularly attractive since the growth temperatures and rates were within the limitations of the Skylab multipurpose furnace.

$Pb_5Ge_3O_{11}$ was grown at temperatures in the vicinity of $750^\circ C$ and at a cooling rate of $1/2^\circ C$ per minute. Nucleation was accomplished with a thermocouple bead rather than seeds. When nucleation was observed the thermocouple was rotated and slowly withdrawn from the melt with the crystal attached. Several small crystals up to 10 mm long and 25 mm^2 cross-section were grown. To investigate the growth of $Pb_5Ge_3O_{11}$ from glass solution, several solvents were developed based on the dissolution of the lead germanate in $PbO \cdot 2B_2O_3$.

Concurrent with the $LiNbO_3$ crystal growth experiments from $Li_2O \cdot 2SiO_2$, work was conducted on the development of additional solvents. Use was made of differential thermal analysis (DTA) to identify the approximate crystal growth temperature. The compositions containing $LiNbO_3$ dissolved in $Li_2O \cdot Al_2O_3 \cdot 8SiO_2$ and SiO_2 would require processing temperatures in the range of 1100°-$1200^\circ C$. Lithium silicate with SiO_2/Li_2O ratios of 1.5 to 2.0 required processing temperatures at $980^\circ C$ as found from the crystal growth experiments. Reducing the SiO_2/Li_2O ratio did not lower the processing temperature.

Experiments were conducted on the flat single crystal platelet growth of lithium niobate using the glass solvent technique. Dual-objective experiments were conducted to optimize the parameters for making thin single crystal films

that could be heated without destroying their film structure. The lowest temperature for the formation of a clear glass film was determined.

Thin glass films were formed on loops of platinum wire. Films were crystallized in both an initially cold furnace or by inserting the loops directly into a hot furnace. Both methods resulted in polycrystalline films of lithium niobate.

An aqueous solution solvent growth experiment for the preparation of triglycine sulfate (TGS) in space was defined. The preliminary design was carried out for growth in the experimental cell designed for space by the slow cooling of a saturated solution and the localized cooling with a thermoelectric actively cooled tip. A flight experiment incorporating both the aqueous solution growth of TGS and the growth of tin crystals was designed.

Work was started toward the development of a characterization plan for TGS. Under subcontract the Materials Research Laboratory at Pennsylvania State University worked on the statistical characterization of triglycine sulphate crystals using Raman Spectroscopy. Work was concentrated on crystals grown by slow evaporation at constant temperature since this technique represents the state-of-the-art in crystal perfection. This work will provide a baseline for the comparison of crystals grown by slow cooling.

Spectral changes at the Curie temperature, hydrogen bonds and structural ordering and the influence of amino acid doping were investigated. The vibrational spectra were in agreement with the other physical property measurements concerning the second order, order-disorder nature of the phase transition in TGS. Spectra taken in the mid-range and high-range frequencies at temperatures of $55^{\circ}C$ are essentially identical to the room temperature spectra. The conclusion can be drawn from the vibrational spectra that the alanine dopant must act on the scale of the individual domains rather than at the molecular level. The increase in sharpness of the lattice modes as the temperature is lowered to $78^{\circ}K$ indicates that a considerable ordering of the hydrogen bond network is taking place.

RECOMMENDATIONS

(1) Growth of Germanate Crystals from Glass Solvents

Growth of crystals from glass solvents offers the possibility of reducing convective effects because of the generally high viscosity of molten glass solutions. Melts of compositions equivalent to the stoichiometric crystals, e.g., $Pb_5Ge_3O_{11}$, are extremely fluid yet crystallize essentially instantaneously on being cooled to the melting point. Crystals of this composition have been grown by the Czochralski technique under the current

program. It is recommended that the development and growth of germanate crystals by appropriate heat treatment of previously prepared glass-based solutions be studied.

Solutions of lead germanate in a lead borate glass were prepared in the earlier studies. Stable amorphous glasses were obtained even with melts containing only 10% of $PbO \cdot 2B_2O_3$ when melts were rapidly cooled. Reheating of these compositions resulted in devitrification and development of the lead germanate crystalline phase. Melts containing the highest amounts of the germanate phase (80 and 90 w/o) resulted in rapid formation of many fine crystals. It was found that a melt of 60 w/o lead germanate devitrified more slowly with fewer nucleation sites.

It is proposed therefore to study further the development of lead germanate from lead borate glass solutions. The objective would be to study the possibility of seeding the solution then to apply appropriate heat treatments to encourage exsolution of the dissolved phase onto the seed. X-ray diffraction data from devitrified crystals has been shown to closely match the data from single crystals grown from the melt.

Some work was initiated on the introduction of Al_2O_3 into the melt to retard the nucleation of numerous crystals and increase the melt viscosity. It is hoped that the improved melt stability will improve the quality of crystal

growth. It has yet to be established that addition of Al_2O_3, or other potential components of a glass melt, can be done without detriment to the crystal properties. A feature of recommended work would therefore be to establish the conditions for stable crystal growth in seeded melts and then to carefully characterize the resulting growth by comparison with melt-grown crystals. Recommended work should be centered on establishing optimum growth conditions for bismuth germanate, as well as lead germanate.

(2) Aqueous Solution Growth of TGS Crystals

Earlier work has established conditions for the growth of TGS crystals from aqueous solutions suitable for study in space experiments. Experimental mock-ups were devised, fabricated, and operated to produce crystals by slowly cooling saturated solutions. Further work is needed to enable precise definition of experimental conditions appropriate to the Space Vehicle environment. Critical areas for further study would include determination of the temperature profile for optimum growth conditions and the thermal control requirements for the system.

System definition should include development of seeding techniques and cooled nucleation points with emphasis on the extraction of the grown crystal from the cell after the experiment. Solution concentrations and growth temperatures have been established in terrestrial experiments but the time frame for near zero-g conditions remains to be defined. In the absence of convection,

diffusion processes dominate the growth process in the space environment; therefore, experimental time frames must be related to diffusion coefficients. Further experimental data is required with TGS solutions and with low temperature modeling systems to establish material transfer rates and potential material yields for experiments to be performed in near zero-g.

Data gathered from TGS experiments is of course also relevant to the glass solution growth processes with appropriate extrapolation to account for differences in diffusion coefficients, etc. The relative importance of such factors as seeding techniques or cooled nucleation sites are much more readily studied in detail in the low-temperature aqueous system.

Interesting characterization techniques have been shown to be applicable to the observation of growth from aqueous solutions under terrestrial conditions. For example, convective disturbances in growth solutions may be observed with the aid of ruled grids placed behind the growth cell. Density changes in the solution cause distortion of the grid pattern which can be recorded photographically during growth. Efforts should be made to relate deliberately introduced disturbances in solutions to the observed crystal growth and to crystal properties during future work in the TGS system.

(3) Growth of Crystals Above 1000°C

An experimental study is recommended for the evaluation of growth of refractory oxide crystals requiring solution temperatures higher than 1000°C. Future space processing facilities will not be limited to low temperatures and

there are many crystals of high technological value which have high melting points. Solution growth of course enables refractory crystals to be produced at temperatures below their melting point but this may nevertheless be over $1000^{\circ}C$ for optimum growth of some oxidic crystals.

Crystals that may be produced from high temperature solutions include several rare-earth garnet compositions and potassium tantalate/niobate structures. Extension of growth conditions into these higher temperature regimens should be a logical extension of the proposed studies with germanate materials and also relate to the earlier data obtained from solutions of lithium niobate and potassium sodium niobate which also required processing at temperatures above $1000^{\circ}C$.

(4) Characterization of Solution Grown Crystals

The basic structural, dielectric, and electro-optic properties of the solution grown germanate should be characterized to isolate and describe the influence of diffusion and convection on these properties. Crystals with varying concentrations (major component and trace impurities) should be characterized. The continued characterization of TGS is recommended. Work should shift to crystals grown by slow cooling. Characterization will center on the study of dielectric loss. The pseudo-conductivity will be tied to the controlling defects and the quality of the crystal. The next step would be to correlate measurable

imperfections with the dielectric loss. It is important to know which of the

identifiable imperfections are responsible for the conductivity of TGS. A series

of crystals should be grown under different conditions that would produce crystals

with different concentrations of dislocations and volume defects. The dielectric

loss would be measured and compared with the concentration of different kinds

of imperfection.

I. INTRODUCTION

The growth of electronic crystals has been identified as one of the principal fields which may benefit from the microgravity of space. While some of the crystals can be grown in usable sizes and qualities in a terrestrial environment, they generally fall far short of their theoretical figures of merit due to the imperfections introduced during the growth process. Experimental evidence indicates that the primary sources of the imperfections are due to the convection and sedimentation present in the growth solutions.

The preparation of crystals in space has intrigued man for over a decade at least since float zone refining and crystal growth in space was first suggested by Pfann* in 1958. Other crystal growing processes which have since been considered are vapor growth and Czochralski or melt growth. Emphasis has been placed on the growth of metallic and semiconductor single crystals utilizing these techniques.

In this study the growth of electronic ceramic single crystals from solution was investigated. The work included growth from fused or glass solvents and aqueous solutions. The objectives of the study were:

1. To study the technique of crystal growth from a fused solvent system for application in the environment of space.

---

*Pfann, U. G., Zone Melting, 1st Edition, John Wiley & Sons, 1959, p. 93.

2. To identify materials that can benefit by production with this technique in space.

3. To develop an optimum method for growing electronic ceramic single crystals from a fused solvent in space.

The literature pertinent to the growth of crystals of electronic ceramic materials has been surveyed and reviewed. Crystals and compositions have been identified which have technologically important and useful properties but which cannot be grown as large and perfect single crystals at the present time. An analytical study has been made of the methods used to grow these crystals. Obstacles to adequate crystal growth which most likely are gravity dependent and which may benefit from zero-gravity processing were identified.

Utilizing the information generated, crystals were chosen for further study based on the importance of the crystal material and the anticipated probability of a successful space experiment. The experimental work centered on the definition of the variables needed to design a zero-gravity single crystal growth experiment from fused solvents and aqueous solutions. Based on this information the preliminary design and definition for a space experiment was carried out.

Since the characterization of crystals grown in space will be very important, work was initiated to analyze the different characterization techniques and tools which may be applicable to the selected materials. Work was also initiated on the development of a future characterization plan. The question to be answered: How can the quality of space-grown and terrestrially grown crystals be compared?

II. CRYSTAL IDENTIFICATION AND SELECTION

A. Economic Demands and Areas of Applications

An econometric study[*] on the growth of electronic single crystals in space concluded that the newer and sophisticated ceramic oxide and compound semiconductor single crystals, which now comprise about 20% of the electronic single crystal market, are the basis for many of the emerging and advanced electronic technologies of the 1980's. Strong economic and technical justification was shown for pursuing the preparation of these electronic crystals with maximum perfection, purity and size to achieve high performance components and devices. It is believed that the near absence of gravitational effects for prolonged times in space will very markedly help to achieve the desired improvements in perfection.

Six areas of application were identified which will provide a substantial demand for high quality crystals. These are:

1. Computer Memories

2. Optoelectronics

3. Optical Communications

4. Pyroelectric Detectors

5. Surface Wave Acoustics

6. Ultrasonics

---

[*] D. R. Ulrich, A. M. Chung, C. S. Yan and L. R. McCreight, "Economic Analysis of Crystal Growth in Space", Final Report, Contract NAS 8-27942, July 1972.

Magnetic bubble computer memories are expected to provide the single greatest demand for high quality single crystals. The second and third sources of demand will be for electrooptic and optoelectronic crystals. Of these, ceramic crystals will meet the needs and requirements of the first two sources of demand and compound semiconductors the third. In view of this the survey will center on the identification of the unique compositions of these crystals and their performance restrictions due to growth-limited size and perfection.

B. Defects in Electronic Ceramic Crystals

The major defects which make solution grown crystals unsuitable for electronic devices are striations, trapped flux and flux inclusions, constitutional supercooling, strain, hopper growth and layer growth. Strain results in optical birefringence. Striations are parallel bands that show up as local index of refraction changes, color changes, or birefringence changes in the crystal. They usually can only be eliminated by elimination of the convection currents during crystal growth which arise from temperature variations. Other defects, such as dislocations and point defects, are usually present. Dislocations can be overlooked, but point defects, if caused by electrically active or optically absorbing impurities, can restrict the usefulness of the crystal. The aforementioned defects with the exception of vacancy point defects are related to the growth of the crystals.

The investigations of ceramic crystal defects and their relation to growth conditions have centered on crystals grown from the melt by the vertical pulling technique, the major defects being striations, strains, constitutional super-cooling and faceting. Perfection studies in solution grown electronic ceramic crystals have not been extensive. However, the general principles can be applied, at least in part, to all methods of crystal growth including solution growth from aqueous and fluxed solvents. In addition, the process by which crystals grow from the flux appears to be similar to that for growth from aqueous solutions at lower temperatures.

C. Magnetic Bubble Memory Crystals[*]

1. Ferrites and Magneto-plumbites

An oxide single crystal material which is divided into domains, or regions which are magnetized in different directions, is the key element of a magnetic bubble device. These "domains" can be formed into small "bubbles" which store bits of information. Physically, the bubbles are cylindrical domains whose polarization is opposite to that of the crystal film in which they are embedded. They can be moved from point to point at high velocity.

---

[*]   At the time of writing, the fabrication of bubble memories from amorphous metallic films instead of crystals was announced. The vertical magnetic field which is needed to form bubbles was produced in sputtered films. Bubbles as small as one-tenth of a micron can be made, but controlling them is another problem. Small bubbles will require new techniques such as the electron-beam approach. It is premature to predict the impact on the single crystal magnetic bubble memory.

5

Several classes of crystals exhibit bubble behavior but only a few within these classes meet the requirements for reasonable densities and speed. The single crystal must: (1) sustain small bubble-like regions so that information can be stored more efficiently than before; and (2) permit the bubble to run at a high velocity so that tremendous amounts of information can be processed in a relatively short time.

Crystals usually of rare-earth ferrites were prepared initially by flux-growth methods. These are a special class of ferrities with the chemical formula $RFeO_3$, where R represents yttrium or one or more rare-earth elements. They are grown as single crystals by mixing the raw ingredients with a suitable flux, melting the mixture in a crucible, and allowing the melt to cool over a period of several weeks. Another method is to pull single-crystal rods directly from the melt and cut wafers from the rods.

In general, the bubble size of the orthferrites is too large. This is unsuitable for the very high density required for mass storage. Samarium terbium orthoferrite comes close to satisfying the need for a bubble mobility which will allow a data-processing rate of a million bits per second, however, it fails to attain the packing density of a million bubbles per square inch because the bubbles are three times too large, i.e. 25 microns in diameter. Another family, the magneto-plumbites such as $BaFe_{12}O_{19}$ can be grown but the resultant bubbles are too small for practical devices. The smallest bubbles - one micron in diameter - have been observed in hexagonal lead ferrite ($PbFe_{12}O_{19}$), but they move too slowly.

6

2. Rare Earth Iron Garnets

Single crystal rare earth garnets such as europium terbium iron garnet with the proper composition can yield bubbles of 6 micron diameter. The preferred properties of bubble materials as exemplified by the garnets are shown in Figure 1. Flux techniques for growth are well established. However, the most economical device configuration will probably involve a structure wherein a liquid-phase epitaxial single crystal film has been produced. Reproducible films reportedly have been grown by liquid phase epitaxy (LPE) on substrates which have been dipped while undergoing axial rotation and which are positioned in a horizontal plane. Chemical vapor deposition (CVD) of magnetic garnet thin films is also employed. Special compositions include the deposition of single crystals of erbium europium gallium iron garnet, terbium erbium iron garnet, gadolinium terbium iron garnet and yttria iron garnet in solution grown substrate crystals of $(RE)Ga_5O_{12}$ where Ga represents gallium and RE, rare earth oxides of dsyprosium, gadolinium, samarium up through neodynium in the Periodic Chart.

The garnets have zero magnetrostriction but exhibit the largest and most uniform uniaxial regions which are needed to form cylindrical magnetic domains in the absence of a bias field. The easy direction of magnetization should be perpendicular to the plate to support bubbles with 5 to 25 micron diameter. The uniaxial anisotropy is thought to be induced by the ordering
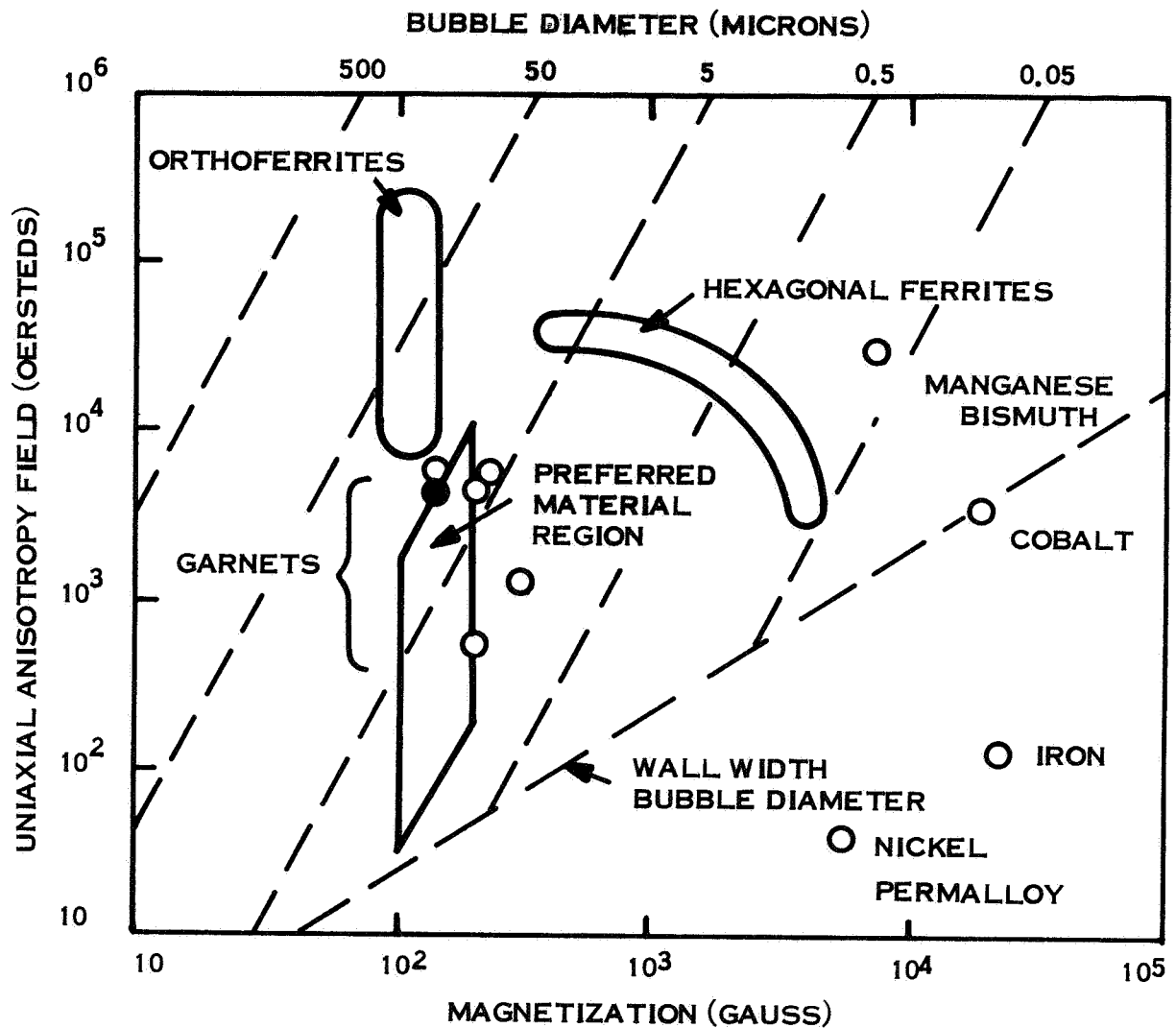
Figure 1. Properties of Magnetic Bubble Crystals. Uniaxial Anisotropy vs. Magnetization and Bubble Diameter. (Bobeck and Scovil, 1971).

resulting from growth and not from uniform stress in the film. The regions of uniaxial anisotropy are growth bands or striations. They are compositional variations and result from temperature fluctuations during the growth process. These are thought to be process-independent and gravity related. The fluctuations are caused by thermal convection currents which are driven by the force of gravity. If growth striations are responsible for uniaxial anisotropy in rare earth iron garnets, microgravity growth may be of interest to develop crystal growth techniques which will allow this effect to be controlled.

3. Rare Earth Garnet Substrate Crystals

The control of rare earth gallium garnet substrate defects is of considerable importance since several types of defects are readily replicated. The replicated defects generally have adverse effects on bubble properties. Gadolinium gallium garnet ($Gd_3Ga_5O_{12}$) single crystals are widely employed as substrates for both LPE (Liquid Phase Epitaxy) and CVD (Chemical Vapor Deposition) deposition of bubble films. The substrates are cut, wafered, and polished from crystal boules grown from the melt by the Czochralski technique. Metallic particles, strained faceted regions, gadolinium precipitates, growth bands, cores, and dislocations have been identified in this crystal system.

Growth bands, which are attributed to small compositional fluctuations in the substrate, and cores, associated with the development of facets on the

9

substrate crystal solid/liquid interface during growth from the melt, are two

types of defects which are replicated. While replications of bands and cores

are observed in various compositions of gallium substituted rare earth and

yttrium iron garnet epitaxial films prepared on rare earth gallium garnet

substrates, the fidelity of replication in films prepared by liquid phase epitaxy

was lower than in chemically vapor deposited films. Unsubstituted yttrium iron

garnet films deposited on garnet substrates by CVD do not reproduce the growth

bands and cores. Instead defects which are associated with high local strains

are reproduced.

D. Electrooptic Crystals

1. Scope

The second largest demand appears to be for high quality electrooptic

crystals such as lithium niobate ($LiNbO_3$), lithium tantalate ($LiTaO_3$), barium

sodium niobate ($Ba_2NaNb_5O_{15}$), bismuth germanate ($Bi_{12}GeO_{20}$), lead germanate

($Pb_5Ge_3O_{11}$), lead germanium silicate ($Pb_5Ge_2O_{11}$), bismuth titanate ($Bi_4Ti_3O_{12}$),

gadolinium molybdate $Gd_2(MoO_4)_3$, lithium iodate ($LiIO_3$) and triglycine sulfate.

There are a wide range of compositions and solid solutions here since electrooptic

phenomena are used across the total range of the cited applications. The crystals

are used as optical storage media and page composers in holographic memories,

light modulators in optical communications systems, pyroelectric detectors in

infrared thermal imaging systems, surface wave acoustic delay lines in radar,

navigation and communications systems and ultrasonic filters in the communications

industry.

2. Lithium Niobate

Lithium niobate ($LiNbO_3$) is one of the most significant crystals for electrooptic applications. It is used as the optical storage media in holographic memory systems, as modulators, harmonic generators and parametric devices in laser communication systems, as well as for surface wave acoustic devices.

Lithium niobate is grown from the melt using the Czochralski technique. Although crystal boules as large as one inch in diameter and six inches in length can be prepared in this manner, dynamic growth at elevated temperatures introduces chemical imperfections and compositional inhomogeneities. Compositional nonuniformity along the length of the crystal, nonuniform growth regions, and compositional differences from crystal to crystal arise from variations in the melt composition, rate of growth, crystallographic axis of pull, etc.

Compositional nonuniformity along the length of the crystal can cause variations in index of refraction, birefringence and optical single harmonic generation. The efficiency of phase matching interaction is reduced and the second harmonic peak power is depressed, thus limiting nonlinear optical activity.

Distortion of holographic patterns in $LiNbO_3$ will arise from long range refractive index variations. In addition surface polishing

introduces scattering centers causing short-range refractive index variations. Since optically induced electrical conductivity is the basis of holographic storage in these materials, a high defect density will probably interfere with the photo-induced charge transfer requirement of holographic storage.

For surface wave acoustic applications, surface perfection is as essential as internal crystal perfection. Growth ridges on the surface of $LiNbO_3$ interfere with the propagation of the high-frequency surface waves. Because of mechanical damage and imperfections introduced during even careful lapping and grinding, polishing surfaces do not transmit a signal as undistorted as that expected from an equally, large flat natural surface.

For high frequency operation, size becomes most important concurrent with surface smoothness. Long crystals of $LiNbO_3$ which are six to ten inches in length are desired for dispersive delay lines. Currently a long delay cannot be obtained in one crystal. In addition, at Gigahertz frequencies the linewidths of surface electrodes deposited on the crystals are in the range of the crystal surface roughness dimensions.

3. Lead Germanate

Lead Germanate ($Pb_5Ge_3O_{11}$) is a new ferroelectric crystal having large electrooptic and nonlinear optic constants as desirable switching properties for electrooptic device applications. Of particular importance has been the discovery of switchable optical rotary power. Crystals which are 4 x 4 x 0.4 mm in size are grown by the Czochralski method. However, switching time is strongly sample dependent due to the crystal inhomogeneities.

4. Bismuth Germanate

Bismuth germanate ($Bi_{12}GeO_{20}$) crystals are grown by the Czochralski technique. Because of the low elastic wave velocity, low losses and moderately strong piezoelectric coupling properties of $Bi_{12}GeO_{20}$, it is a foremost candidate for surface wave devices and for storage information at VHF and microwave frequencies. Bismuth germanate has a slower acoustic velocity, i.e., 1.6×10^5 cm/sec as compared to 3.5×10^5 cm/sec for $LiNbO_3$, and is, therefore, a first choice for devices requiring long delay times. The growth of large crystals of $Bi_{12}GeO_{20}$ with a minimum of surface ridges and internal stresses is required to prevent the surface waves from becoming dispersive. In severe cases this could cause a prohibitive attenuation loss of the propagating wave.

5. Barium Sodium Niobate

Barium sodium niobate ($Ba_2NaNb_5O_{15}$), along with potassium lithium niobate ($K_3Li_2Nb_5O_{15}$), have tungsten-bronze structures with large nonlinear coefficients and are resistant to optical damage. The large birefringence of lithium niobate and barium sodium niobate make these crystals applicable for harmonic generators, barium sodium niobate is about two times as effective. Crystal boules of barium sodium niobate which are one inch in length and 5 millimeters in diameter can be grown. However, yields are low, the density of artifacts is high. There are many kinds of defects, cracking and striations

13

which degrade its efficiency as a second harmonic generator or parametric oscillator. In addition compositional nonuniformity causes inhomogeneities in the index of refraction and reduction in conversion efficiency.

6. Lithium Tantalate

Piezoelectric crystals such as lithium tantalate ($LiTaO_3$) and quartz are the fundamental materials for electronic delay lines and filters in the communications industry. While monolithic quartz crystals can do some jobs extremely well, there is a severe limitation on the available bandwidth which is associated with the weak electromechanical coupling in quartz crystals. Lithium tantalate has all the desirable features of quartz. In addition it has a stronger electromechanical coupling and a wider bandwidth. The bandwidth is close to that of piezoelectric ceramics; however, $LiTaO_3$ does not require the costly shaping, assembly and testing of ceramic devices. For frequency applications above 50 MHz surface-wave filters become available which are fabricated from $LiTaO_3$ flat plates. Lithium tantalate crystals will also be used as light modulators for future optical transmission systems and as a detector of light frequencies in the IR region. Lithium tantalate is also capable of recording volume holograms.

For these applications, clear, large aspect ratio crystals of $LiTaO_3$ are required. Lithium tantalate is grown by the Czochralski technique.

7. Bismuth Titanate

Bismuth titanate ($Bi_4Ti_3O_{12}$) is a ferroelectric whose optical behavior is completely different from other ferroelectric crystals such as barium titanate, triglycine sulphate and potassium dihydrogen phosphate. It provides nearly maximum transmission in the intensity of transmitted light and a most attractive material for a high-speed page composer for holographic memories. The lameller crystals of $Bi_4Ti_3O_{12}$ are grown by the flux method. At most they are about 1 mm thick and possess a face area which is too small for practical display purposes. Efforts to grow them by other techniques have proven unsuccessful. To obtain a crystal area suitable for memory storage and display applications, it would be necessary to grow large crystals and to cut the plate-like crystals parallel to specific planes and stack narrow slices side by side.

8. Gadolinium Molybdate

Gadolinium molybdate, $Gd_2(MoO_4)_3$, is a ferroelectric-ferroelastic crystal which shows promise as a page composer for holographic memories. It is grown by the Czochralski technique and must be defect free so that it can be switched an indefinitely large number of times without fatigue. However, temperature fluctuations in the melt during crystal growth cause the boule diameter to change discontinuously. Thus, severe strains are introduced which influence the threshold field. In addition stoichiometry in the melt must be closely controlled and a flat solid-liquid interface maintained.

9. Triglycine Sulfate

Triglycine sulfate $(NH_2CH_2COOO H)_3 H_2 SO_4$, is the basic crystal for a new family of infrared detectors which provide significant advantages over the conventional infrared thermal detectors. Triglycine sulfate and triglycine selenide derivatives are responsive to a wide range of frequencies from optical to microwave. They have high detectivities and fast response times and are replacing conventional devices as the universal room temperature detector. In general TGS and its derivatives are generally superior to other crystals such as barium strontium niobate, lithium sulphate, sodium nitrate, lithium niobate and lead titanate.

Very thin lamellar sheets of highly perfect TGS are required. Crystals grown by present aqueous solution techniques result in crystals with flaws and solvent inclusions. Polishing and lapping of the crystals to a few tens of microns thickness result in surface imperfections. Cutting of the crystal to obtain orientation of the surface perpendicular to the polar axis introduces strain and defects. Because of growth-induced size-perfection restrictions, infrared detectors currently made with TGS crystals fail to achieve their theoretically expected performance.

10. Other Aqueous Solution Crystals

Crystals such as potassium dihydrogen phosphate (KDP), ammonium dihydrogen phosphate (ADP), and deuterated potassium dihydrogen phosphate (KD*P) are used for electrooptic applications in spite of their low electrooptic

properties and deliquescence. This is mainly because of the ease of growing large, good quality optical crystals from aqueous solutions. There are other electrooptic crystals which have much better electrooptic figures of merit and physical properties but which cannot be grown in large sizes with good quality. Lithium iodate is a good example.

Lithium iodate ($LiIO_3$), is in demand because of its high second-harmonic efficiency for $YAGNd^{3+}$ (yttrium aluminum garnet: Nd^{3+}) and ruby lasers. It is grown in aqueous solution at ambient temperatures up to 20 by 50 millimeters. Its figure of merit is four times that of potassium dihydrogen phosphate. In comparison to lithium niobate and lithium tantalate it has better optical homogeneity and higher resistance to damage from visible light. However, with increasing size, haze, occlusions and growth striations occur. This is thought to be caused by thermal convection. The striae from growth discontinuities cause a severe distortion of the laser beam which is similar to that caused by striations in barium sodium niobate. Potassium iodate, sodium iodate, and alpha-iodic acid are other aqueous solution grown crystals whose use is in demand, but restricted, because of growth striations and hopper growth.

11. Other Crystals

Several other crystals were identified as being technologically important. In some cases the current quality of the crystals as grown is considered to be satisfactory. For example, single crystals of lead molybdate

17

($PbMoO_4$) are important components in solid state acousto-optic light deflectors. The acousto-optic interaction is very large and has great advantage in optical deflection systems for holographic memories. Boules of 15 mm in length can be grown. The quality of these is acceptable for use.

In other areas of application, there are requirements for size, shape and/or perfection improvements. The crystalline lasers are presenting new material problems. Yttrium aluminum garnet (YAG or $Y_3Al_5O_{12}$) is currently the most important host crystal utilizing neodynium (Nd^{3+}) fluorescence for laser action. For optical sources they are pumped by light emitting diodes (LED's). YAG is well suited for continuous power applications. Using the conventional rod design, however, high averaged pulsed power cannot be produced. The crystals are limited in size and certain defects are introduced during high temperature growth. The YAG laser with its high power capability and fast chopping rates also demands a faster nonlinear optical crystal capable of withstanding power densities of 150 megawatts.

Barium strontium niobate is superior to TGS as a pyroelectric detector in certain respects such as fast response at room temperature. However, the high temperature growth process introduces chemical non-uniformity in the boule and a high density of imperfections. Other crystals are finding less well-publicized use in surface wave acoustic delay line memories. Yttrium iron garnet, spinel ($MgAl_2O_4$), $Y_3Ga_5O_{12}$ and $Y_3Al_5O_{12}$ are candidates for producing low

18

attenuation at high frequencies. Ferrimagnetic gadolinium iron garnet films can be used for high-density magneto-optical beam addressable memories. However, at this time the arrays are limited in density by the laser beam wave length and the lack of deflectors to address large field sizes.

E. SUMMARY

Several crystals have been identified which are technologically important but whose theoretical figures of performance cannot be attained because of size or perfection limitations. These are classified in Table 1 according to application. The predominant growth-related problems of the most important crystals whichare grown from aqueous and fluxed solutions or from melts are listed in Table 2.

F. PROSPECTS FOR CRYSTAL GROWTH IN SPACE

While the crystals discussed in Sections D and E can be grown in useable sizes and shapes, they generally fall short of their theoretical figures of merit during performance because of growth-induced imperfections. Experimental evidence has shown that the imperfections can be attributed to the convection and sedimentation in the growth solutions. Growth of crystals from solution in the microgravity of space offers an alternative approach for minimizing the defect levels in the crystals.

Table 3 projects what improvements one might expect in the crystals discussed in Sections C and D.

G. CRYSTAL SELECTION FOR FURTHER STUDY

Based on the results of the literature survey, lithium niobate, triglycine sulphate, lead germanate, and bismuth germanate were selected for further study. These represent candidates for low and high temperature solution growth. Triglycine sulphate was selected for growth from aqueous solution using slow cooling or constant temperature evaporation. The high temperature growth crystals were selected for investigating their growth from seeded glass solvents. The rational for this selection is discussed in Section VII. The growth of lead germanate and bismuth germanate from their melts was also studied. The crystals and methods selected are summarized in Table 4.

Table 1

CRYSTAL IDENTIFICATION

COMPUTER MEMORY CRYSTALS

   MAGNETIC BUBBLES

      RARE EARTH IRON GARNETS

      RARE EARTH GALLIUM IRON GARNETS

   HOLOGRAPHIC

      LITHIUM NIOBATE, BISMUTH TITANATE

      GADOLINIUM MOLYBDATE

OPTICAL COMMUNICATIONS SYSTEMS

      LEAD GERMANATE, LITHIUM IODATE

PYROELECTRIC SENSORS

      TRIGLYCINE SULFATE

SURFACE WAVE ACOUSTICS

      BISMUTH GERMANATE

ULTRASONIC DEVICES

      LITHIUM TANTALATE

21

Table 2

GRAVITY DEPENDENT GROWTH PROBLEMS

RARE EARTH IRON GARNETS

    GROWTH BANDS CONTROL BUBBLE SIZE
    FACETS CONTROL UNIAXIAL REGIONS

LITHIUM NIOBATE

    LARGE SIZE: GROWTH STRIATIONS AND COMPOSITIONAL NON-
    UNIFORMITY CAUSE E-O VARIATIONS AND HOLOGRAPHIC
    DISTORTION

LEAD GERMANATE

    GROWTH STRIATIONS CONTROL OPTICAL ROTARY SWITCHING
    POWER

LITHIUM IODATE

    HAZE, OCCLUSIONS, AND GROWTH STRIATIONS DISTORT E-O
    PROPERTIES

TRIGLYCINE SULFATE

    FLAWS AND SOLVENT INCLUSIONS REDUCE IR DETECTIVITY

BISMUTH GERMANATE

    SURFACE FLAWS DISTORT SONIC PROPAGATION

Table 3

PROJECTED SPACE PROCESSING IMPROVEMENTS TO CERAMIC CRYSTAL GROWTH

Crystals	Applications	Growth Method	Terrestrial Growth Problems	Projected Space Growth Improvements
Rare earth iron garnets or rare earth gallium iron garnet films	Magnetic bubble memories	LPE from fluxed melt	Growth bands gravity-related. Control bubble diameter. Natural facets control uniaxial regions.	Gravity-related turbulence and growth striations controlled
Rare earth gallium garnets	Magnetic bubble film substrates	Melt	Facets and hillocks	Flat solid – liquid interface to control facets
Lithium niobate	Optical storage media for holographic memories	Melt	Compositional non-uniformity causes variations in E-O properties. Surface ridges. Surface polishing-defects and roughness	Decreased turbulence, increased optical quality
Triglycine sulfate	Pyroelectric sensors	Aqueous solution	Flaws, solvent inclusions. Polishing and orientation cutting-surface imperfections and stresses	Large crystals. Flaw and inclusion elimination

23

TABLE 4
(cont'd)

Material	Application	Growth method	Problems	Objectives
Lithium iodate	Laser communi- cations systems, electrooptic	Aqueous solution	Size, haze growth striations	Optical quality. Increased size.
Lead germanate	Electrooptic	Melt	Small size. Switching time dependent on inhomogeneity	Large size. Improved homogeneity
Sodium iodate	Electrooptic	Aqueous solution	Hopper growth	Decreased turbulence. Decreased hopper density.
Bismuth titanate	Page composer for holographic memory	Flux	Face area too small Composition inhomogeneity	Growth of large platelet crystals.
Lithium tantalate	Ultrasonic filters	Melt	Thin sheets. Flat surfaces. Surface perfection.	Growth of large platelet crystals.
Bismuth germanate	Surface wave acoustic devices	Melt	Surface imperfections	High quality crystals.
Gadolinium molybdate	Page composer holographic memory	Melt	Temperature fluctuations causes boules to change discontinuously. Stoichiometry problems	Decrease turbulent convection advance of flat liquid–solid interface.

Table 4

CRYSTAL MATERIALS SELECTED FOR FURTHER

STUDY

LOW TEMPERATURE GROWTH

    TRIGLYCINE SULFATE (TGS)

        AQUEOUS SOLUTION TECHNIQUE

HIGH TEMPERATURE GROWTH

    LEAD GERMANATE

        MELT, GLASS SOLVENT

    BISMUTH GERMANATE

        MELT, GLASS SOLVENT

    LITHIUM NIOBATE

        GLASS SOLVENT

H. BIBLIOGRAPHY

The volume of literature published on the subject of crystal growth is extensive. While exercising some discrimination, a list of significant references has been compiled which have some pertinence to: (1) the identification of technologically important, but performance-limited, ceramic electronic crystals; and (2) the identification of potential gravity-dependent growth problems with ceramic electronic crystals. In essence the literature survey has been based on the following publications. Therefore, the references are organized under the topical headings of process interactions and defects, solution growth, magnetic bubble memory crystals and electrooptic crystals.

1. Process Interactions and Defects

Bardsley, W. and Cockayne, B. in Crystal Growth (H. S. Peiser, ed.), Pergamon, Oxford, 1967, p. 109.

Basterfield, J., Prescott, H. and Cockayne, B., J. Mater. Sci., 3 33 (1968).

Brice, J.C., Opt. Laser Tech. 2 (4) 206-208 (1970).

Brice, J.C., J. Cryst. Growth, 6, 205 (1970).

Brice, J.C., and Whiffin, P.A.C., Brit. J. Appl. Phys., 18 581 (1967).

Brice, J.C., J. Cryst. Growth, 2 395 (1968).

Charvat, F., Smith, J.C. and Nestor, D.H., in Crystal Growth (H. S. Pieser, Ed.), Pergamon, Oxford, 1967, p. 45.

Carruthers, J.R., J. Electrochem. Soc., 114 1077 (1967).

Carruthers, J.R., Can. Met. Quart. 5 55 (1966).

Carruthers, J.R. and Benson, K.E., Appl. Phys. Letters 3 100 (1963).

Chandrasekhar, S., Hydrodynamic and Hydromagnetic Stability, Clarendon Press, Oxford, 1961.

Cockayne, B. and Gates, H.P., J. Mater. Sci. 2 118 (1967).

Cockayne, B., Robertson, D.S., and Bardsley, W., Brit. J. Appl. Phys. 15 1165 (1964).

Cockayne, B., J. Mat. Sci. 3 224 (1968).

Cockayne, B., J. Cryst. Growth 3, 4 60-70 (1970).

Cockayne, B., Chesswas, M. and Gasson, J. Mat. Sci. 3 224 (1968).

Cockayne, B., Chesswas, M., Plant, J.G., and Vere, A.W., J. Mater. Sci. 4 565 (1969).

Cole, G.S. and Winegard, Can. Met. Quart. 6 233 (1967).

Cole, G.S. and Winegard, J. Inst. Metals 93 (153 (1964-1965).

Chedzey, H.A. and Hurle, D.T.J., Nature 210 233 (1966).

Curtis, B.J. and Dismukes, J.P., J. Cryst. Growth, 19 128 (1972).

Giess. E.A., Cronemeyer, D.C., Rosier, L.L. and Kuptsis, Mat. Res. Bull. 5 495 (1970).

Hurle, D.T.J., Solid State Electronics 3 142 (1961).

Hurle, D.T.J., Solid State Electronics 3 37 (1961).

Hurle, D.T.J., Jakeman, E. and Pike, E.R., J. Crystal Growth, 3, 4 633 (1968).

Hurle, D.T.J. and Jakeman, E., J. Cryst. Growth, 5 227 (1969).

Hurle, D.T.J., in Crystal Growth (H. S. Peiser, Ed.), Pergamon, Oxford, 1967, p. 659.

Hurle, D.T.J., J. Cryst. Growth 13, 14 39-43 (1972).

Kim, K.M., Witt, A.F. and Gatos, H.C., J. Electrochem. Soc. 119, 1218 (1972).

Morizane, K., Witt, A.F. and Gatos, H.C., J. Electrochem. Soc. 113 51 (1966).

Morizane, Witt, A.F. and Gatos, H.C., J. Electrochem. Soc. 115 747 (1968).

Parfitt, H.T. and Robertson, D.S., Brit. J. Appl. Phys. 18 1709 (1967).

Utech, H.P., Brower, W.S. and Early, J.G., in Crystal Growth (H. S. Peiser, Ed.) Peragamon Press, Oxford, 1967, p. 201.

Utech, H.P. and Flemings, in Crystal Growth (H. S. Peiser, Ed.) Pergamon Press, Ox ford, 1967, p. 651.

Van Uitert, L.G., Levinstein, H.J., Rubin, J.J., Capio, C.D., Dearborn, E.F. and Bonner, W.A., Mat. Res. Bull. 3 47 (1964).

Wilcox, W.R. and Fullmer, L.D., J. Appl. Phys. 36 2201 (1965).

Witt, A.F. and Gatos, H.C., J. Electrochem. Soc. 113 808 (1966).

Witt, A.F. and Gatos, H.C., J. Electrochem. Soc. 114 413 (1967).

Witt, A.F. and Gatos, H.C., J. Electrochem. Soc. 115 70 (1968).

2. Solution Growth

Chase, A.B., in Preparation and Properties of Solid State Materials (R. A. Lefever, Ed.), Dekker, Inc., New York, 1971, pp. 183-264.

Elwell, D. and Neate, B.W., J. Mater. Sci. 6 1499 (1971).

Hoselitz, K., J. Cryst. Growth 3, 4 5-12 (1968).

Laudise, R.C., Linares, R.C., and Dearborn, J. Appl. Phys. 335 1362 (1962).

Lefever, R.B., Chase, A.B. and Torpy, J.M., J. Am. Ceram. Soc. 44 141 (1961).

Laudise, R.A., The Growth of Single Crystals, Prentice Hall, Englewood Cliffs, N.J.

Laudise, R.A., Carruthers, J.R. and Jackson, K.A., in Annual Review of Materials Science, Volume 1, 1971 (R. A. Huggins, R. H. Bube, and R. W. Roberts, Eds.), Annual Reviews Inc., Palo Alto, Calif. 1970, pp. 253-288.

Nielson, J.W., J. Appl. Phys. 31 51 (1960).

Scheel, H.J. and Schulz-Dubois, J. Cryst. Growth 8 304 (1971).

3. Magnetic Bubble Memory Crystals

Anon., Solid State Tech., 16(5) 25 (1973).

Belt, R. F., J. Appl. Phys. 40 1644 (1969).

Blank, S. L., Shick, L. K., and Nielsen, J. W., J. Appl. Phys. 42 (4) 1556-1558 (1971).

Bobeck, A. H. and Scovil, H. E. D., Scientific American 224 (6) 78 (1971).

Bobeck, A. H., Fisher, R. F., Perneski, A. J., Remeika, J. P. and Van Uitert, L. G., IEEE Trans. Mag. MAG-5 (3) 544-553 (1969).

Bobeck, A. H., Spencer, E. G., Van Uitert, L. G., Abrahams, S. C., Barnes, R. L., Grodkiewicz, W. H., Sherwood, R. C., Schmidt, P. H., Smith, D. H., and Walters, E. M., Appl. Phys. Lett. 17 (3) 131-134, 1970.

Callen, H., Mat. Res. Bull. 7 (10) 931-938 (1971).

Ghez, R. and Giess, E. A., Mat. Res. Bull. 8 31-42 (1973).

Glass, H. L., Mat. Res. Bull. 8 43-52 (1973).

Glass, H. L., Mat. Res. Bull. 7 385-   (1972).

Glass, H. L. and Hamilton, T. N., Mat. Res. Bull. 7 761-768 (1972).

Kooy, C. and Enz, U., Philips Res. Repts. 15 (1) 7-29 (1960).

Laudise, R. A. and Van Uitert, L. G., Bell Labs Record 49 (8) 238-243 (1971).

LeCraw, R. C., Wolfe, R., Bobeck, A. H., Pierce, R. D., and Van Uitert, L. G., J. Appl. Phys 42 (4) 1641-1642 (1971).

Lefever, R. A., Chase, A. B., and Torpy, J. W., J. Amer. Ceram. Soc. 44 (3) 141-145 (1961).

Matick, R. E., Proc. IEEE 60 (3) 266-289 (1972).

Quon, H. H. and Potvin, A. J., Mat. Res. Bull. 7 (5) 463-472 (1972).

Shick, L. K., Nielsen, J. W., Bobeck, A. W., Kurtzrg, A. J., Michaelis, P. C., and Reekstin, J. P., Appl. Phys. Lett. 18 (3) 89-91 (1971).

Van Uitert, L. G., Sherwood, R. G., Bouner, W. A., Grodkiewicz, W. H., Petroski, L. and Zydrik, G., Mat. Res. Bull. 5 (2) 153-162 (1970.

Varnerin, L. J., IEEE Trans. on Mag. Mag-7 404 (1971).

4. Electrooptic Crystals

Amodei, J. J., Phillips, W. and Staebler, D. L., Applied Optics 11 (2) 390 (1972).

Amodei, J. J. and Staebler, D. L., RCA Review 33 (1) 71 (1972).

Anderson, L. K., Microwaves 4 42 (1965).

Anderson, L. K., Ferroelectrics 3 69 (1972); IEEE Trans. Sonics & Ultrasonics SU-19 69 (1972).

Anon., Amer. Ceram. Soc. Bull 51 (9) 732 (1972).

Anon., Bell Labs Record 45 20 (1967).

Anon., 1971 British Crystal Optical Physics Conference, Optics and Laser Technology, Special Supplement, 3 5-13, May, 1971.

Anon., Laser Focus 8 (2) 15 (1972).

Anon., Optical Spectra 5 (1) 16 (1971).

Anon., Optical Spectra 5 (1) 34 (1971).

Beerman, H. P., Bull. Am. Ceram. Soc. 46 (8) 737 (1967).

Bergman, J. G., Ashkin, A., Bellman, A. A., Dziedzic, J. M. Levenstein, H. J. and Smith, R. G., Appl. Phys. Lett. 12 (3) 92 (1968).

Brezina, Mater. Res. Bull. 6 (6) 401 (1971).

Broy, A., Dures 89-94, May, 1971.

Broy, A., New York Times, August 29, 1971.

Bordogna, J., Keneman, S. A., and Amodei, J. J., RCA Review 33 (1) 227 (1972).

Bowers, K. D., Bell Labs Record 49 (5) 139 (1971).

Byer, R. L. and Rounidy, C. B., IEEE Trans Sonics & Ultrasonics SU-19 (2) 333 (1972).

Chang, J. T., Dillon, J. F. and Gianola, U. F., J. Appl. Phys., 36 1110 March 15, 1965.

Chapman, D. W., Proc. 1970 IEEE Int. Computer Group Conf. (Washington, D.C. June 16-18, 1970), p. 56.

Cummins, S. E., and Luke, T. E., IEEE Trans. Sonics & Ultrasonics SU-19 (2) 125 (1972).

Dixon, R. W. and Chester, A. N., Appl. Phys. Lett. 9 (5) 190 (1966).

Dougherty, J. P., Sawaguchi, E. and Cross, L. E., Appl. Phys. Lett. 20 (9) 364 (1972).

Fay, H., Alford, W. J. and Dess, H. M., Appl. Phys. Lett. 12 (3) 89 (1968).

Geusic, J. E., Levinstein, H. J., Rubin, J. J., Singh, S. and Van Uitert, L. G., Appl. Phys. Letters 11 269 (1967).

Giordmaine, J. A., Phys. Rev. Lett. 8 (1) 19 (1972).

Glass, A. M., Appl. Phys. Lett. 13 (4) 147 (1968).

Glass, A. M. and Abrams, R. L., J. Appl. Phys. 41 (11) 4455 (1970).

Hasegawa, T. and Sato, H., IEEE Trans. Sonics & Ultrasonics SU-19 (2) 183 (1972).

Hoselitz, K., J. Cryst. Growth 3, 4 5 (1968)

IEEE Trans. Microwave Theory Tech. 17 No. 11 (1969) (Collection).

Iwasaki, H., Sugii, K., Nuzeki, N. and Toyoda, H., Ferroelectrics 3 157 (1972).

Johnson, K. M., Microwave Journal 7 51 (1964).

Kaminow, I. P. and Turner, E. H., Applied Optics 5 1612 (1966).

Kimmitt, M. F., Ludlow, J. H. and Putley, E. H., Proc. IEEE 56 (7) 1250 (1968).

Kino, G. S. and Matthews, H., IEEE Spectrum 6 (8) 22 (1971).

Konstantinova, V. P., Sil'vestrova, and Aleksandrov, K. S., Kristallografia 4 69 (1959).

Kumada, A., IEEE Trans. Sonics & Ultrasonics SU-19 (2) 115 (1972).

Kurtz, S. K. and Perry, T. T., J. Appl. Phys. (July, 1968).

Laudise, R. A., Bell Labs Record 46 (1) 3 (1968).

Lytollis, J., Optics Technology 1-10 November, 1968.

Matick, R. E., Proc. IEEE 60 (3) 266 (1972).

Matsumura, S. and Uematsu, Mat. Res. Bull 7 (1) 45 (1972).

Midwinter, J. E., Appl. Phys. Lett. 11 (4) 128 (1967).

Midwinter, J. E., J. Appl. Phys. 39 (7) 3033 (1968).

Phillips, W., Amodei, and Staebler, D. L., RCA Review 33 (1) 94 (1972).

Pinnow, D. A., Van Uitert, L. G., Warner, G. W., and Bonner, W. A., Appl. Phys. Lett. 15 (3) 83 (1969).

Putley, E. H., Semiconductors and Semimetals 5 259 (1970). Edited by R. K. Willerdam, et. al.

Putley, E. H., Optics and Laser Technology, 150, August 1971.

Putley, E. H., Watton, R. and Ludlow, J. H., IEEE Trans. Sonics & Ultrasonics SU-19 (2) 263 (1972).

Ramberg, E. G., RCA Review 33 (1) 5 (1972).

Spencer, E. G., Lenzo, P. V. and Ballman, A. A., Proc. IEEE 55 2074 (1967).

Sugii, K., Iwasaki, H. and Miyazawa, S. Mat. Res. Bull. 6 (6) 503 (1972).

Tsuya, H., Fukino, Y. and Sugibuchi, K., J. Appl. Phys. 41 (6) 2557 (1970).

Vollmer, J. and Gandolfo, D., Science 175 (4018) 129 14 January 1972.

White, G. L., Digest of Technical Papers, pp. 22-38 to 22-45, IEEE International Conference on Communications, San Francisco, June 8-10, 1970.

White, G. L., Bell Sys. Tech. J. 50 (8) 2607 (1971).

White, R. M., Proc. IEEE 58 (8) 1238 (1970).

Yamaka, E., Hayashi, T. and Matsumoto, M. Infrared Physics 11 (4) 247 (1971).

III. AQUEOUS SOLUTION GROWTH OF TGS

As discussed in Section II, tryglycine sulfate (TGS) is a technologically important ferroelectric material whose application in devices is presently limited by the perfection of available crystals. TGS is an ideal material to use as the basis for a study of crystal growth in space since, in addition to its technological significance: (a) it can be grown readily from aqueous solutions; (b) the temperature of growth is relatively low and presents no safety hazard; (c) it has high solubility in water so that a small volume of solution could provide a significant amount of crystal product for study; (d) the power requirement for an aqueous growth experiment will be low; (e) the simple experimental procedure can be fully automated and have a high probability of successful completion; (f) experimental materials are non-toxic and relatively harmless in the event of an accident; and (g) growth of TGS under terrestrial conditions is well advanced and crystals are available for detailed characterization and comparison between space grown and terrestrial crystals (see Section IV).

TGS has typically been grown from aqueous solution in the laboratory by introducing a seed crystal into a supersaturated solution then maintaining the supersaturation during growth by (a) slowly cooling the solution, (b) controlled evaporation of the solution at constant temperature, or (c) controlled replenishment of the growth solution with fresh TGS to replace that deposited onto the seed. For the purposes of this program and to satisfy the criteria for simplicity, as denoted above, the process of growth by controlled cooling of the solution

('a' above) was chosen. The best quality terrestrial crystals have, to date, been obtained from slow evaporation of solutions at constant temperature ('b' above) but this is not readily adaptable to the space environment (see Section IV). There is merit to the method (c) above in which two vessels are linked so that fresh saturated solution from one vessel is continually added to the growth vessel maintained at a slightly lower temperature.

Our initial studies were all based on growth on nucleating pins fixed in the solution and cooled by conduction to external pins or actively by a thermoelectric device. Again this procedure eliminates the possibility of disturbing the solution by introducing a seed and also eliminates the need for a mechanism for seed handling. However, this unseeded solution has a greater tendency for spurious nucleation on the walls of the vessel and not at the desired site, unless careful precautions are taken. All growth runs were performed by cooling solutions below the Curie temperature (49°C) but recent data (see Section IV) suggests that greater perfection is obtained in crystals grown above the Curie temperature. In the proposed arrangement growth would occur at all temperatures below the nucleation (supersaturation) temperature but it may be of interest in future work to start growth at, say 60°C, so that parts of the crystal form above the Curie temperature and parts below it. This would provide an additional source of characterization data when comparing terrestrial vs. space-grown crystals.

The preliminary definition of a crystal growth experiment and the design of an experimental system suitable for use in a manned mission profile is discussed in subsequent sections.

A. Preliminary Definition and Design of Experiment

Exploratory work for the growth of TGS crystals from aqueous solutions by the method of slow cooling was performed using commercial TGS crystals (from Eastman Kodak). Later experiments employed multiple recrystallized material using the above crystals as source material. Saturated solutions were prepared in accordance with the data in Figure 2. Solutions saturated at $40^{\circ}C$ were generally used so that in cooling, to say $25^{\circ}C$, a growth of about 15 gms of TGS per 100 cc's of water would be possible. In the interests of compactness, growth vessels of 50 cc capacity were chosen and allowing for the volume of thermometers, nucleation, pins, and stirrers a solution volume of 40 ml was used in most experiments so that a yield of 5 gms of TGS was feasible from this cell.

The initial experiments were designed to make use of the Apollo mission electrophoresis boxes*, the design of which had passed quality control from a NASA interface standpoint and was chosen as a flight experiment on the Apollo 16 mission. The mock-up unit (approximately 10 x 12 x 16 cm), shown in Figures 3 through 5, was self contained and required only an electrical power supply and the use of a Hasselblad camera for data collection. The arrangement of the crystal growth box relative to the camera is shown in Figure 3.

The camera field of view of the front face of the experimental unit is shown in Figure 4. The mock-up unit had two crystal growth cells, each of 40 ml

*E. C. McKannan, et al, NASA TM X-64611, August 29, 1971
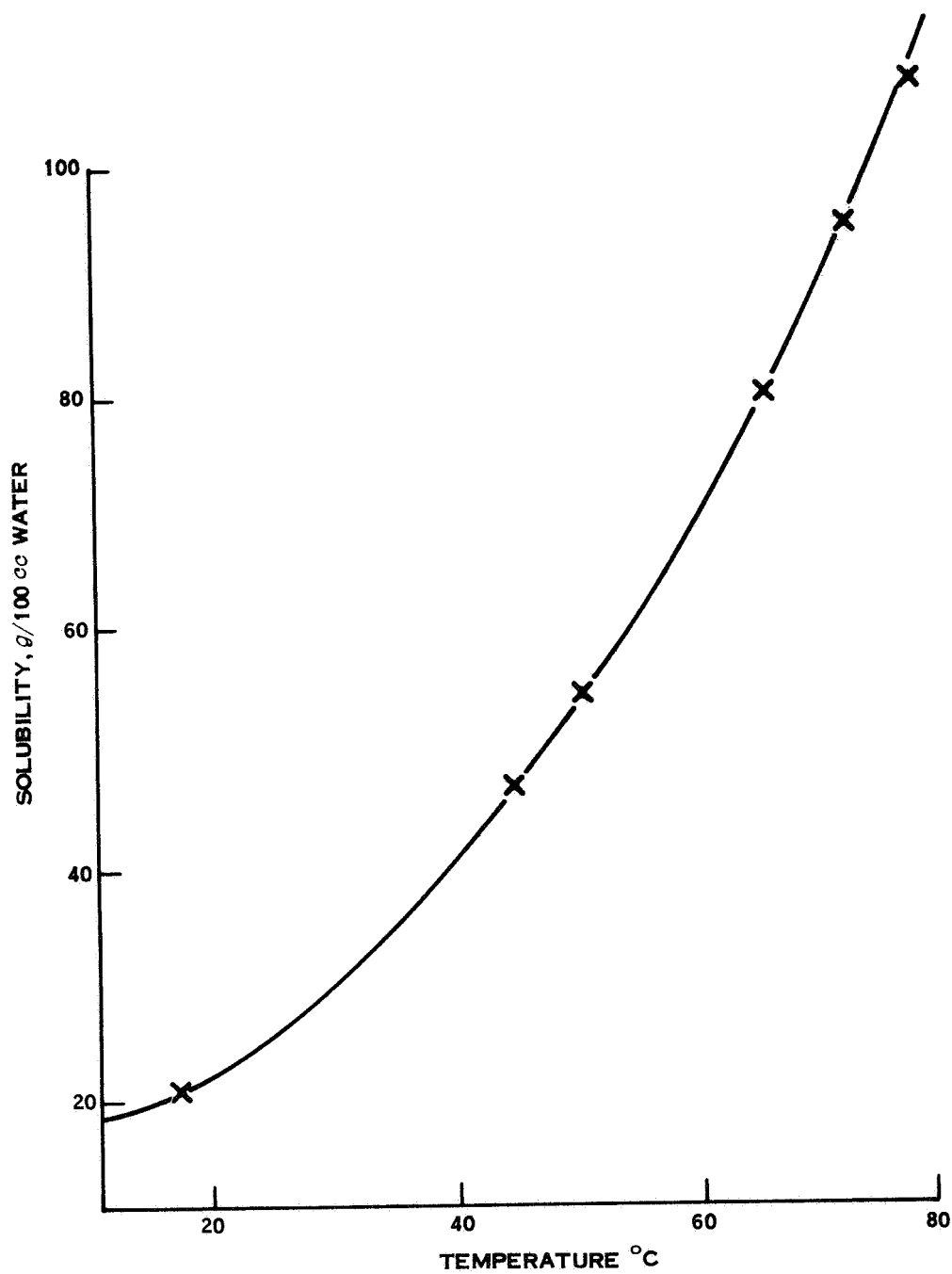
Figure 2.   The Temperature Dependence of the Solubility of Triglycine
Sulfate in Water (Konstantinova, Sil'vestrova, and
Aleksandrov, 1959).
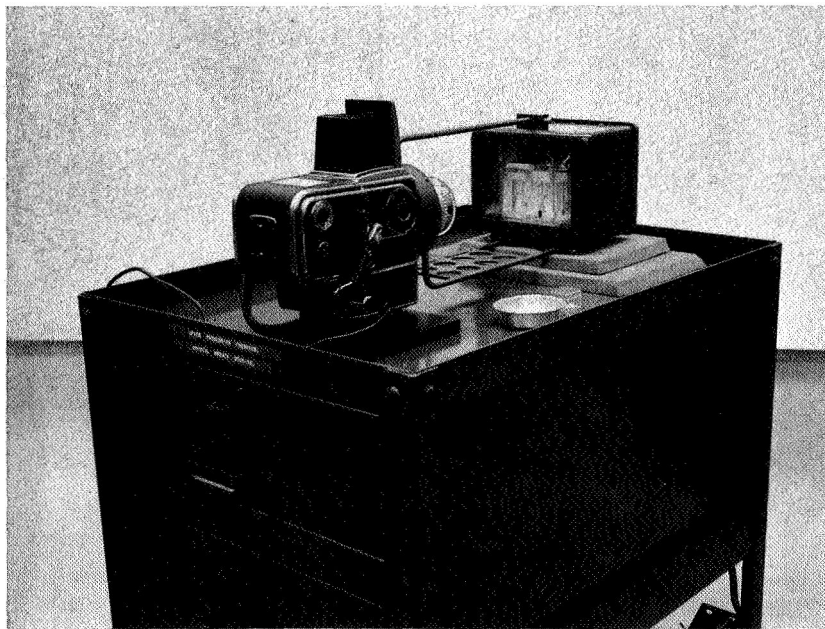
Figure 3.   Arrangement of Apparatus for Studying Crystal Growth
             from Aqueous Solutions in a Zero-G Environment.

THERMOMETER

PINS USED AS
NUCLEATION SITES

CHRONOMETER
(MOCK-UP)

MIRROR FOR
SIDE VIEW
OF CELLS

SIDE VIEW OF
NUCLEATION
SITES

GROWTH CELLS   HEATER IN BASE OF CELL
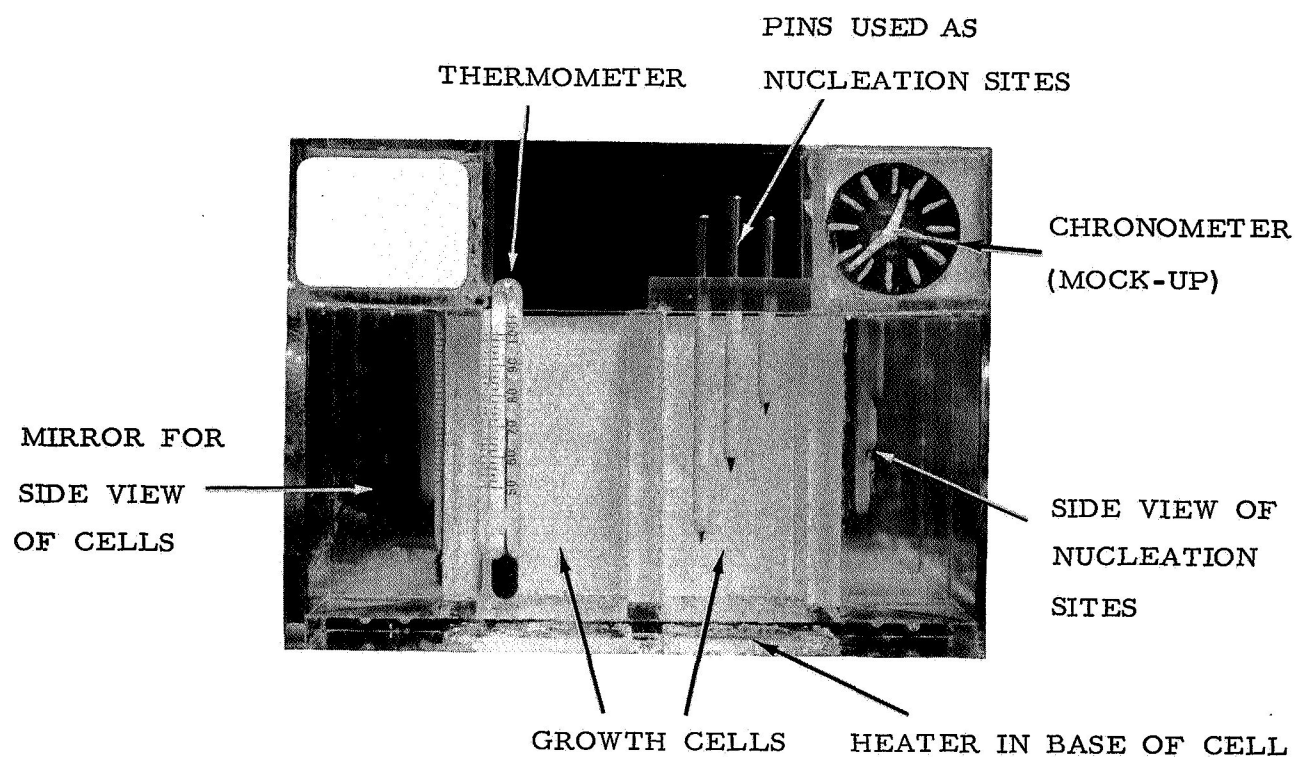
Figure 4.   Field of View of the Camera for a Crystal Growth
Experiment in the Demonstration Unit for Growth
from Aqueous Solutions.

39

capacity, in which two separate solutions could be studied simultaneously. Each cell contained two thermometers to indicate temperature at top and bottom of the cell, and three actively cooled stainless steel pins to serve as nucleation sites for crystal growth. All data from the growth experiments was recorded photographically by a sequential camera, typically at five minute intervals during the growth process. The final design concept was arranged to incorporate provisions for a simple and rapid recovery of the grown crystals so that return of the complete unit after a growth experiment would not be necessary. A small resistance heater was embedded in the base of each cell and the total power requirement for the heating the solutions during the initial period of growth was about 7 watts. The field of view of the camera also included an electrical chronometer with calendar to indicate elapsed time during crystal growth. Illumination of the cells and indicators was provided internally in the mock-up unit by a small fluorescent lamp behind a white screen. Side views of crystal growth in each of the cells were provided by mirrors at each side of the unit. The arrangement of the wiring and components in the growth box is shown in Figure 5.

Several preliminary growth experiments of triglycine sulfate (TGS) from aqueous solutions were performed using the growth cells of the mock-up unit. The procedures for a typical growth experiment were as follows: The unit was sealed with each cell containing solutions of chosen concentrations of TGS so as to form saturated solutions when heated to about 40°C. The heaters were then turned on until a temperature of 40°C was reached in the cell and all

POLISHED METAL
REFLECTOR

WHITE DIFFUSER
SCREEN

BACK OF BOX WITH
POWER CONNECTOR
AND FOAM INSULATION

FLUORESCENT
LAMPS

STARTER FOR
LAMPS
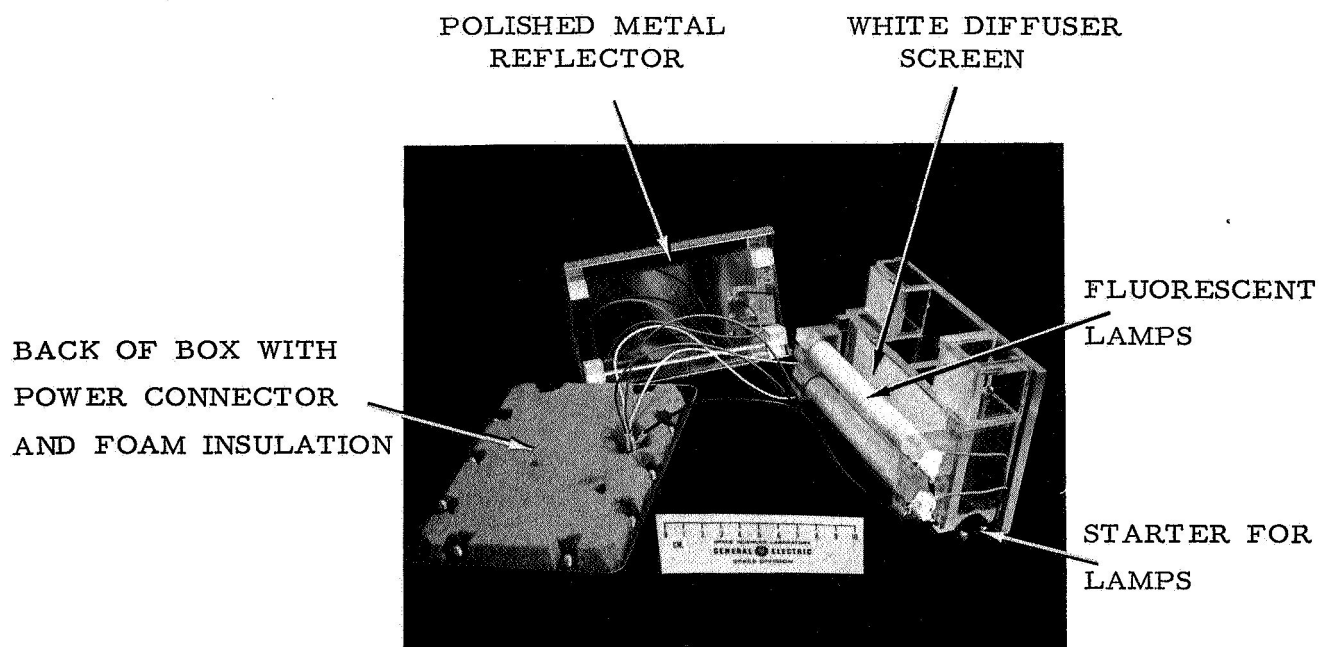
Figure 5.   Arrangement of Components and Wiring Within the
Growth Cell Box

41

the TGS was dissolved after which only the cell illumination was left on as the cells were allowed to cool. The sequential camera was then activated and exposures were made at appropriate intervals for several hours until the cells cooled to room temperature. Growth was usually completed within 6 to 10 hours in the mock-up unit: the illumination source provided a small background heating effect within the unit and the walls of the box were internally lined with polyurethane foam insulation to encourage slow cooling.

B. Experimental Results

The major objective in assessing the results of the crystal growth experiments was to assess the reproducibility and reliability of this simple concept for producing TGS crystals. In the experiments performed on this program the crystals generally formed rapidly (relative to established practice for high quality crystals; i.e. refer to Section IV) and commonly consisted of multiple nucleations on both the growth sites (metal pins) and cell walls. Overgrowths, veils, and possibly solvent inclusions were common growth features with no significant difference being observed between as-received source crystals and multiply recrystallized material. The resultant crystals were predominantly plates with rhombus-like outlines and had largest dimensions of between 2 and 10 mm.

Improvements in the construction of the metal pin nucleation site (stainless steel or aluminum) were made to increase the probability for nucleation on the pin. The pin was cooled by attaching it to a 1/8" diameter

aluminum or copper rod which extended out of the heated growth cell into the cooler laboratory atmosphere. The surface of the rod was insulated from the solution by a 1/8" thick sleeve of Teflon tubing so that only the point of the pin was exposed to the growth solution. Nucleation was reproducibly obtained on this pin design although occasionally more than one seed was nucleated and growth of two or more adjacent crystals resulted. Enhanced cooling of the pin by a small thermoelectric device* was used in some experiments but generally led to high cooling rates and spontaneous nucleation throughout the solution. A low power device of this type could readily be incorporated into the growth unit if an external cooling environment (pins or fins extending out of the unit) is not practicable in space.

Spontaneous nucleation of many small crystals in the solution was a feature of several experiments designed to complete growth of crystals in only a few hours (less than 10 hours). To avoid this it was necessary to cool slowly, about 0.2°C/hr., during nucleation and the first few hours of growth, and then to increase the cooling rate to 0.5°C/hr. for 10-20 hours and finally cool at 1 to 2°C/hr. to ambient temperature. Cooling was controlled by regulating the power input to the heater at the base of the cell using a small Variac. In these laboratory experiments it was necessary to stir the solution with a small teflon-coated magnetic stirrer to avoid severe density (and concentration) gradients in the solution during growth. In the absence of gravity this would of course not be

---

* Cambridge Thermionic Corporation

necessary and growth would take place in a much more stable environment. The total growth time for a typical experiment was now about 60 hours and crystals up to 3 gms weight were obtained with individual faces over 1 cm^2 area. For the size of cell used in the mock-up, a maximum crystal size of 5 gms could be obtained from a single-seed nucleation using the conditions described above.

A complete photographic record of several growth experiments (using an air cooled aluminum pin as the nucleation site) was obtained using a Hasselblad camera and lapsed-time photography similar to the procedure expected to be followed in the flight unit.

The experimental setup is shown in Figure 6. The growth of a TGS crystal with slow cooling over several days is shown in Figure 7. The as-grown crystal is shown in Figure 8 after removal from the aluminum pin. A crystal with a rhombus-like outline with a face over 2 cm^2 area is shown in Figure 9. An example of spurious nucleation resulting in the growth of many small crystals on the aluminum tip as well as in the Teflon tubing is shown in Figure 10.

While our efforts at General Electric were concentrating on the design of a space experiment and the determination of the technique and initial parameters for that method, Pennsylvania State University was primarily concerned at this point with growing the best crystals possible by conventional terrestrial techniques (controlled solvent evaporation) so that work could commence on the characterization plan (Section IV).

44
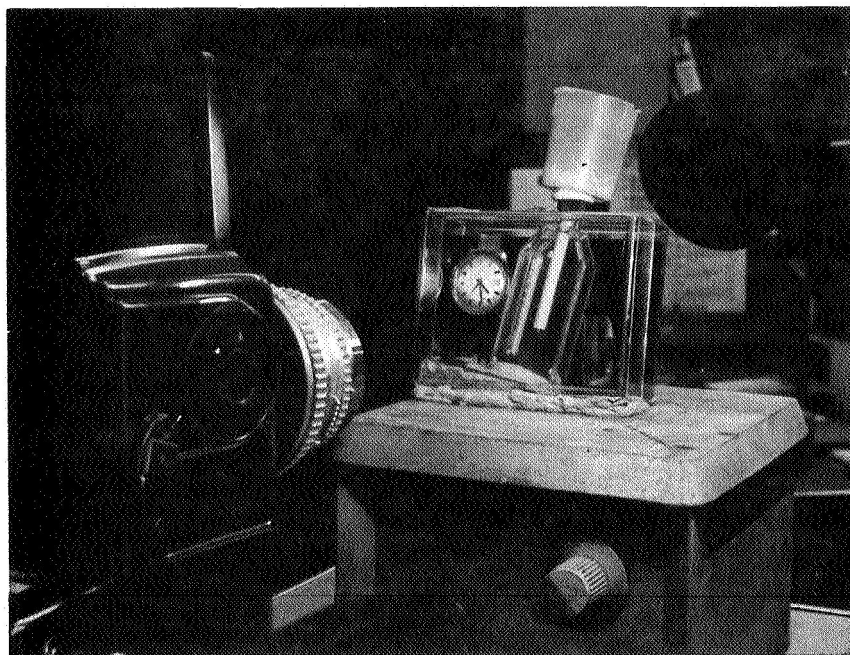
(A)
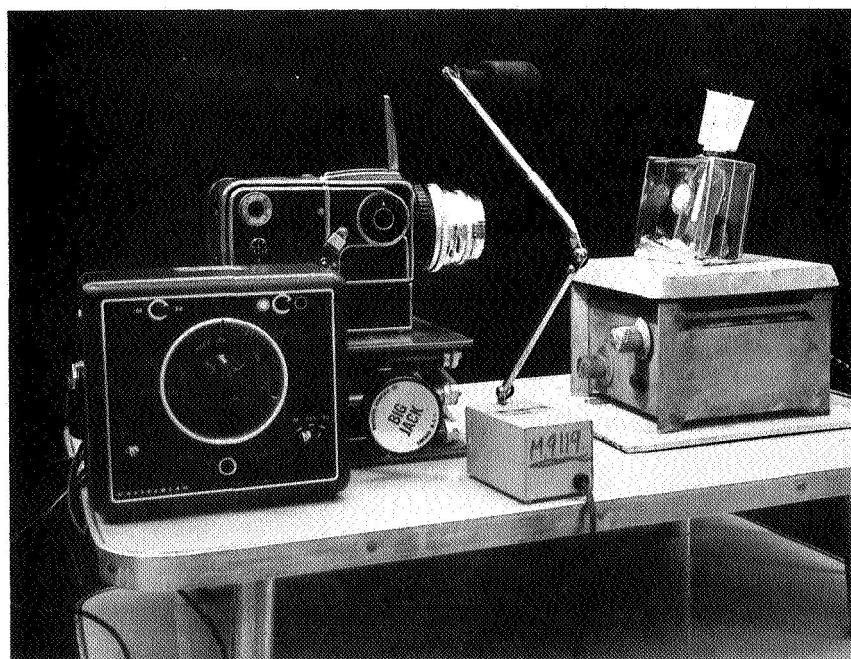
(B)

Figure 6. Experimental Set-Up for Simulation of TGS Space Growth
Procedure. (A)   Front View Showing Cell Cooling Tip and
Chronometer; (B)   Side View Showing Camera and Cell.

45
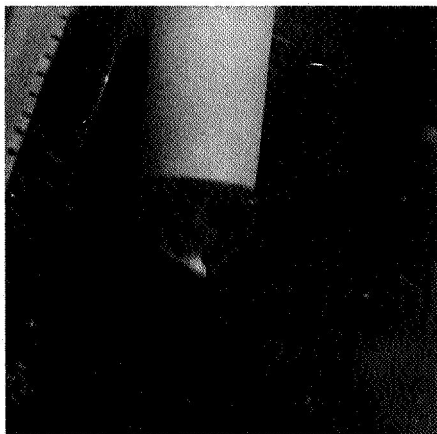
24 hours
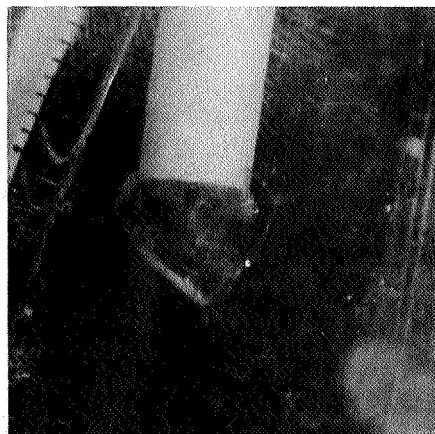
72 hours
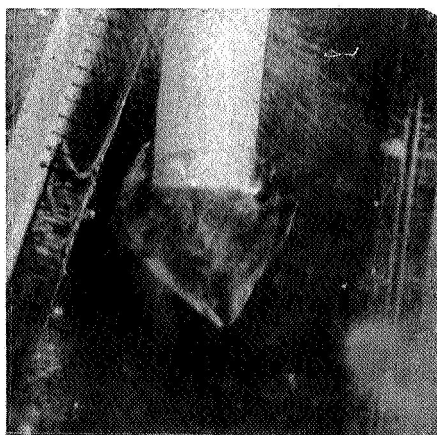
116 hours
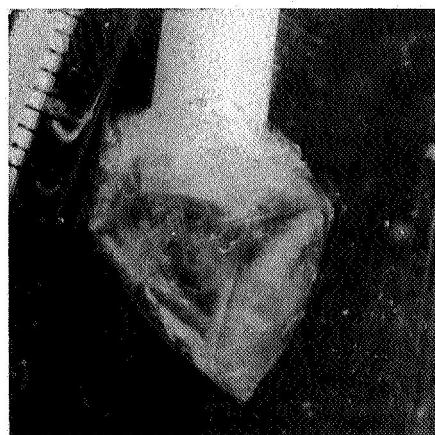
140 hours

Figure 7. Growth of a TGS Crystal from Cooling Tip in Simulated Space Growth Experiment over 140 Hours.

Figure 8.   As-Grown TGS Crystal After Removal from Cooling Tip
             in Simulated Space Growth Experiment.

⊢————⊣
  CM

Figure 9.   TGS Crystal with Rhombus-like Outline Grown in
             Simulated Space Growth Experiment.

47
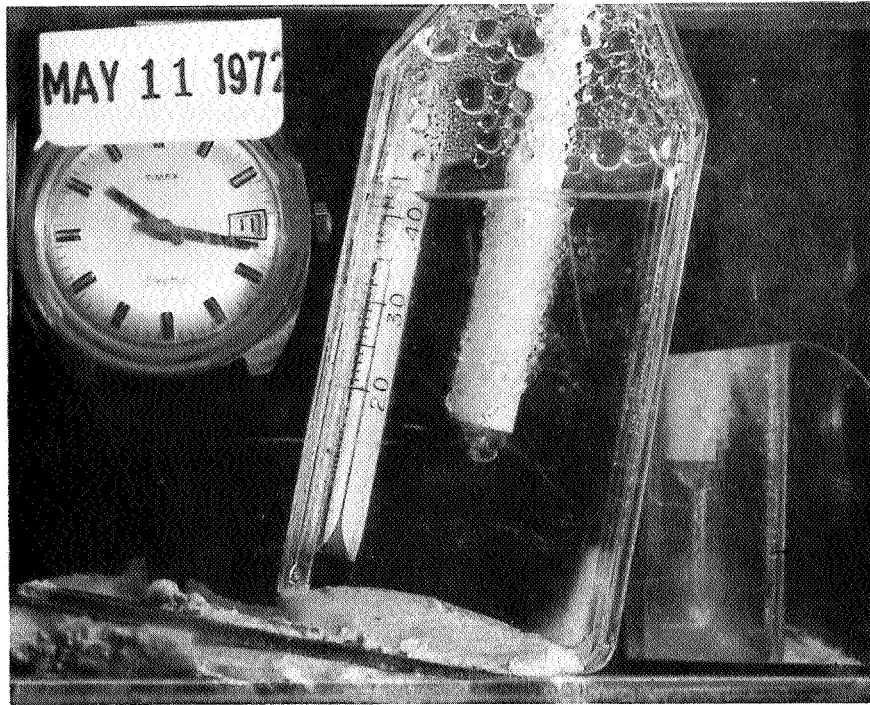
Figure 10. Cooling Tip Showing Results of Spurious Nucleation in Simulated Space Growth Experiment

47A

C.   Observation of Inhomogeneities in Solutions during Crystal Growth

Inhomogeneities occur within crystal-growth solutions as a result of variations in concentration, density, and temperature which in terrestrial experiments give rise to convective disturbances in the solutions. It is well established that these inhomogeneities and disturbances cause variations in the crystal-growth process and therefore lead to imperfect crystal structures. In terrestrial experiments, these inhomogeneities are generally alleviated by encouraging forced convection or by actively stirring the solution. In a space environment under nearly zero-g conditions, convection currents would not be set up since differences in density have reduced significance. Therefore, in principle, a stable motionless crystal-growth solution could be established and the growth of crystals under these conditions could be studied.

In this zero-g condition crystal growth can occur by diffusion of the crystallizing species to the growth site along concentration, density, or temperature gradients. This process will be slow, orderly, and well controlled, and should result in highly-perfectly crystals. However, the nature of these gradients during growth will not be well known from the normal photographic data recorded during growth.

A simple technique was established which greatly facilitated the detection and observation of inhomogeneities and disturbances in crystal-growth solutions. This technique consisted of viewing the crystal-growth cell against a background of a Moiré pattern grid (a black and white print with 5 lines/mm

was found to be adequate). By this technique, any inhomogeneities in the solution were manifested as distortions of the line pattern and could be readily observed and photographed. The distortions arise because changes in concentrations, density, or temperature within the solution cause slight changes in the refractive index of the liquid which in turn causes distortion of the image of the grid pattern.

This procedure was used during the growth of TGS from aqueous solutions in the crystal growth unit mock-up described above and is shown in Figure 11. Convection currents, density stratification, and small disturbances near the growing crystal surface were shown to produce distortions in the observed grid pattern without interfering with the view of the growing crystal. Attempts to produce Moire interference patterns by the addition of a similar line pattern on a film in front of the growth cell proved unsuccessful and were not studied in detail because the film grid interfered with the prime objective to observe the growing crystal.

The technique described was easily adapted to the existing growth cell designs and the mock-up unit for crystal growth studies by simply replacing the white background screen with an appropriate black and white line pattern. It is planned to use this technique in future crystal growth experiments and growth-cell mock-ups.
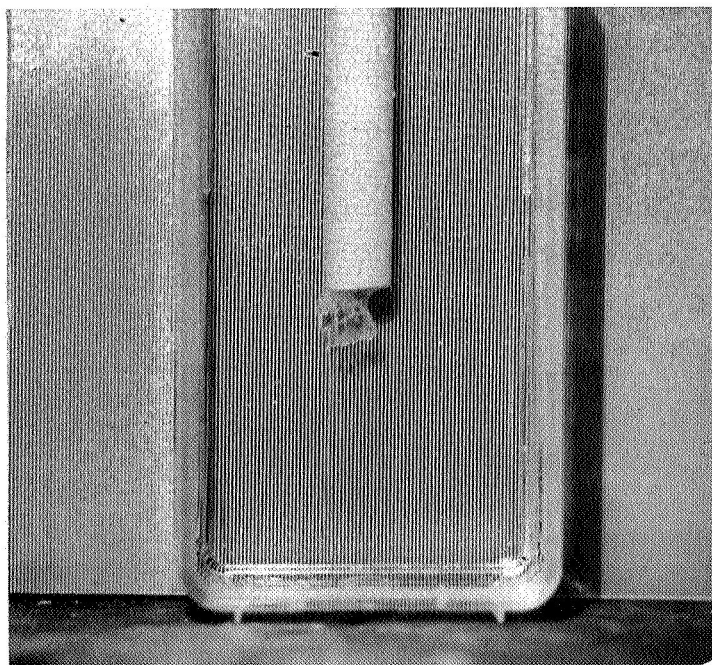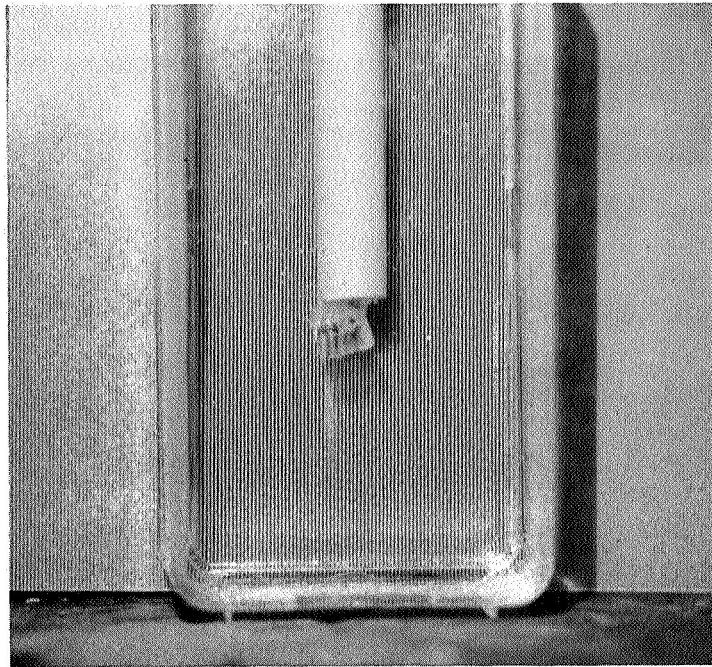
Figure 11. View of Crystal Growth Cell Against a Moiré Pattern in Simulated TGS Space Growth Experiment.

D. A TGS-Tin Experiment Design

In a separate internal study NASA has investigated the effect of gravity on the microstructure of small single crystals of tin*. As part of the current program, the possibility of incorporating a small module for the growth of tin crystals in the same box as used for aqueous solution growth was investigated. A modified growth unit was designed to permit the performance of a dual experiment to grow both TGS and tin crystals and some preliminary operational feasibility experiments were performed.

The dual growth unit was designed such that the tin growth module fitted into the rear of the illumination tube of the unit shown in Figure 5 and was bolted to the back plate of the box. The module consisted of a multi-chambered graphite crucible in a small resistance wound furnace within a ceramic foam insulation block. The heat would be extracted from this module in a space experiment by a direct metal contact between one end of the crucible and a finned block on the back plate of the box. Heat from the tin experiment may be used to pre-heat the box and growth solutions for subsequent growth of TGS. In the space experiment only a temperature indicator for the tin module would need to be added to the existing display for photographic recording.

The graphite crucible contained four chambers each 3 mm in diameter with nichrome wire to form the resistance furnace. The winding and crucible thermocouples were held in place by a ceramic cement.

---

* NASA TM X-53999, March 1970.

51

For initial laboratory experiments the furnace and crucible were placed into a machined hole in a 6 cm cube of ceramic insulating brick. There was provision for greater heat loss from the base of the crucible by means of an aluminum rod inserted through a hole in the brick. This arrangement ensured that solidification would be initiated at the conical base of the chambers. Temperature records showed that a gradient of up to 10°C could be maintained between the top and the conical end of the chambers by using a rod 1 cm diameter in contact with the alumina crucible and extending out of the brick structure, as shown in Figure 12. The cooling rate of this construction was too fast for acceptable crystal growth as recommended from the previous NASA work. Therefore, experiments were performed by cutting the power input to the furnace by a known fraction of that required for melting (instead of a direct switch off) so that a cooling rate of as low as 1°C per minute was achieved.

The construction shown in Figure 12 required a power input of 10 watts to achieve a temperature of about 270°C within 30 minutes. With the power switched off, the arrangement cooled at about 20°C per minute and solidification of all 4 slugs was achieved over a two minute period (solidification plateau). This is undesirable and almost certainly resulted in spurious nucleation of a polycrystalline slug (characterization of solidified slugs was not completed). Slow cooling rates were achieved by reducing the power input to the furnace after a temperature of about 280°C was reached in the furnace. Figure 13 shows data from an experiment in which the power input was cut to about 8 watts after melting so that a cooling rate of about 1.5°C per minute was achieved up to solidification.

THERMOCOUPLES { T M B

INSULATING BRICK

ALUMINA CRUCIBLE

FURNACE WINDING

ALUMINUM ROD

T M B

TIN SLUGS

GRAPHITE CRUCIBLES
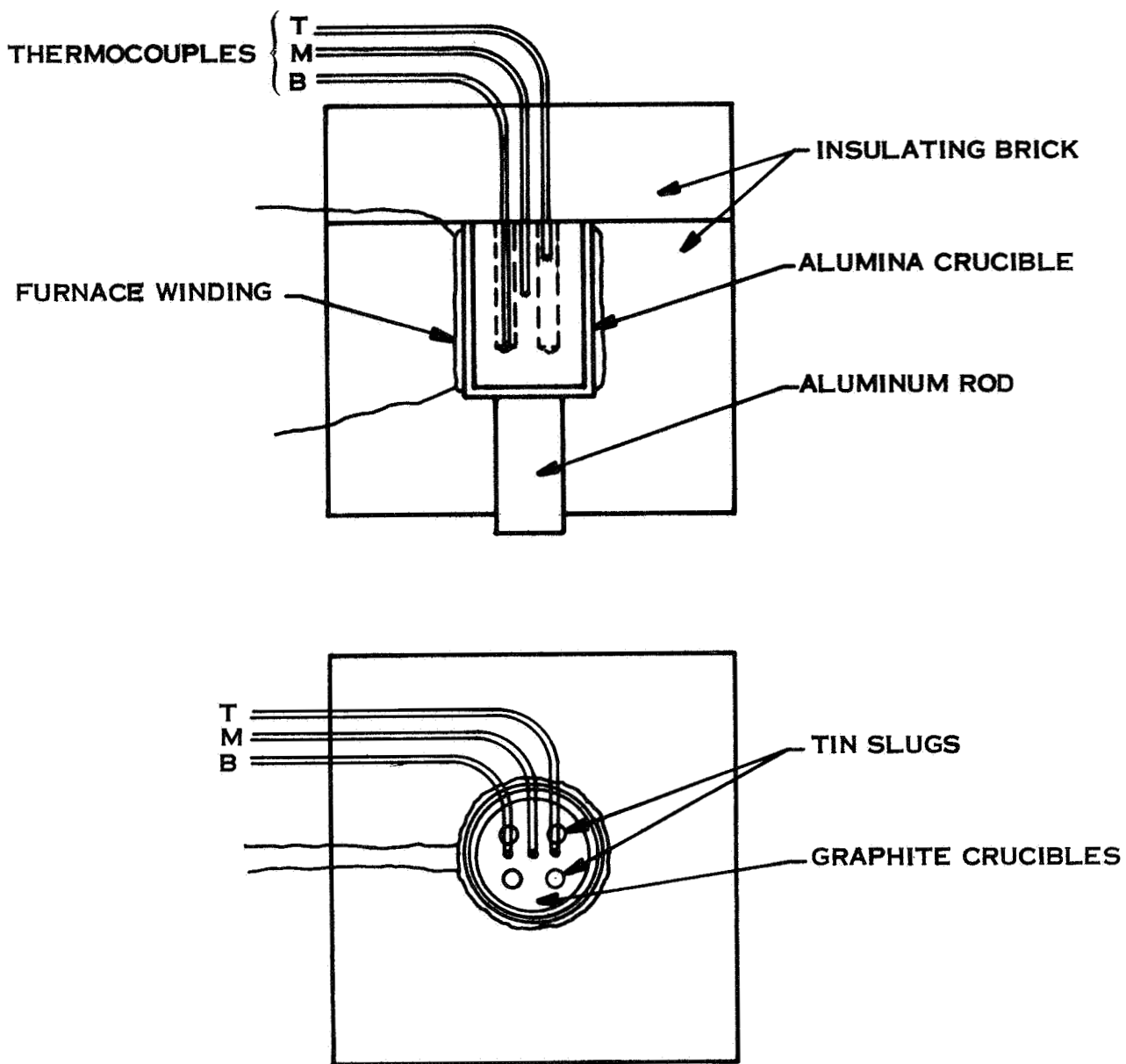
Figure 12.   Arrangement Used for Studies of the Solidication of Tin.

The equilibrium temperature at this power input was 210°C so that the cooling rate during and after solidification was less than 1°C/min. It is significant that four distinct solidification exotherms were observed corresponding to the solidification of each of the four tin slugs. In Figure 13, the recorded degree of supercooling was about 3, 6, 8 and 10°C for slugs 1 to 4 respectively (the melting point of tin is 231°); additional data for various cooling rates was obtained using recorders of higher sensitivity than that used for Figure 13.

The difference in temperature between top and bottom of the crucible was not large in the data shown in Figure 13: a difference between top and bottom of about 5°C is indicated by the arrows. (The original data showed a different color for each point, top, middle, and bottom, of the crucible which is not shown in Figure 13.) The temperature difference resulting from the solidification exotherm is far greater than the temperature gradient and results in an overall increase in crucible temperature of about 10°C as each slug solidifies. The solidification of each slug, therefore, has an influence on the thermal environment of each of the others and consequently affects the solidification and crystal growth of the others. Refinement of this system such as isolating each slug chamber from the others was considered but not pursued.

The tin crystals grown in the above unit were examined briefly and etched sections showed similar features (growth striations, etc.) to those reported in the earlier NASA work. Feasibility designs were completed to enable the tin growth unit to be incorporated if necessary into the aqueous growth mock-up. Further work on growth of tin crystals was not pursued.

54
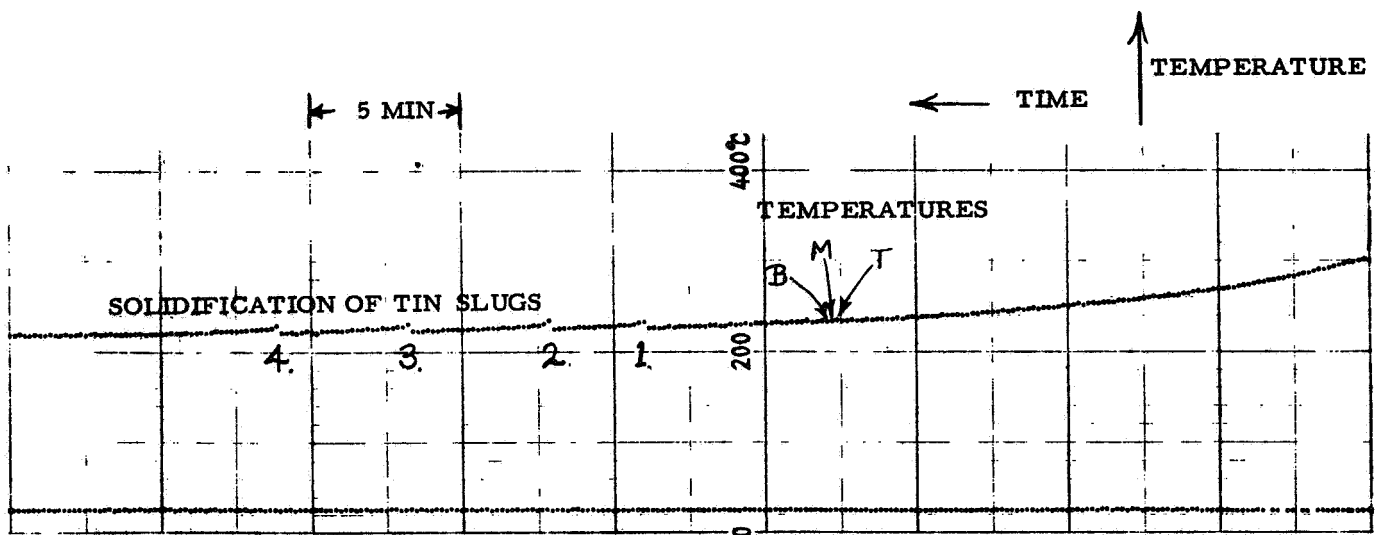
Figure 13.   Data Obtained from the Experimental Arrangement Shown
in Figure 12.

55

IV. CRYSTAL CHARACTERIZATION OF TGS

A. Introduction

The growth of crystals in space is based on the condition that the absence of a gravitational field would significantly improve the quality of the crystals as compared to terrestrially grown materials. The subject of this section is: How can the quality of space grown crystals and terrestrially grown crystals be compared?

The possible sequences for the characterization of triglycine sulfate have been investigated with a view to providing a system of measurements tailored to the evaluation of defect - and structurally - sensitive properties which appear to be gravity dependent. Triglycine sulfate has been selected since the general description by which crystals grow from high temperature solutions appears to be generally similar to that for growth from aqueous solution (Elwell and Neste, 1971).

Since the best available TGS crystals are grown by the constant evaporation technique, these were used to establish the initial baseline for comparison with space grown crystals. The next logical step would be to extend this work to TGS grown by the slow cooling method.

A possible sequence of characterization schemes for comparison of space-grown and terrestrially grown crystals is illustrated in Figures 14 and 15

The exact selection of analyses depends on the particular crystals grown. As a generalization, however, the information needed for a comparison breaks down into three broad categories:

1. Purity

2. Perfection

3. Perfection-sensitive properties

Recrystallization is often used as a purification procedure and carefully grown crystals may have a lower concentration of impurities than the starting materials. Usually the uptake of impurities is controlled by the rate of growth and the comparison is therefore a useful indication of the fluctuations in growth conditions. For most crystals of great technological interest, impurity levels must be in the part per million range or below. Methods of analysis are therefore critical and usual techniques may not be applicable.

Perfection of crystals refers to the density (or concentration) of a variety of dislocations, low angle grain boundaries, stacking faults, clusters of included materials, voids, bubbles, and veils. The uniformity of concentration of imperfections is also a good measure of the stability and control of the crystal growth process. Most applications of single crystals are perfection-limited and even under the most carefully controlled conditions, imperfection concentrations may be too high.

The final test of any comparison of crystal growth techniques
is the relevant physical property itself. As will be shown later in the case
of triglycine sulfate, the values of the permittivity at the phase transition,
and of the coercive field are very sensitive to the purity and perfection of the
crystals. When these relations have been established, measurement of the
property can also be a characterization tool. This is somewhat analogous
to the common practice of evaluating quality of germanium by its resistivity.
However, property measurement is not characterization as such -- it must
always first be established that the property to be measured in fact varies in
a sensitive way with some known characterization variable.

The major point that we make with the flow sheets of Figures 14 and 15 is
that characterization is a <u>system</u> of measurements tailored to a specific
material with a specific application.

B. Growth and Characterization of Triglycine Sulfate

1. Introduction

The design of crystal growth experiments for initial reconnaissance
of materials processing in space should include the following criteria:

i. Maximum data return: Comparison of growth in zero gravity

with laboratory growth on earth should be of significance.

ii. The material should be technologically significant.

iii. Experiment should consume maximum weight and volume

and yet be as fool-proof as possible.

iv. Experiment should be automated to consume minimum

crew time.

58
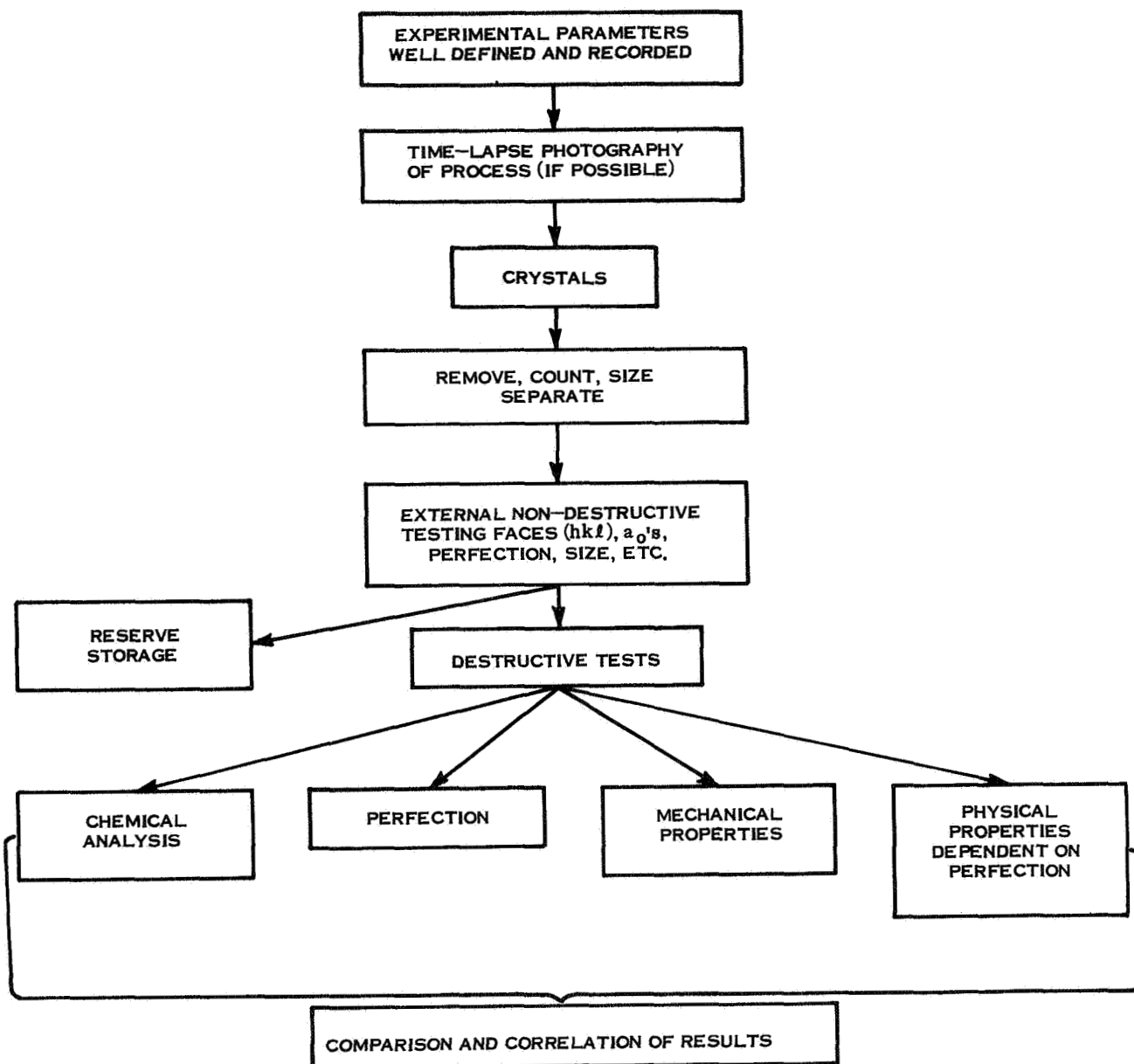
Figure 14. Flow Sheet Showing Handling, Testing and Evaluation
Procedure of Space Grown Crystals.
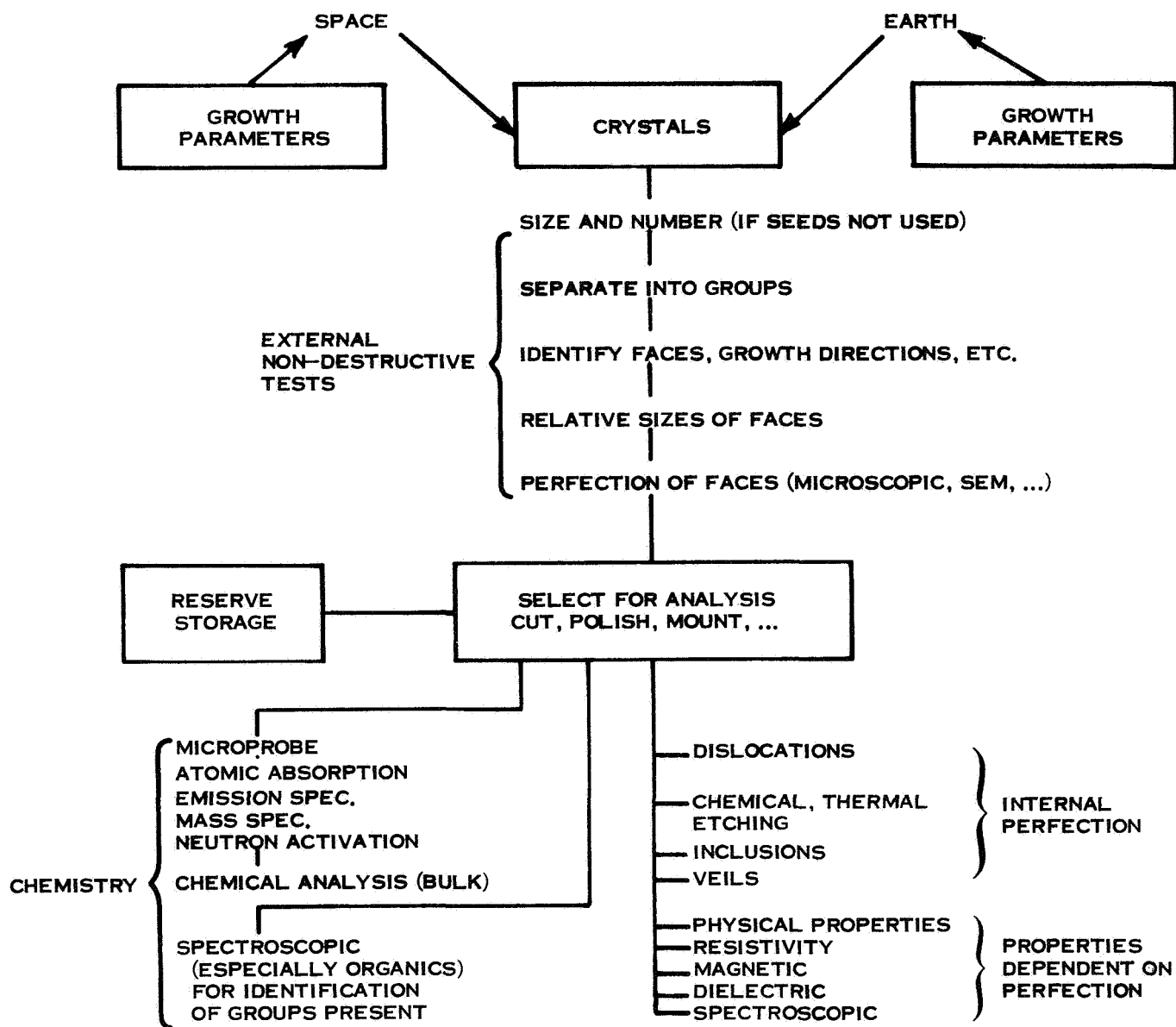
Figure 15. Characterization Scheme for Comparison of Space-Grown and Terrestrial Grown Crystals.

v. Power requirement should be low.

vi. Chemical compatibility: Experimental materials should be nontoxic to minimize risk of accident and to minimize hazard to crew if an accident should occur.

A substance which meets these criteria is the amino acid salt, triglycine sulfate. TGS has a wide range of applications as a pyroelectric material for use in infrared detectors. Its present application is perfection-limited and the size of individual crystals used in detectors is extremely small (1.5 x 1.5 mm x 40 μm). This section of the report reviews the present status of crystal growth and characterization of TGS as applicable to a possible space experiment.

2. Properties and Device Applications

The ferroelectricity of triglycine sulfate was discovered in 1956 by Matthias and others at the Bell Telephone Laboratories. It has become one of the most extensively investigated ferroelectrics because the ferroelectric phase transition is near room temperature and because of the ease with which large crystals can be grown. The Curie temperature is 49°C. The crystal belongs to monoclinic space group $P2_1$ in the ferroelectric phase and the onset of the paraelectric phase is induced by the introduction of a mirror plane to raise the symmetry to $P2_1/m$. The dielectric properties and domain structure of TGS are summarized by Jona and Shirane (1962). A summary of the physical properties of TGS is given in Table 5.

61

Table 5. PROPERTIES OF TRIGLYCINE SULFATE

Space Group $\quad\quad$ $P2_1 (T<49°)$ $\quad\quad$ $P2_1/m (T>49°)$

Unit Cell Constants

$a = 9.15$

$b = 12.69$ $\quad\quad\quad$ Hoshino et al. (1959)

$c = 5.78$

$\beta = 105°40'$

Optical Constants

$n_\alpha = 1.484$

$n_\beta = 1.556_5$

$n_\gamma = 1.584_5$

$X = b$ $\quad\quad$ Dion (1959)

$Y \wedge c = 3°$

$Z \wedge a = 18°40'$

$2V = 61°18'$

Density $\quad\quad\quad$ 1.69 gm/cm^3

Dielectric Properties $\quad\quad$ $T_c = 49°C$

$\quad\quad$ Spontaneous Polariz. $= 3.07 \text{ } \mu C/cm^2$

$\quad\quad$ Curie Constant $\quad\quad = 2950°C$ $\quad\quad$ Quoted from Malek et al.
(1969)

$\quad\quad$ Max. Permittivity $\quad = 2.5 \times 10^4$

$\quad\quad$ Coercive Field $\quad\quad = 590 \text{ V/cm } (25°C)$

Dielectric Constant (23°C) $\quad$ $\varepsilon_{11} = \varepsilon_a = 8.6$

$\varepsilon_{22} = \varepsilon_b = 43$ $\quad\quad$ Jona and Shirane (1962)

$\varepsilon_{33} = \varepsilon_c = 5.7$

The building block of the TGS structure is the glycine molecule, NH_2CH_2COOH. When the amino acid is reacted with sulfuric acid to form the $Gly_3H_2SO_4$ acid salt, two of the amine groups are protonated by the sulfuric acid to form glycinium ions (glycine-I and glycine-III in Hoshino et al's notation) and the remaining glycine assumes a zwitterion form so that the detailed formula could be written $NH_3^+CH_2COOH \cdot NH_3^+CH_2COO^- \cdot NH_3^+ CH_2COOH \cdot SO_4^{-2}$. The glycine molecules are nearly planar and are stacked in the unit cell cross-linked by hydrogen bonds on planes nearly parallel to 010. The glycine-I molecules lie close to the $y = 1/4$ and $y = 3/4$ planes with the molecular plane canted to the crystallographic plane by about 12°. The ferroelectric polarization involves a displacive movement of glycine-I across the $y = 1/4$, $3/4$ planes and thus there is an easy dipole reversal under an applied electric field. Domain switching also requires the exchange of one proton across a short hydrogen bond between glycine III and glycine-II (the zwitterion) thus effectively exchanging their roles. At temperatures above the Curie temperature, a mixture of the two orientations appears so that the $y = 1/4$ and $y = 3/4$ planes become the mirror planes of $P2_1/m$ and the spontaneous polarization vanishes. This basic picture of the TGS structure and of the mechanism of ferroelectric switching and phase transformation was proposed by Hoshino, Okaya, and Pepinsky (1959) and remains the accepted mechanism. New crystal structure refinements (Itch and Mitsui, 1971) have not changed the basic picture.

It is apparent from the structure that the desirable physical

properties are tied to the hydrogen bond network and that the perfection of

this network will be tied to the perfection of the crystal.

More detailed information on the hydrogen bond network and the ferro-

electric mechanisms of TGS and its isomorphis triglycine selenate and triglycine

fluoroberyllate is provided by a series of NMR experiments (Hoshino, 1962;

Lundin et al., 1960; and Blinc and his co-workers, 1961, 1967, 1971-a,

1971-b; Kato and Abe, 1972). These show that the NH_3^+ group is freely rotating

at room temperature. The origin of the spontaneous polarization in the

displacement of glycine-I is confirmed. Likewise confirmed is the Hoshino,

Okaya, and Pepinsky model for the cooperative displacive phase transition of

the order-disorder type including the rotation of the tetrahedral molecule and the

equivalence of glycine-II and glycine-III in the paraelectric state.

TGS crystals cooled through the Curie temperature exhibit the

spontaneous formation of a domain structure in common with other ferroelectrics.

As required by the crystal structure, these are antiphase domains with the

polarization axes oriented along the crystallographic b axis. The domains are

usually circular or elliptical in cross-section and cylindrical or cone-shaped in

long dimension (parallel to b). Domain motion is easy in TGS and the crystals

can easily be poled into single domain form by application of an electric field.

As will be discussed later, the presence of impurities and imperfections in the

TGS crystal affects domain wall motion and thus the switching characteristics. This in turn affects energy losses due to wall motion (Gilletta, 1972-a). There is some evidence of nonferroelectric surface layers on TGS crystals which affect the nucleation of domains during the cooling of the crystal through the Curie temperature (Gilletta, 1972-b); Distler and Kobzareva, 1972). Other blockages on domain wall motion appear in the phenomenon of aging (Stankowska and Stankowski, 1960) observed in TGS that has been subjected to heat treatment or to an a.c. electric field for a considerable period of time. A double hysteresis loop is observed in the aged specimens. The effect can be greatly enhanced by deliberately doping the crystal with $CuSO_4$.

The most significant use for TGS has been in the fabrication of pyroelectric bolometers for infrared detection. This application has been reviewed in comparison with other pyroelectric materials by Beerman (1971). A typical device contains a single crystal active element 1.5 x 1.5 mm in cross-section and 50 m thick. The crystal must be cut perpendicular to the crystallographic b-axis. One of the best such devices examined by Beerman had a detectivity $D^* = 9.2 \times 10^8$ cm Hz $^{1/2}$/w. Kunz (1972) in a critical evaluation of all design characteristics of pyroelectric bolometers succeeded in producing TGS-based devices with $D^* = 1.3 \times 10^9$ cm Hz $^{1/2}$/w by optimizing geometrical and electrical circuit characteristics. The theoretical maximum detectivity for a pyroelectric bolometer operating at $300°K$ is 1.8×10^{10} (calculated by Putley, quoted in Beerman, 1971). It can thus be seen that about

an order of magnitude improvement can be made in infrared sensing devices

of this type by materials improvement. At present, the devices appear to

have been optimized to the materials limit. Improvement can be made by

decreasing the dielectric loss of the material (i.e. decreasing the conductivity)

which implies a reduction in dislocations and volume defects in the crystals.

The response of the detector, of course, is a function of ambient temperature.

The relative response of TGS is compared with several other materials in

Figure 16. It can be seen that the sensitivity falls off very rapidly near the

Curie temperature.

The detectivity of pyroelectric bolometers compares very favorably

with other types of infrared detectors (such as InSb detectors) particularly in

the long wave infrared and they have the tremendous advantage, particularly for

airborne and satellite applications, of not needing cryogenic cooling. Among

the pyroelectric detector materials, TGS continues to be a leading contender

and it is significant that TGS detectors were selected by NASA for use in the

Nimbus E and F series cloud-scanning radiometers.

3. Crystal Growth of Triglycine Sulfate

a. Synthesis of TGS

Triglycine sulfate is almost absurdly simple to prepare. Solutions

of glycine in water and sulfuric acid in water are prepared with volumes

corresponding to the 3:1 stoichiometric ratio. Typically the sulfuric acid

solution is about 50% by weight H_2SO_4 in H_2O. The sulfuric acid is poured into
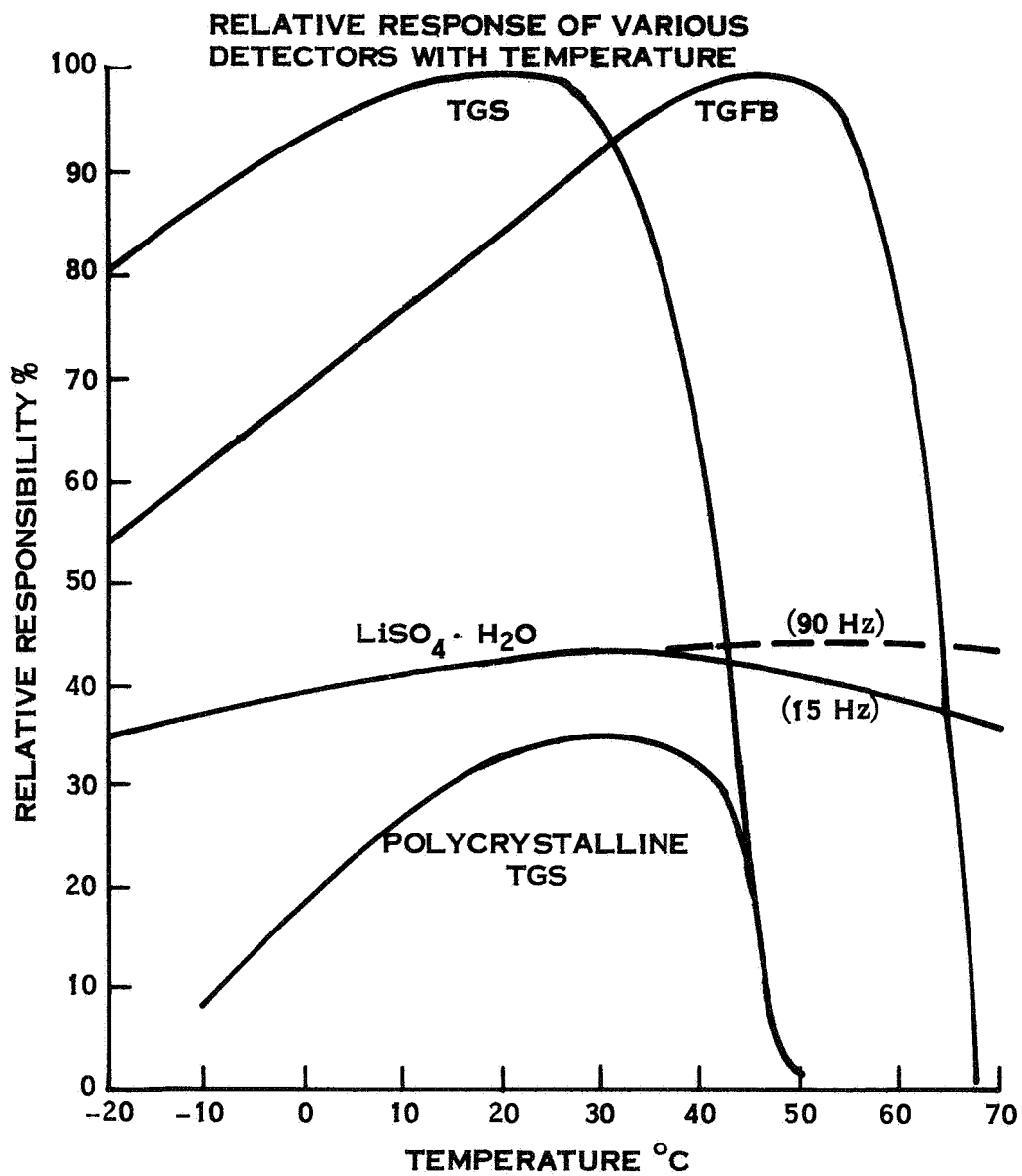
Figure 16. Relative Response of Infrared Detectors Prepared with Active Elements of Triglycine Sulfate, Triglycine Fluoroberyllate, and Lithium Sulfate Hydrate.

67

a hot solution of glycine and the mixture stirred and allowed to cool. Crystals

of triglycine sulfate precipitate out on cooling. These can be filtered off,

redissolved in ultrapure water and again recrystallized. Usually two or three

recrystallizations are carried out to obtain a material of suitable purity before

beginning the crystal growth experiments.

Triglycine sulfate is quite soluble in water. The solubility curve

of Konstantinova et al (1959) is shown in Figure 2. Likewise the slope of the

solubility curve with temperature is high, leading to easy recrystallization by

cooling hot solutions.

Chemical impurities, metal ions in particular, are known to

increase the density of volume defects ($1000 \overset{o}{\text{A}}$ diameter) in TGS crystals

(Moravec, Malek, Sulcek and Hrdlicka, 1970) and, perhaps as a result, to

affect dielectric properties deleteriously (Koldoboskaya, Meleshina, Rez,

Mironova, Gavrilova Safronov, 1967; Moravec and Kanstantinova, 1968;

Hikzer, Malek, Moravec and Strajblova, 1969; Malek, Moravec, Strajblova

and Novotny, 1970; Moravec and Novotny, 1971). Thus, efforts have been

made to determine impurities and to reduce trace element levels to minimal

values. Literature reports on qualitative and quantitative analysis of impurities

seem restricted to determination of the inorganic ions present and their

concentrations, through the use of atomic absorption and atomic emission

spectrophotometry (Malek, Moravec and Strajblova, 1969; Malek, Moravec,

Sulcek and Hrdlicka, 1970; Moravec and Sulcek, 1971). The question of purity

in terms of organic components does not seem to have been considered; the term "impurity" in what follows refers only to inorganic ions.

Synthesis of TGS for crystal growth requires two compounds, sulfuric acid and the amino acid, glycine. As sulfuric acid of very high purity is commercially available (Merck "Suprapur"), research on the effects of reducing impurity levels in TGS have involved treatment of only the glycine used in synthesis. Recrystallization alone results in substantial reduction of impurity concentrations (Malek, Moravec and Strajblova, 1969; Moravec, Malek, Sulcek and Hrdlicka, 1970; Moravec and Sulcek, 1971); treatment by ion-exchange alone results in lower overall impurity levels (Moravec, Malek, Sulcek and Hrdlicka, 1970; Moravec and Sulcek, 1971); and a combination of the two methods would produce glycine of the highest purity (Moravec and Sulcek, 1971). The results of a number of purification schemes are given in Table 6. An analysis of commercially available, semi-conductor purity, glycine is also presented for comparison. The relatively high ion data compiled from Moravec and Sulcek, 1971 and Novotny and Moravec, 1971, level for ion-exchange treated glycine (4.00 ppm) is not due to inefficiency of the ion-exchange resin for removing Fe^{+3} or Fe^{+2}. Removal of 10 ppm introduced Fe^{+3} or Fe^{+2} ions is quantitative. Evidently the iron present in the glycine used is present in a form which is not absorbed strongly by the resin. In any event, the iron impurity would be reduced by one or more crystallizations, and in a usual preparation at least two crystallizations would be standard.

Table 6. IMPURITY LEVELS IN GLYCINE, ppm

Sample	Ca	Mg	Fe	Cu	Na
Not purified	22.00	5.10	9.30	0.90	12.30
Purified on Dowex A-1(H^+ form)	0.67	0.07	4.00	0.07	0.27
Single crystallization	7.20	0.80	0.93	0.07	3.34
Triple crystallization	1.00	0.40	0.7	0.07	1.47
Semiconductor grade	3.32	0.10	2.19	0.07	7.32

Data from Moravec and Sulcek (1971)

b. Crystal Growth Experiments Reported in the Literature

Crystallization from water solutions is the usual method for producing TGS single crystals. A single crystal seed is introduced into a supersaturated solution of TGS, and the rate of growth is controlled by maintaining supersaturation by one of three methods: by slow isothermal evaporation of the solution; by a programmed decrease of the temperature of the solution (in a closed container); or by controlled introduction of additional TGS into the growth solution to replace that deposited on the crystal (Walker-Kohman isothermal crystallizer). Since rapid cooling or heating or indelicate physical manipulation can introduce defects, care must be taken in thermally equilibrating the finished crystal and in handling it.

Proper crystal growth from solution is influenced by several factors:

1. The degree of supersaturation

2. The hydrodynamic conditions present in the crystallizer

3. The temperature of crystallization.

4. The quality of the seed crystal and of the initially deposited material.

There is, in all of the above, a choice of temperature range over which to conduct the experiments. Growth below the Curie temperature results in the formation of polydomain specimens and these appear to be of lower perfection than crystals which are grown above the Curie temperature and then cooled as single crystal masses into the ferroelectric region.

Since the research group at the Institute of Radio Engineering and Electronics in Prague, Czeckoslavakia currently produce the highest quality TGS crystals, it is worth examining their methods in some detail. What follows summarizes two recent communications by Novotny (1971) and Novotny and Moravec (1971).

The key feature of the Czeckoslavakian experiment is to maintain constant supersaturation and constant hydrodynamic conditions for the duration of growth. This is accomplished by a three-cell crystallizer of the Walker-Kohman type illustrated schematically in Figure 17. The outer water-bath is broken into three comparments by dividers and each has its own independent heating and stirring system. The central compartment contains a cylindrical vessel with triglycine sulfate source material. The solution over the source material is stirred and allowed to come to equilibrium saturation at temperature T_s. The saturated solution leaves the source vessel through a microporous filter and enters a temperature stabilizing chamber. From the base of this chamber, a screw pump drives the solution at a flow rate in the range of 0 to 6 liters/hour into the growth chamber which is held at a slightly lower temperature, T_g. The ideal supersaturation at the seed is therefore given by the concentration ratio

$$\sigma = \frac{C_o(T_s) - C_o(T_g)}{C_o(T_g)}$$

72
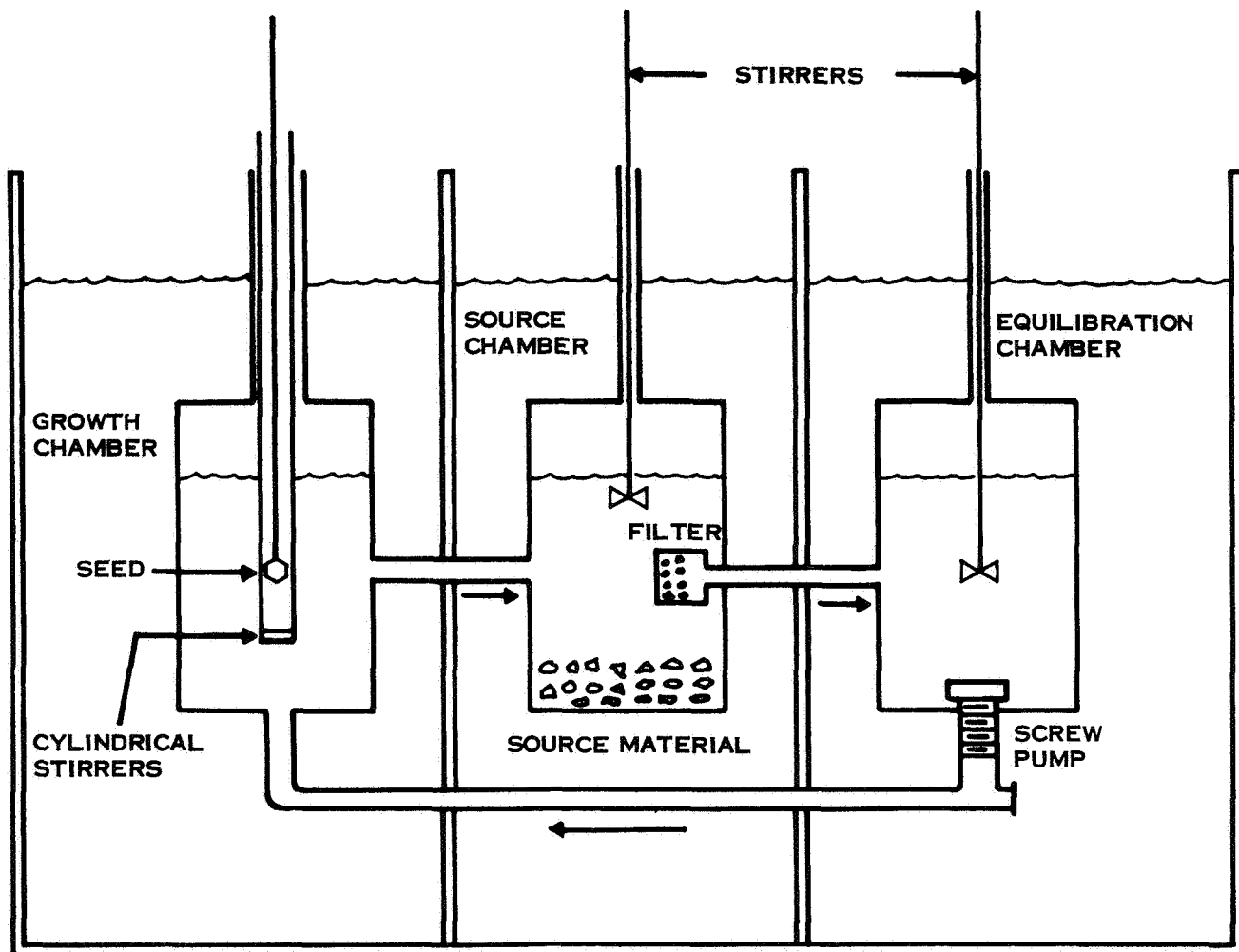
Figure 17. Simplified Schematic of Three Chamber Crystallizers
Used by Novotny (1971).

73

and remains constant throughout the experiment. The background temperature ambient of the bath is likewise kept constant, and mass transport of material from the solution to the growing crystal is driven only by the small temperature gradient $T_s - T_g$ which is on the order of 0.1 degrees. Very accurate overall temperature control is therefore needed and temperature variations in the growth chamber of no more than $0.002^{o}C$ have been claimed.

Hydrodynamical control is obtained by using a cylindrical seed with the cylinder axis parallel to the c-axis of TGS. The seed is surrounded with a cylindrical stirrer which rotates at a constant velocity. The flow dynamics in the zone immediately adjacent to the seed is characterized by a Reynolds number, R_e defined by

$$R_e = \frac{d^2 np}{\eta}$$

where d = diameter of stirrer
       n = number of revolutions
       ρ = density of solution
       η = kinematic viscosity

and from an empircal equation from chemical engineering practice, the thickness of the laminar boundary layer around the seed can be calculated

$$\delta = \frac{a}{0.16} (R_e^{0.62} S_c^{0.5})^{-1}$$

where S_c is the Schmidt number, and a is a constant of the system. An optimized experiment was obtained with $R_e = 3.4 \times 10^3$, $S_c = 1690$, and a = 0.02 meters. The thickness of the boundary layer then calculates as 20μ m and it is this layer that forms the diffusion barrier for crystal growth.

Novotny and Moravec have conducted growth experiments at a variety of supersaturations but maintain the ambient at $52^{\circ}C$, just above the transition temperature. Growth rate data obtained with this apparatus at a saturation level of 6.32×10^{-3} are shown in Figure 18.

Although many laboratories have grown TGS crystals (see particularly the Soviet papers cited in the bibliography) most use either programmed cooling at rates of fractions of a degree per day (which also requires good temperature control on the baths) or isothermal evaporation of the solutions.

An alternative circulating system has been used (Nitsche, 1958) which permits more rapid growth of crystals and is sketched in Figure 19 because of its possible application in an orbiting laboratory situation. A lower chamber contains the source material at some temperature T_s. An upper chamber contains a seed held in solution at slightly lower temperature T_g. The seed is rotated by means of a small motor and the solution is forcibly circulated by means of a magnetic pump. Extraneous crystals that nucleate on the seed or supporting members fall off and drift back into the source chamber where they are reused. As in the Czech experiments, supersaturation and thus growth rate can be controlled by controlling the temperature gradient $T_s - T_g$. Nitsche claims to have grown $2 \, cm^3$ size crystals in 48 hours with this apparatus compared with the ten days or so needed to reach these dimensions
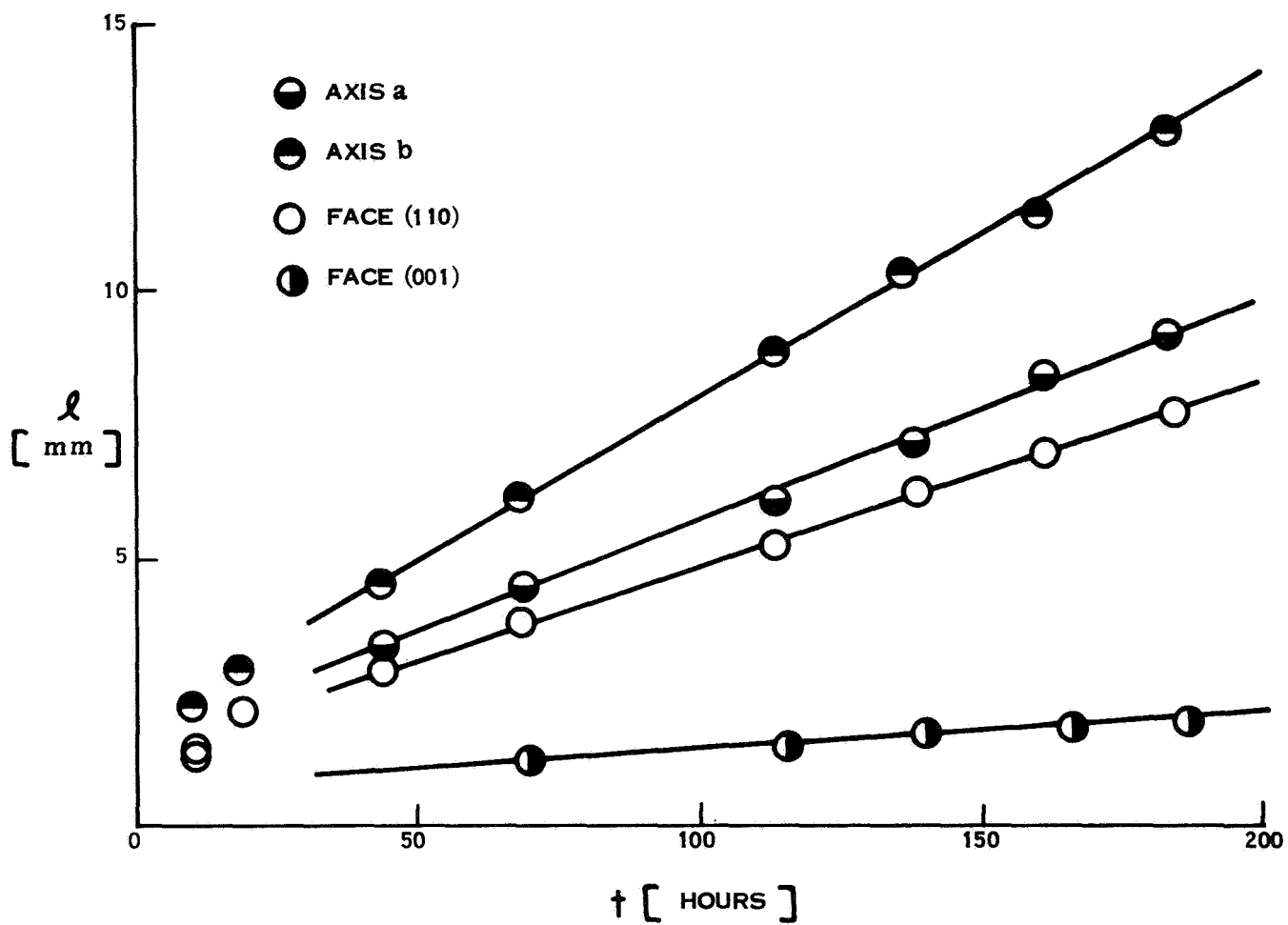
Figure 18. Rate of Growth of Principal Crystallographic Directions
of TGS. (Novotny and Moravec, 1971).
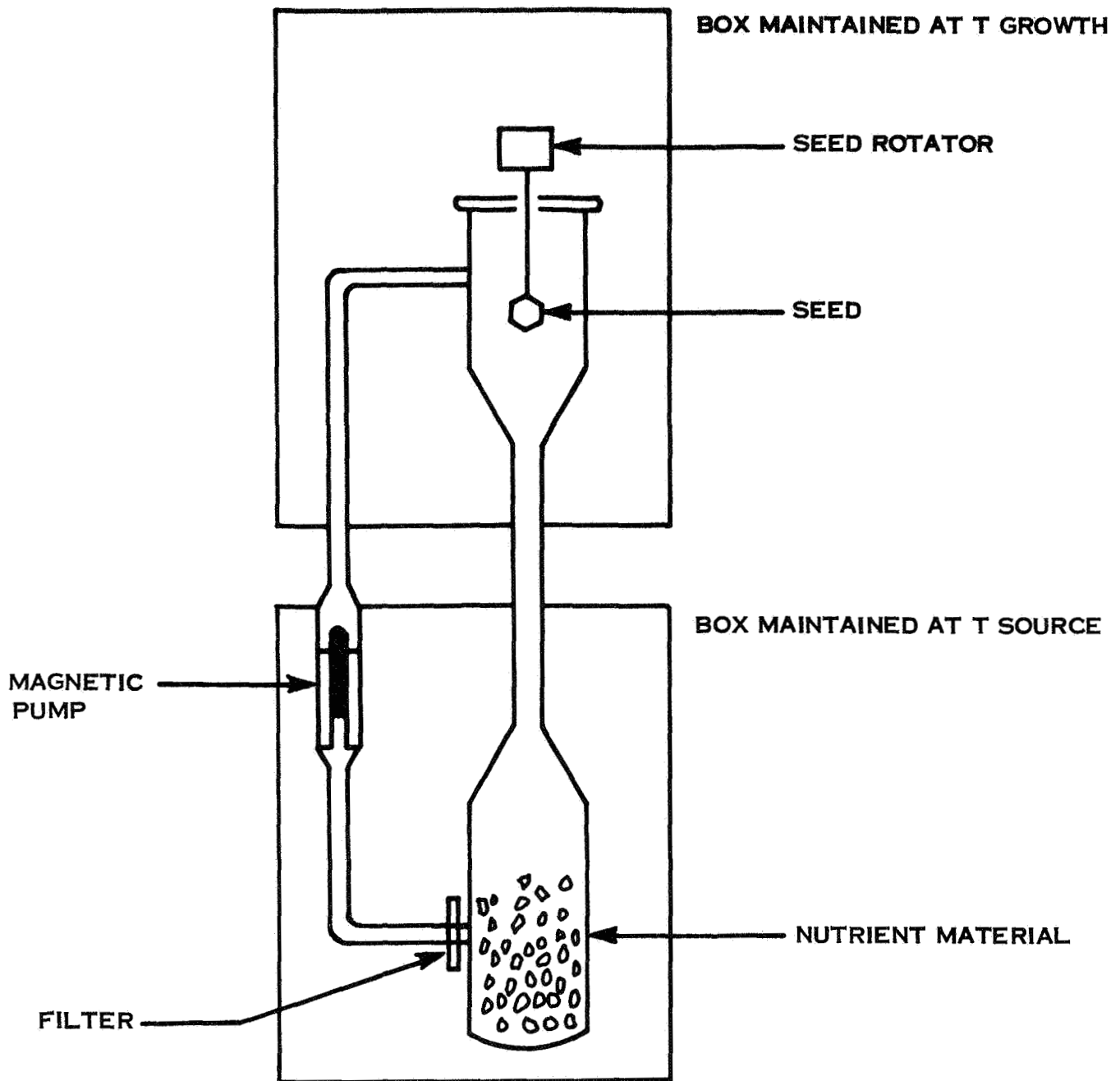
Figure 19. Schematic of TGS Growth Arrangement of Nitsche (1968).

in the Novotny apparatus. Nitsche does not, however, offer any evidence for the degree of perfection of his rapidly grown crystals.

Films of TGS have been grown on silicon substrates by a spinning technique (Keester and Jacobs, 1972). A drop of aqueous solution of TGS placed on the silicon disc leaves a uniform film, approximately 1μ m in thickness, by evaporation when the disc is spun. The film has a two-dimensional spherulitic texture with the fiber axes of the spherulites elongate along the c-crystallographic axis.

c. Growth Experiments by Isothermal Evaporation

To evaluate the difficulties in carrying out aqueous solution growth experiments and to get some first hand experience with the difficulties involved, a series of growth experiments were carried out in the laboratory. We chose to use the isothermal evaporation technique which requires somewhat less stringent temperature control and to keep growth rates from being excessive, a temperature of 30° was chosen. The growth baths were 20 liter glass vats filled with water. Temperature control was obtained by a commercial controller which allowd control to a few tenths of a degree centigrade. The growth vessels were 400 cm^3 "no lip" beakers. All growth runs were seeded but the seeds were not rotated.

Saturated aqueous solutions of TGS were prepared at $35^{\circ}C$. The warm solutions were gravity filtered into a clean dry beaker using fine mesh filter paper. After filtering, the solutions were cooled slowly to $32^{\circ}C$, covered with a clean watch glass to prevent evaporation, and placed securely in the

78

water bath. The solutions reached equilibrium after 24 to 36 hours and the few crystals at the bottom of the beaker ceased growing. The solutions were then transferred to similar vessels and placed back in the bath. Seed crystals were attached to nylon threads, rinsed with demineralized water to prepare a fresh surface, and hung in the decanted solutions. Evaporation control was achieved only by varying the degree of cover on the growth vessel. Bath temperature for the growth runs was maintained at $30^{\circ}C$ and stabilized to less than $0.2^{\circ}C$.

Typical growth runs required periods up to four weeks. Good quality crystals from 0.5 to 2.0 cm in long dimension were obtained. The successful runs produced well faceted crystals without veils and without obvious inclusions of solution. Temperature fluctuations apparently produce veiling and some small included bubbles of solution. About an order of magnitude improvement in temperature control seems to be called for. The principal difficulty was to obtain uniform growth on the seeds. Unless very perfect seed crystals were selected, carefully handled and surface-etched, hollows and voids developed between the seed and the overgrown layers resulting in a highly flawed crystal.

It does not appear to us that the controlled evaporation technique has been fully exploited. Instead of free evaporation into the atmosphere as has been used in the past, a modified design could be developed in which the evaporated solvent would be condensed in a cooler chamber connected to the

growth chamber as a closed system. Evaporation rate could then be controlled by controlling the temperature difference between the two chambers. This design would have more applicability in an orbiting facility than would the open bath technique. The recent work on domain wall motion also suggests that growth temperatures should be kept above the Curie temperature, a regime that results in too rapid evaporation rates with the usual system. Closed systems would not have this limitation.

d. Crystal Habit and Habit Modification

TGS crystals typically grow with an equant prismatic illustrated in Figure 20. The (001) is the slow growth direction as illustrated in Figure 18 and this results in the (001) faces as the dominant facets on most crystals. The fast growth direction is along (010) and as a result b-axis faces are small or absent. This has important implications for the growth of detector crystals. Since the b-axis is the polar axis, one would ideally prefer to grow (010) platelets of the correct dimensions directly to avoid the damage that necessarily results from cutting and polishing operations. An (010) platelet seems highly unlikely from any aqueous growth experiment unless drastic habit modification can be achieved.

Novotny and Moravec (1971-a) showed that the habit is modified by growth at higher supersaturations. As the supersaturation increases the (110) faces become more dominant until at $\sigma = 10^{-2}$, the habit is a prism with (110) side faces and terminated by (001) faces. Similar results can be achieved by deliberately doping the crystals with transition metal ions (Moravec and Novotny, 1971). Ni^{2+} has a relatively minor effect on the usual habit; Fe^{2+}
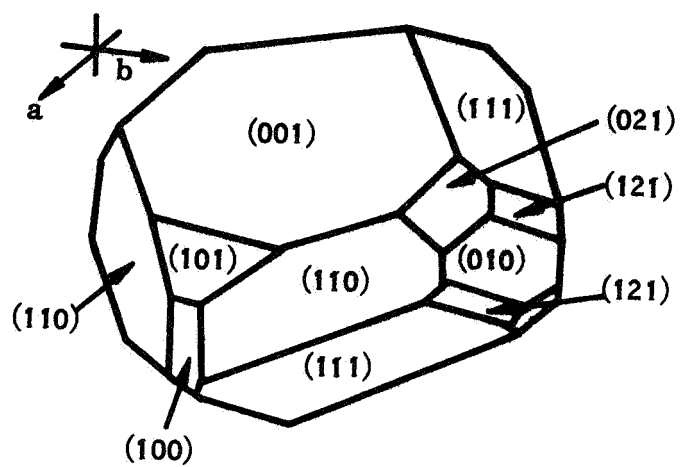
Figure 20. Typical Habit for Triglycine Sulfate Grown from
Aqueous Solution.

completely changes the areas of the faces; and Cu^{2+} produces a prismatic

habit with dominant (110) faces similar to that obtained at high super-

saturations. No dopants thus far investigated produce dominant (010) faces.

4. Modifications of Triglycine Sulfate

It is possible to prepare derivative structures of TGS in which the

physical properties can be varied in a desired manner. Growth of these

materials can be achieved by the methods previously discussed and they form

a set of alternative materials for crystal growth experiments.

a. Irradiation Experiments

It has been found that the X-irradiation of TGS single crystals in the

presence of a strong bias field (on the order of 10 kV/cm) produces a modified

structure with different physical properties. Irradiated crystals are permanently

poled and the hysteresis loops are displaced from the origin with a bias of about

1500 V/Cm. A crystal structure analysis of an irradiated crystal (Fletcher

et al., 1971) indicates that the structure is distinctly different from unirradiated

material. In particular, the planar glycine I molecule is nonplanar in irradiated

crystals, while the nonplanar glycine II molecules have become planar. It

suggests that glycine-I is the zwitterion in irradiated crystals and thus that

there has been a major rearrangement of the hydrogen bond network. Spectro-

scopic studies (Dodd, 1960) indicate changes in ultraviolet absorption which

shows that some kind of defect center must also be created in addition to the

structural changes.

b. Solid Solutions

The triglycine sulfate structure can be deuterated to form a complete series of solid solutions between TGS and $ND_3^+ CH_2COO^- \cdot 2ND_3^+ CH_2COOD \cdot SO_4^{-2}$. The deuteration is accomplished by recrystallizing TGS from aqueous solutions containing a known fraction of D_2O. The principal effect of deuteration on the electrical properties is a shift in Curie temperature from 48.4^o to 60.7^oC in the particular crystals examined (Brezina and Smutnu, 1968).

The tetrahedral molecule in TGS can be substituted by SeO_4^{-2} or by BeF_4^{-2} to form triglycine selenate or triglycine fluoroberyllate, both known ferroelectrics. Solid solutions can also be prepared between the end members. Again the solid solutions exhibit Curie temperatures that vary smoothly and almost linearly with composition. It is therefore possible to prepare crystals with any intermediate Curie temperature (Brezina and Smutny, 1966; Brezina, Safrankova and Kvapil, 1966; Brezina, 1971).

c. Amino Acid Substitutions

Perhaps the most interesting solid solutions synthesized to date are TGS crystals containing small (0.1 to 2.0 mole %) amounts of other amino acids. It was observed by Lock (1971) that substitution of some 2% alanine in TGS produced a crystal that was permanently poled into a single domain state with bias fields as high as 80 kV/cm. The crystal is therefore permanently polarized and the hysteresis loop is displaced from the origin. These crystals

remain pyroelectric to higher temperatures and detectors have been fabricated from them that operate to 70°C with only about a factor of 2 loss in sensitivity from the room temperature values.

The crystals are grown from aqueous solutions in the usual manner but with varying amounts of α-alanine dissolved in the solution. To produce a crystal with 2 mole percent α-alanine in solid solution requires a liquid solution containing about 60% alanine. It is not known at the present time if the solubilities of amino acids observed in the solid state represent equilibrium saturation values (Bye, Whipps and Keve, in press).

The mechanism proposed for this behavior (Keve, Bye, Whipps and Annis, 1971) requires that the substituent amino acid enter the TGS structure by replacement of glycine-I. Domain wall switching is achieved by the displacement of glycine-I across the y = 1/4, 3/4 planes, essentially transforming the molecule into a mirror image of itself. Since glycine has two hydrogens on the carbon atom connected to the amine group, the molecule and its mirror image are equivalent. In alanine one of these hydrogens is replaced with a methyl group so that the molecule and its mirror image are no longer equivalent. This means that polarization reversal cannot take place in the region immediately surrounding the alanine molecule. This in turn sets up a large strain field in the surroundings which locks the domain into a single orientation. The strain field is sufficiently long range that only a small number of dopant amino acid molecules are necessary to permanently pole the crystals.

84

Permanent poling and displaced hysteresis loops are also observed when TGS crystals are doped with other amino acid molecules, providing that the substituent molecule contains an unsymmetrical carbon bonded to the amine group. The effect is observed when the substituent is serine, α-amino-n-butyric acid, or sarcosine. When the substituent molecule has a symmetric carbon next to the amine group as does α-amino-iso-butyric acid and β-alanine, normal hysteresis loops are observed.

Amino-acid-doped TGS has become an interesting material because pyroelectric bolometers can be constructed that will operate at higher ambient temperatures than will undoped TGS and also is useful when permanent poling is desired. The ultimate sensitivity is not much different than that obtained with TGS alone, presumably for the same reasons. Growth and characterization of the amino-acid-substituted material is also of interest for this reason.

5. CHARACTERIZATION OF TRIGLYCINE SULFATE

Triglycine sulfate crystals grown with ordinary care are single crystals, well faceted, and water clear with no visible evidence of large voids, veils, flaws, multiple grains, or surface damage. Discussion is restricted, therefore, to the less obvious structural imperfections. These are mainly of three types: dislocations, domain walls, and volume defects. The techniques most often applied to the characterization of these defects are chemical etching, Lang x-ray topography, and light scattering ultramicroscopy.

a. Dislocations

Dislocation densities in TGS have been reported to vary from $10^4/cm^2$ to $100/cm^2$ depending on the method and conditions of growth. They can be revealed by various etching techniques using etchants mainly based on glacial acetic acid (HAc). A few favorite recipes are given in Table 7. Etch pits in TGS are typically elongated in shape with sharp bottoms. Those etched on (010) faces reveal the two-fold symmetry of the unique monoclinic axis. Etch pits on other faces tend to be elongate but irregular. Pits are observed with the light microscope, although scanning electronic microscope images have also been taken.

An extensive series of etching experiments in this laboratory confirms etch techniques as one of the most useful characterization tools. Scanning electron microscope images are also good representations of the etch pits but do not seem to reveal more information than can be obtained with a good light microscope.

X-ray topography utilizing the Lang camera technique proves a very useful way of determining dislocation distributions in triglycine sulfate crystals. Many studies including those of Konstantinova et al (1972). Miuskov et al (1969) and Malek et al (1972) demonstrate the technique. The

Table 7. ETCHANTS FOR TRIGLYCINE SULFATE

Etchant	Treatment	Reference
Dislocation Etches		
Glacial HAc:H_2O(1.4%):HNO_3 (0.7%)	Immersion for 5-10 sec	Konstantinova (1963)
30 ml glacial HAc 0.0236 gm α alanine 0.04 ml 60% HNO_3	Immersion for 0.5 to 4 min. Reveals both dislocations and domains	Meleshina (1964)
Domain Wall Etches		
Glacial HAc:H_2O(0.7):Zn	1-2 min immersion. Opposite sign domains have different reflectivity	Konstantinova (1963)
H_2O	Water rubbed on crystal surface with cloth	Sawada and Abe (1967)

advantage of topographic technique is that it gives a projection of the three-dimensional distribution of dislocations rather than merely revealing their intersection with a surface as do the etching techniques. From the topographic work comes an important conclusion: the distribution of dislocations in TGS is very non-uniform. Bulk regions of carefully grown crystals may be as low as a few hundred per cm^2. In the boundary region between the seed and the overgrowth, dislocation densities become very high and propagate out into the overgrowth crystals. Volume defects, the included bubbles of mother liquor, act as sources for dislocations. Additional flexing or mechanical strain on the crystal such as might take place during cutting and polishing will then generate many more dislocations from these sources. Dislocation densities become as high as $10^6/cm^2$ in the vicinity of some of these sources.

The dislocation density of TGS crystals is a very sensitive function of the way in which the crystal is grown. In general, it may be said that the slower the growth, the lower the dislocation density. This is illustrated by data from Malek et al (1972) in Figure 21. By carrying out the growth experiments at very low supersaturations, dislocation densities as low as $25/cm^2$ could be achieved and at extremely low supersaturation, dislocation-free regions of crystal were obtained.
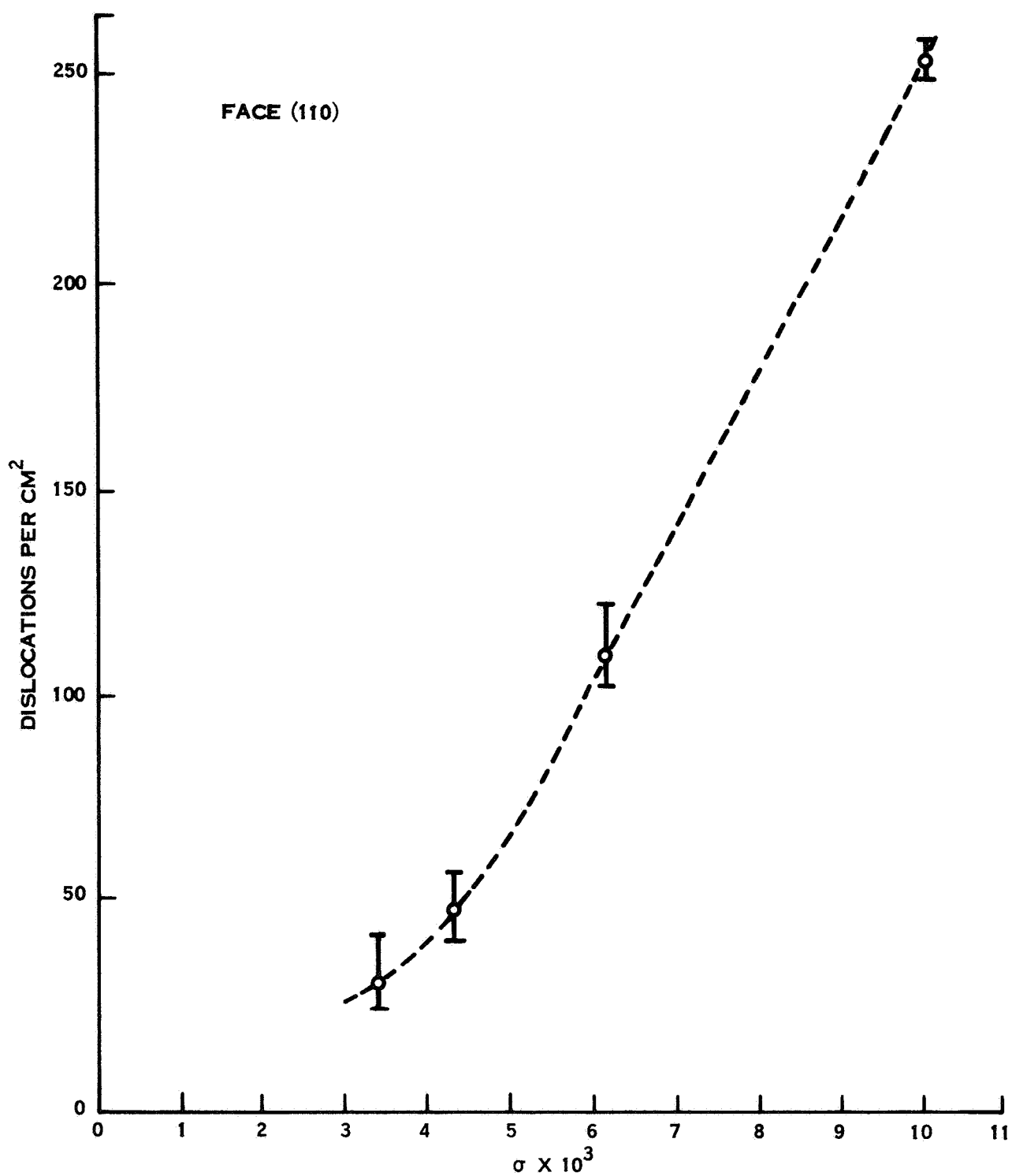
Figure 21. Dislocation Density of (110) Face of TGS as a Function of
Supersaturation of Solution During Growth (Malek, et al, 1972).

b. Domain Walls

Triglycine sulfate possesses only 180° domains and these have the polarization such that the optical indicatrix is invariant under domain switching. This means that domains in TGS differ only in the sign of their polarization; they cannot be observed optically. The domains tend to be elongate regions parallel to the polar b-axis. Domain walls on (010) surfaces tend to be irregular, perhaps roughly elliptical regions. Walls observed on (h0k) sections are seen as stripes parallel to the b-axis.

Because the two ends of the polar domain tend to dissolve at slightly different rates, domain walls can be revealed by etching (Table 7).

Lang camera x-ray topographs can be used to image domain walls just as it will image dislocations (Petroff, 1969). Domain structure can also be revealed by several decoration techniques. Dispersing a platinum sol onto the crystal surface for two or three minutes is a useful way of labeling small domains (Distler and Konstantinova, 1969). The platinum-decorated surface is coated with a thin carbon layer in a vacuum chamber, the water-soluble crystal dissolved, and the platinum-carbon replica floated off. Transmission electron microscope examination of the replica then produces a final picture of the domain pattern. Gold (Distler et al 1968) and silver (sputtered onto the crystal surface) (Konstantinova and Distler, 1970) have also been used with good results.

A rather unique technique for revealing domain walls (Fausek et al, 1966) involves the condensation of isobutyl alcohol vapor. The crystal is placed in a closed chamber connected to a vessel containing saturated vapor of the alcohol (the key feature of the vapor is that it should have a reasonable dew point and should not dissolve the crystal to any appreciable extent). On the other side of the chamber is a rubber bulb for sucking the vapor into the chamber. The process is observed through a light microscope. When the vapor is drawn into the slightly cooler chamber containing the crystal, small liquid droplets (dew) condense on its surface. Because of the difference in polarity, the droplets settle preferentially on the surface and image the characteristic lenticular domains.

c. Volume Defects

Growing crystals of triglycine sulfate tend to include tiny bubbles or droplets of the growth solution (mother liquor) into the overgrown layers. At worst, these appear as veils, surfaces of tiny bubbles that contour the surface at times when the growth rate became too rapid. More typically, however, they appear as individual defects randomly scattered throughout the crystals. The larger voids, those greater than one micron in diameter can be observed and counted in a light microscope since the crystals are transparent. Defects smaller than one micrometer are not observable this way, but are expected to be present in large numbers.

91

Smaller volume defects can be measured by light scattering experiments. Although the roughly spherical volumes are too small to be imaged in a light microscope, the large difference in refractive index between the solution contained in the bubble and the surrounding crystal is sufficient to cause the light to scatter. The minimum diameter defect observable is about 1000 $\overset{o}{A}$ when incoherent sources such as xenon arcs are used; about 100 $\overset{o}{A}$ if a laser source is used.

Moravec et al (1970) and Malek et al (1972) measured actual concentrations of volume defects using a xenon arc in a Tyndall scattering experiment. Since they could correlate the measured volume concentrations directly with their carefully controlled supersaturations and growth rate, their data are plotted in Figure 22. Just as in the case of dislocations, it is seen that the concentration of volume defects increases with increasing growth rate.

To carry out additional light scattering experiments, we reconstructed the light scattering apparatus originally invented by Vand, Vedam, and Stein (1966). The basic principle is the same, that of Tyndall scattering, but an image is produced instead of a scattering intensity measurement. Basically, the crystal to be examined is mounted in the path of a small He-Ne las er (1 to 20 mw) and a focusing lens is mounted on a translation mechanism so that the beam is swept back and forth through the crystal in a horizontal plane. The

92
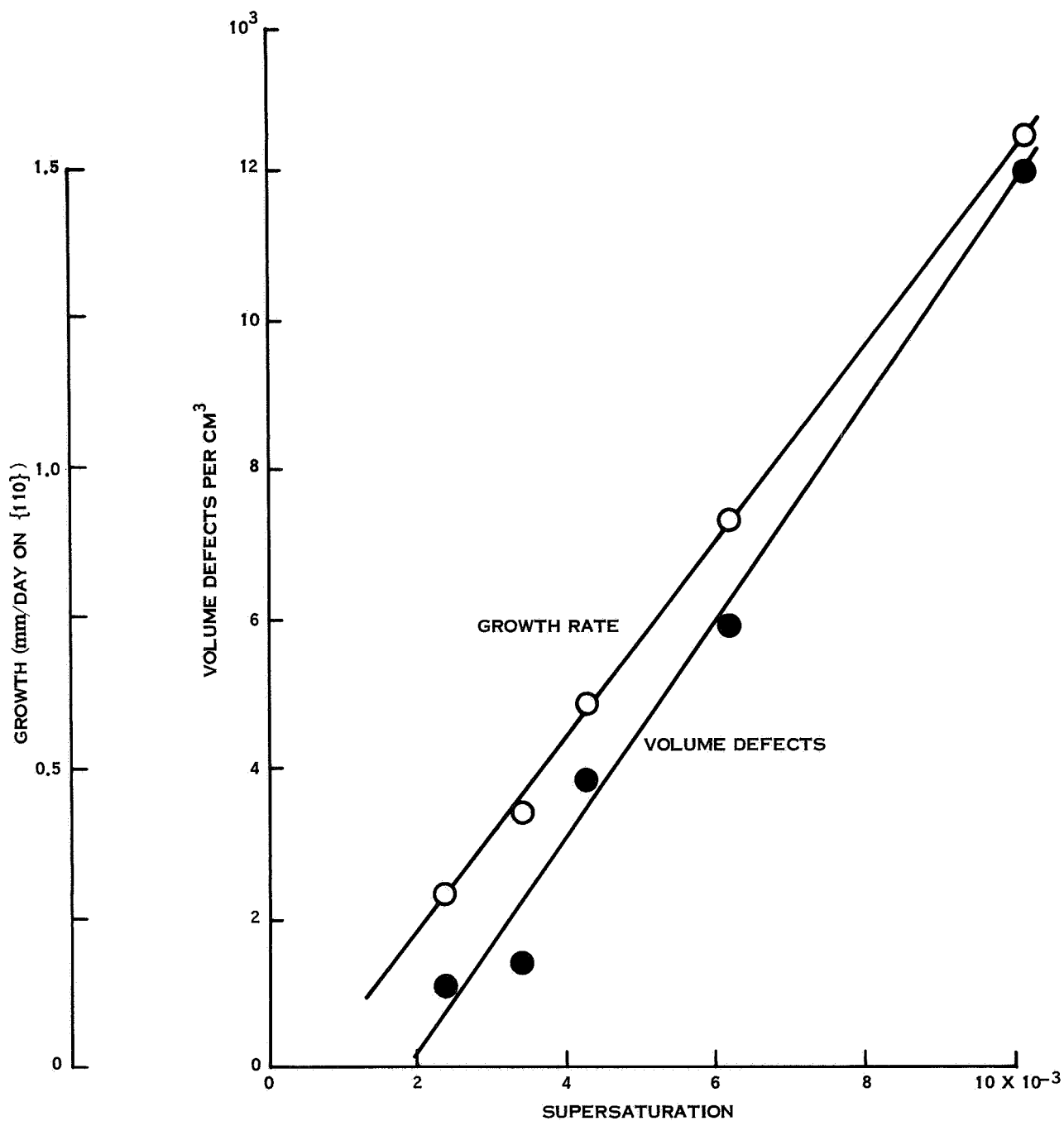
Figure 22. Correlation Between Growth Rate and Concentration of Volume
Defects Determined by Tyndall Scattering Experiments
(Malek, 1972). Growth at 52°C.

crystal is observed in the vertical direction by a camera whose field of view encompasses the plane in the crystal being swept by the laser. Each volume defect in the crystal scatters the laser light giving a flash of light as the beam sweeps by. The camera integrates these flashes and produces an image of the distribution of volume defects with size in the range of a few hundred angstroms and larger. It constructs, in effect, a planar section through the crystal. By translating the crystal along the vertical axis, other sections can be generated and thus a three-dimensional picture of the distribution of volume defects can be constructed.

We achieved results similar to those of the Czech workers for our slow evaporation-grown crystals, although only preliminary measurements were made. Light scattering appears to be an excellent tool for the further investigation of the distribution of volume defects. It is not known at present what influence the volume defects have on the electrical properties of TGS crystals since their presence (Figure 22) is so closely tied to the concentration of dislocations, which do affect the electrical properties. It seems likely that the liquid trapped in these small volumes is the source of much of the dielectric loss that in turn contributes to the loss of effective detectivity in pyroelectric bolometers. This point is worthy of further investigation.

94

d. Characterization of Chemical Purity

The importance of pure starting materials and the significance of impurities in controlling habit and growth was discussed earlier in this report. Impurities have a profound effect on the electrical properties of TGS and these appear to have a threshold at about 1 ppm. Methods for the analysis for metal cations in particular must therefore be effective at this level of concentration. Methods for chemical analysis of trace elements are well established and do not need to be discussed in detail. The most useful of these will be:

i. Emission spectrography specifically set up for metal elements in the ppm region.

ii. Atomic absorption spectroscopy for those elements, alkali metals and alkaline earths for which it is particularly sensitive. This is an exceptionally convenient technique here because the crystals are water soluble and samples are easily prepared. Likewise, metal sensitivities are in the tens to hundreds of parts per billion range compared to emission spectrography where ten ppm is often pushing the limit of sensitivity. Atomic absorption likewise avoids the difficulty of volitilization of the organic molecule in the carbon arc of the emission spectrograph.

iii. Neutron activation analysis will also be a useful technique for many of the metallic trace elements. Its main disadvantage is that the procedures require neutron activation in an atomic pile followed by precision gamma ray spectroscopy. The technique, however, has a sensitivity threshold in the part per billion level for certain elements and would make a valuable adjunct method if available.

iv. Solid state mass spectroscopy also provides a convenient method for the determination of trace element impurites. It does not seem to have been applied to the problem of TGS characterization and was not investigated in the course of the present research.

All of the methods described above have the common disadvantage of being destructive. Crystals grown in an orbiting laboratory facility would be considered valuable specimens. It does appear that representative crystals or fragments must be sacrificed to obtain chemical analyses at the impurity levels deemed pertinent to improved physical properties.

The thresholds described above also largely preclude the effective use of the electron microprobe as a device for either bulk chemical analysis or for the investigation of crystal zoning or impurity concentration during growth. The electron probe has a typical sensitivity of 50 to 100 ppm for most metallic elements under general useage, although with some skill and care sensitivities of 10 ppm can be achieved. This is, unfortunately, about an order of magnitude larger than the purity level desired in the most optimum crystals. The only effective method for the investigation of trace impurity partitioning seems to be an actual dissection of the crystal followed by atomic absorption spectroscopic analysis of the fragments.

6. Influence of Purity and Imperfections on Physical Properties

Many authors have considered the role of chemical impurities, mainly metallic cations, and imperfections, mainly dislocations, on the dielectric properties of TGS. Certainly some combination of these imperfections causes a spread in such parameters as the Curie temperature, the coercive field, the dielectric constant at the phase transition, and the shape of the hysteresis loop. Two mechanisms that have been at least partly identified are the role of impurities themselves, and the role of dislocations, mainly believed to act through the blockage of domain wall motion. In general, it may be said that the details of both electrical effects and of the exact mechanisms that cause them are poorly known. Authors who have addressed these questions include

97

Koldobskaya et al (1967), Malek et al (1970), Malek et al (1969), Meleshina (1970), Helczer (1972), Nakamura and Nakamura (1962), Moravets and Konstantinova (1968), Chynoweth and Abel (1959), and Furuhata (1970).

The effect of impurities is best demonstrated with some data of Malek et al (1969). They deliberately grew crystals from starting materials of high purity, and then other crystals from the same starting materials that had been subject to a three-fold recrystallization. The cation impurities and the variations in the electrical properties are tabulated in Table 8. The variation in dielectric properties is quite apparent, but then it must be noted that the dislocation density of the unrecrystallized material is about two orders of magnitude higher than that of the high quality crystals. The increase in coercive field, in particular, is likely due to impaired domain wall motion due to pinning by dislocations rather than due to the effects of impurity cations themselves.

Other studies of the role of dislocations (particularly that of Nakamura and Nakamura (1962) and the x-ray topographs of dislocations in TGS show quite definitely that dislocations tend to interfere with domain wall motion and thus inhibit switching. Applications, such as memory devices, which require rapid and repetitive domain reversal, will require high perfection crystals.

Table 8. EFFECT OF IMPURITIES ON DIELECTRIC PROPERTIES

(Data from Malek, 1969)

Element (ppm)	Ca	Mg	Fe	Cu	Na
Starting material	22	5.1	9.3	0.9	12.3
3X crystallized	1.0	0.4	0.7	0.07	1.5

Property	TGS from starting material	TGS from recrystallized		
		A	B	C
Dislocations/cm^2	10^4	10^2	10^2	10^2
Number of samples	20	5	10	24
Curie Temperature (°C)	49.19	49.41	49.24	49.23
Max, permittivity	2.5×10^4	5.1×10^4	5.1×10^4	5.3×10^4
Coercive field (V/cm)	590	526	460	460

Pyroelectric applications, however, may be a different story. The pyroelectric bolometer contains a single domain crystal which is kept permanently poled either by the application of a field, or by internal poling through the substitution of another amino acid. It is not clear at this writing whether the detectivity of a pyroelectric bolometer would, in fact, be particularly sensitive to the presence of dislocations in the detector crystal. If the high noise background that limits present detection levels to a tenth of the theoretical limit is really due to the intrinsic resistivity, then impurities trapped along dislocations rather than the dislocations themselves may be the dominant imperfection along with, perhaps, the fluid-filled volume defects.

C. SPECTROSCOPIC CHARACTERIZATION OF TRIGLYCINE SULFATE

1. Introduction

The important physical properties of triglycine sulfate originiate in the long range interaction due to the hydrogen bond network linking the molecules in the unit cell. The state of structural order is therefore of interest and can be investigated by means of infrared and Raman spectroscopy. We undertook a complete re-investigation of TGS with a view to using the spectra as a characterization tool.

Previous studies of the vibrational spectra of TGS have been fragmentary. Dodd (1959) reported single-crystal infrared spectra in the frequency range 4000 to 625 cm^{-1}. The only low frequency IR data available

glycine-III, another glycinium ion are arranged close to each other near the median plane of the crystal (y = 1/2). The planar glycine molecules lie with their planes nearly perpendicular to the polar b-axis. Above the Curie temperature y = 1/4 and y = 3/4 become true mirror planes of space group $P2_1/m$ (C^2_{2h}) and the number of molecules in the unit cell remains the same. No detailed structure analysis of the paraelectric phase seems to be available in the literature and this will require that certain assumptions be made in order to analyze the spectra.

Since triglycine sulfate is a molecular crystal, it is both convenient and valid to separate the vibrational modes into sets of internal modes due to the individual molecules, and translatory and rotational modes due to motions of the molecules against each other. This distribution can be achieved simply by inventorying the degrees of freedom of all atoms in the unit cell and is tabulated in Table 9. Each molecule will contribute 3N-6 internal degrees of freedom where N is the number of atoms in the molecule. The protonated glycinium atoms contain 11 atoms each, the zwitterion 10, and the sulfate ion five. In monoclinic symmetry each degree of freedom will be represented by a distinct normal mode.

It is exceedingly unlikely that all of the 174 internal degrees of freedom will be observable in the IR and Raman spectra. There will be expected 9 bands due to the sulfate ion with a possibility of 18 if the factor group splitting caused by the interaction of the two sulfates in the unit cell is of sufficient magnitude. Deducting these, the remaining internal vibrations are those of the glycine molecules. Although glycine I, II, and III are crystallographically distinct, their internal modes will not differ greatly in frequency. Likewise, the factor group splitting between these units (unless strongly coupled by the hydrogen-bond bridges) will not be large. We would expect, therefore, 9 modes assignable to the sulfate ion and 26 modes assignable to the internal vibrations of glycine.

The spectral bands will fall into three distinct regions. The low frequency region, 10 to 200 cm^{-1} is expected to contain only the transitional and rotational modes. There will be a high frequency region, 2500 to 3500 cm^{-1} that will contain only stretching motions of the hydrogens in the system. There will be an overlap of C-H, N-H, and O-H type vibrations and this region will be of special interest because the nature of the hydrogen

span the range 220 to 30 cm^{-1} (Brodskii and Galanov, 1970). Raman

spectra of TGS over the entire vibrational frequency range at room

temperature were reported by Krishnan and Balasubramanian (1959) and by

Taurel et al (1958). The low frequency range, 10 to 200 cm^{-1} has been the

object of considerable study. Spectra covering the temperature range from

$55^{\circ}C$ (above the Curie temperature) down to liquid nitrogen temperature have

been reported by Savatinova and Simova (1966), Arbatskaya et al (1965), and

Savatinova et al (1971). The most complete data, taken as a function of

temperature on oriented single crystals are those of Quilichini et al (1969).

Brillouin scattering experiments on TGS have been reported by Gammon and

Cummins (1966) from room temperature up through the phase transition.

2. Experimental

Measurements were made on both polycrystal and single crystal TGS

and TGS doped with percent-range concentrations of α-alanine. The

polycrystalline material was obtained by grinding small scraps of single

crystal into powders with a grain size in the range of 10 μm. Single crystals

of both TGS and alanine-doped TGS were grown from water solution by slow

evaporation using methods described previously in the report.

Infrared measurements in the range of 4000 to 275 cm^{-1} were made

on polycrysalline material only using a Perkin Elmer Model 621 spectrometer.

The TGS and ATGS powder was mixed with KBr, and vacuum cold-pressed into transparent pellets for measurement.

Raman spectra were measured on a Spex Model 1401 spectrometer using a 200 mw ionized argon laser source. Both 488 and 514.5 nm excitation wavelengths were available, but most measurements were made using the 488 nm blue line. No obvious evidence of laser damage to the single crystals was noted. Measurements were made on polycrystalline TGS and ATGS by pressing the powder into a thin wafer and mounting the wafer on the goniometer head with double-faced tape. Single crystals were oriented so that the incident beam was along the unique b-axis and scattering could be observed in the ac plane. Measurements were made as a function of temperature using a specially designed cold cell down to liquid nitrogen temperature. Measurements were made above the plane transition temperature by the simple expedient of putting hot water in the same vacuum dewar used for low temperature measurements.

3. Theoretical Analysis

The structure of TGS proposed by Hoshino et al (1959) has been confirmed by more recent structural refinements (Itoh and Mitsui, 1971). The space group of the ferroelectric phase is $P2_1$ (C_2^2) with two formula units in the unit cell. Glycine I (a glycinium ion) and the distorted sulfate ion lie close to the planes $y = 1/4$ and $y = 3/4$. Glycine-II, the zwitterion, and

Table 9. DISTRIBUTION OF DEGREES OF FREEDOM
IN TRIGLYCINE SULFATE

Molecule	Internal	Translational	Rotational
Glycine-I	$2 \times 27 = 54$	6	6
Glycine-II	$2 \times 24 = 48$	6	6
Glycine-III	$2 \times 27 = 54$	6	6
SO_4^{-2}	$2 \times 9 = 18$	6	6
Unit Cell	174	24	24

Total degrees of freedom = 222

Table 10. CLASSIFICATION OF NORMAL MODES IN TRIGLYCINE SULFATE

Irreducible Representation	Total Modes	Internal Modes	Translational Modes	Rotational Modes	Acoustic Modes	Selection Rules
Ferroelectric Phase, C_2						
A	111	87	11	12	1	IR:$E\|\|b$ Raman:$\alpha_{xx}\alpha_{yy}\alpha_{zz}$ α_{xy}
B	111	87	10	12	2	IR:$E{\perp}b$ Raman:$\alpha_{yz}\alpha_{xz}$
Paraelectric Phase, C_{2h}						
A_g	60	48	7	5	—	Raman:$\alpha_{xx},\alpha_{yy},\alpha_{zz},$ α_{xy}
B_g	51	39	5	7	—	Raman:$\alpha_{xz}\alpha_{yz}$
A_u	51	39	4	7	1	IR: $E\|\|b$
B_u	60	48	5	5	2	IR:$E{\perp}b$

bond system should be most obvious there. Finally, the middle frequency region will contain the other internal vibrations of the sulfate and amino acid units and will be the most complicated region of the spectrum.

Analysis of the vibrational behavior of TGS under the restrictions imposed by the crystal symmetry is not very helpful because of the low symmetry of the structure. The point symmetry of the ferroelectric phase is C_2. The factor group analysis is shown in Table 10. There are two irreducible representations, both active in both IR and Raman spectra. Since all atoms are on general positions in the ferroelectric phase, the normal modes are evenly distributed between the two representations. The effect of the symmetry appears only in the polarization properties of the spectra.

The calculations for the paraelectric phase are also shown in Table 10. The creation of the mirror plane induces a center of symmetry in the structure and although no atoms lie on the center of symmetry, the vibrations are split into two sets containing motions that are symmetric and antisymmetric to it. The symmetric modes belong to the irreducible representations A_g and B_g and will be active only in the Raman effect. Those vibrating antisymmetric to the center of symmetry will belong to A_u and B_u and will appear in the infrared.

107

Distribution of normal modes among the four irreducible representations of C_{2h} is to some extent uncertain because of the lack of a detailed structure analysis of the paraelectric phase. The results listed in Table 11 were obtained by assuming that the S-atom and two of the oxygens of the sulfate group have moved onto the mirror plane (which must be true if the mirrors exist). The problem is the glycine-I molecules which are said to be distributed about the $y = 1/4$ and $y = 3/4$ planes in such a way that mirror symmetry is obtained in a statistical sense. For purposes of calculation it was assumed that only the oxygens and carbons of the glycinium ion were in the mirror plane and that the nitrogen and hydrogens project from the plane so that mirror symmetry is obtained statistically.

4. Results

Infrared spectra of TGS and alanine-doped TGS are shown in Figure 23. The spectrum of α -alanine is shown as a comparison. The band shapes and vibrational frequencies are in general in good agreement with the spectra presented by Dodd (1959). The hydrogen stretching region appears as a single intense broad band centered at 3150 cm^{-1}. The remainder of the bands in the spectrum are also diffuse and rather poorly defined compared with the alanine spectrum.

Raman spectra of the middle frequency range are shown in Figure 24. The room temperature data are in fairly good agreement with Krishnan and Balasubramanian's (1959) spectra, except that the laser excited spectra tend
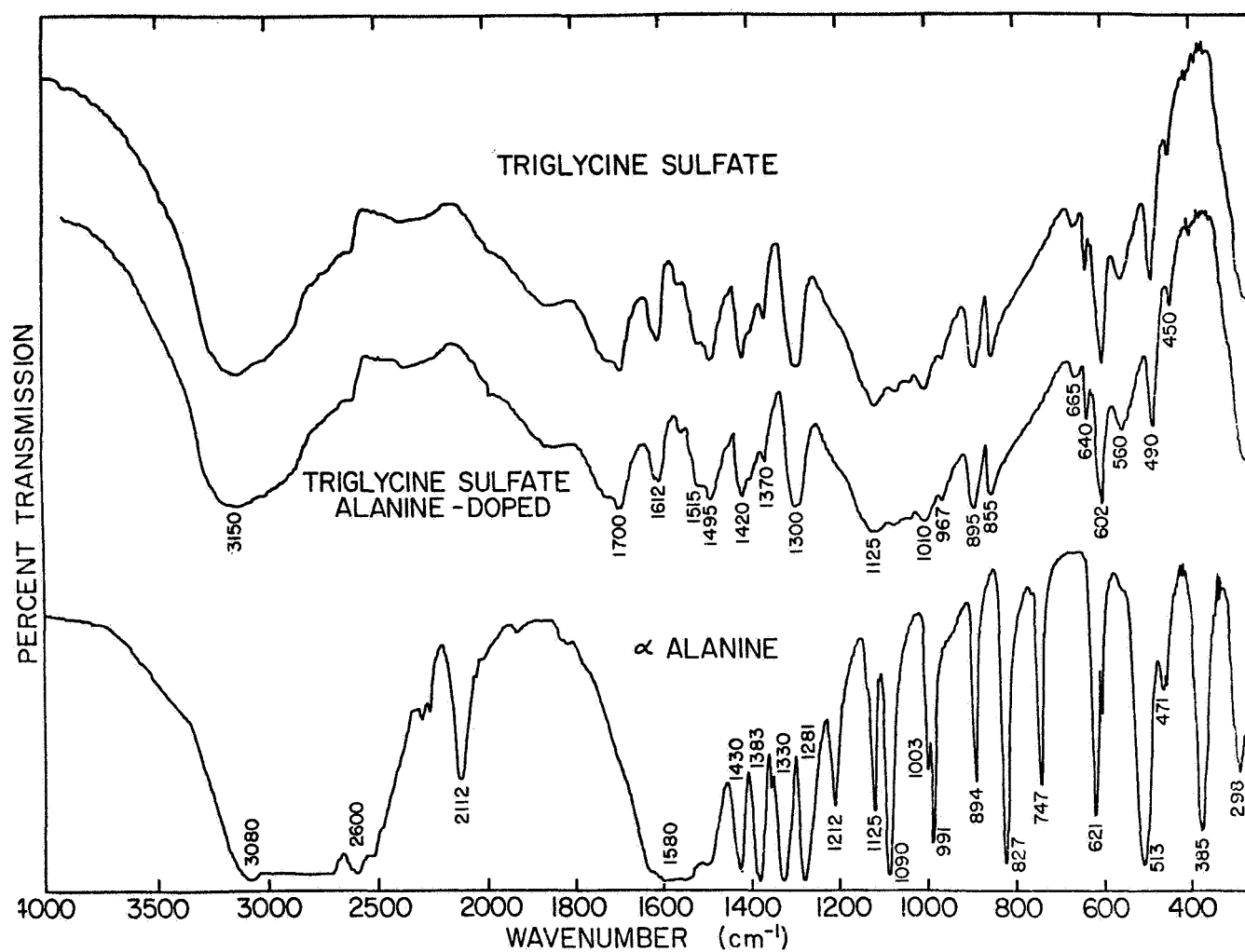
108

Figure 23. Infrared Spectra of Polycrystalline TGS, Alanine Doped TGS, and ∝-Alanine

109
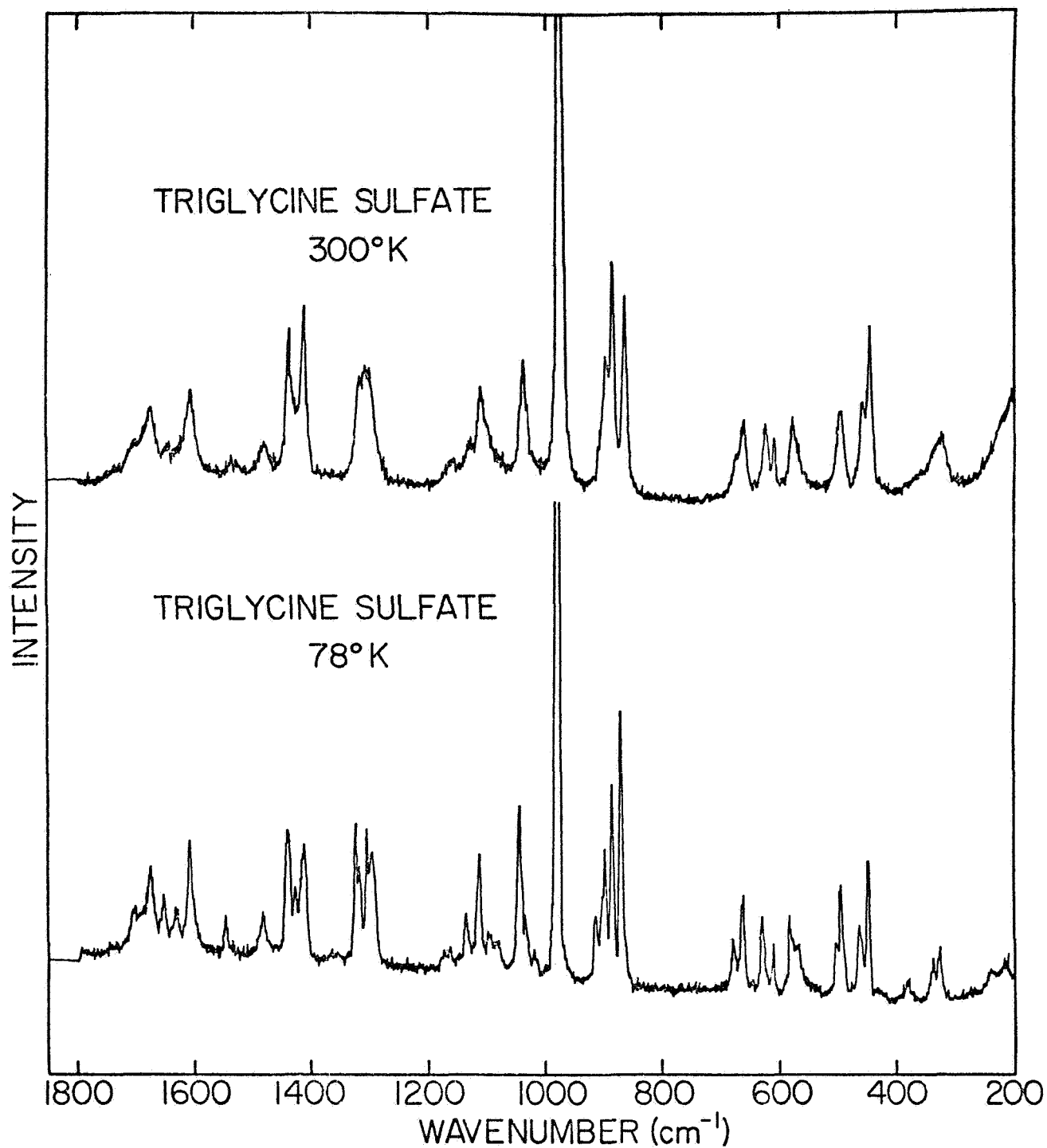
Figure 24. Raman Spectra of TGS at Room Temperature and at Liquid Nitrogen Temperature.

to be sharper and exhibit more detail. Twenty-five distinct bands appear at room temperature. The effect of temperature is rather startling. One would not have expected much temperature dependence from molecular vibrations of this type. At liquid nitrogen temperature, the spectra become much sharper and many of the broader bands split into several components. At least 40 distinct bands appear in the spectrum.

The low frequency lattice vibration region is shown in Figure 25. The effect of temperature here is quite significant although again not as expected. Above the Curie temperature (i.e. $49^{\circ}C$), only 4 bands are identified two sharp bands at 40 and 45 cm^{-1} and two rather broad bands at 68 and 102 cm^{-1}. Several other weak and broad bands can be identified at higher frequencies. When the temperature is lowered through the Curie temperature, the 68 cm^{-1} band splits into two components and a new band becomes discernible at 172 cm^{-1}. The spectra continue to sharpen and the broad bands are resolved into more components as the temperature is lowered still further. At liquid nitrogen temperature, the lowest attainable in our present equipment, at least 15 bands can be identified in the spectra. The spectra of the alanine-doped material is for all practical purposes identical at all temperatures. Small differences visible in Figure 25 are probably due to details of specimen alignment and beam focusing rather than to any real differences between the two materials.
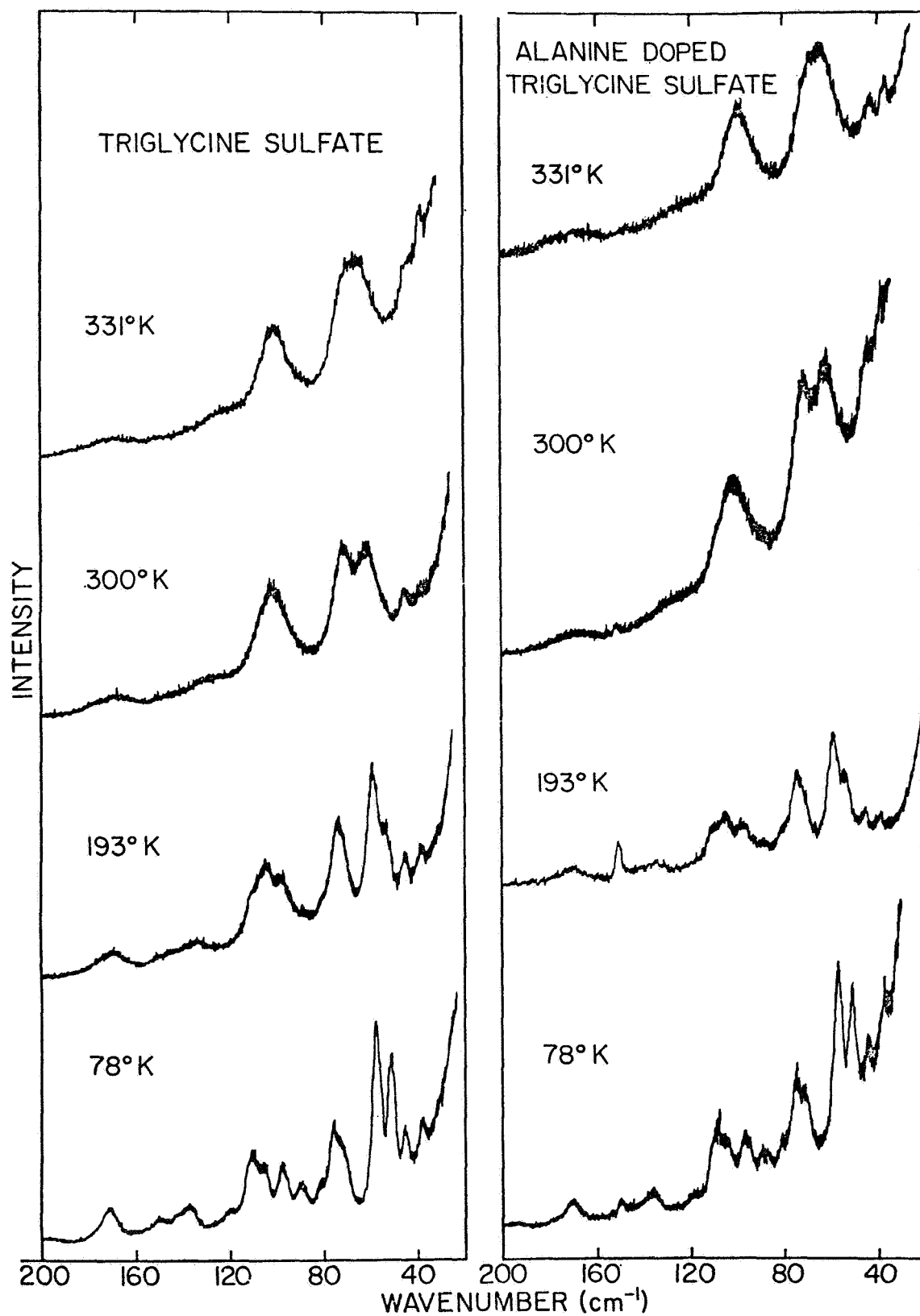
Figure 25. Low Frequency Raman Spectra of TGS and Alanine-Doped
TGS Taken at Various Temperatures.

The high frequency region Raman spectra are shown in Figure 26. The spectra consist of a group of five sharp bands in the region of 3000 cm^{-1} and a broad continuum with a poorly defined maximum at 3135 cm^{-1} at room temperature. The effect of temperature on this set of bands is surprisingly small. The sharp group of bands exhibit some small changes including a splitting of the major peak and some changes in relative intensity. The broad continuum does not change with temperature except for a small shift in the maximum. Again the alanine-doped TGS is essentially identical to TGS itself.

5. Discussion and Conclusions

a) Spectral Changes at the Curie Temperature

The vibrational spectra are in agreement with other physical property measurements concerning the second order, order-disorder nature of the phase transition in TGS. The only evidence for a transition lies in the low frequency lattice bands. At temperatures greater than T_c, glycine-II and glycine-III are equivalent due to the rapid sharing of the connecting hydrogen bond. Statistically at least, whether the molecule on a given site is the zwitterion or the glycinium ion depends on the transient location of the proton. Below T_c, the two molecules are distinct and the lattice mode separates into two components.

Spectra taken of the mid-range and high-range frequencies at temperatures of 55°C (not shown) are essentially identical to the room temperature spectra shown in the figures. The onset of additional disorder with resultant
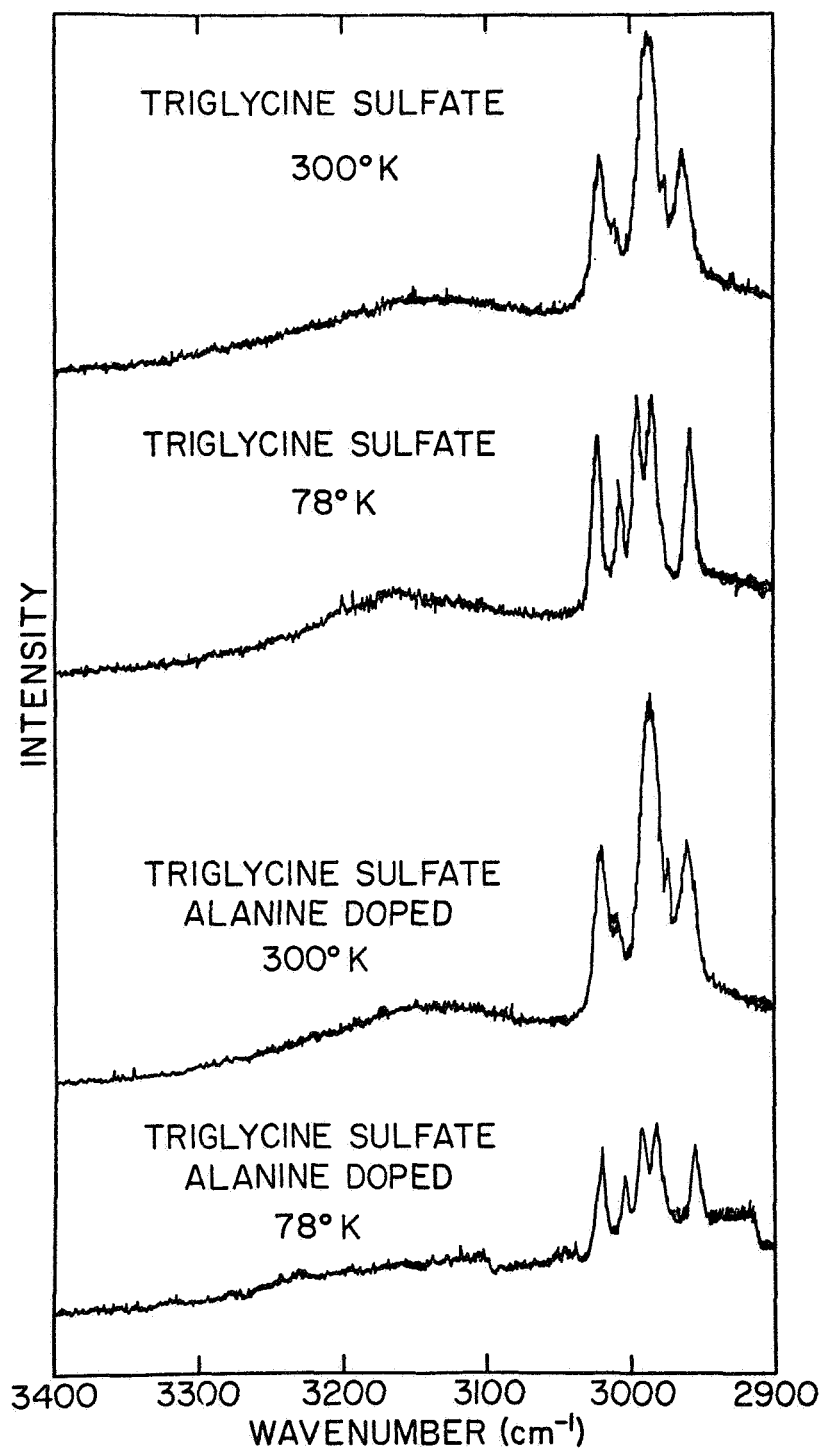
Figure 26. Raman Spectra of TGS and Alanine-Doped TGS in the Hydrogen-Stretching Region.

114

higher symmetry does not reflect in the Raman spectra. In principle, from the factor group calculations, the number of modes should decrease by a factor of two above T_c because of the separation of the vibrations into an IR-active and a Raman-active set. The fact that no such splitting is observed is evidence that the factor group splitting between the two equivalent sets of molecules in the unit cell is very small.

b. Influence of Amino Acid Doping

As shown by the researchers of the Mullard group discussed in an earlier section, the addition of other amino acids in concentrations on the order of one percent produces profound changes in the dielectric properties. The crystals have the property of being permanently poled and there are large changes in the coercive field.

The conclusion to be drawn from the vibrational spectra is that the alanine dopant must act on the scale of the individual domains rather than at a unit cell level. One hypothesis had been that the dopants acted by forcing an ordering of the hydrogen bond network and thus maintained the spontaneous polarization to higher temperatures. Had the hypothesis been correct, the spectra of alanine-doped TGS should have been sharper and better resolved at any given temperature compared with undoped TGS. The observed fact that the spectra of TGS and ATGS are essentially identical in all three measured

spectral regions throughout the investigated temperature range indicates that the alanine must act on the domain structure, not at the molecular level. The stress field around the ananine may indeed block domain wall motion as the Mullard group have suggested but the long-range influence on the hydrogen bond network is small.

c.   Hydrogen Bonds and Structural Ordering

The increase in sharpness of the lattice modes as the temperature is lowered to $78^{\circ}K$ indicates that a considerable ordering of the hydrogen bond network is taking place.   This is also indicated by the additional splitting of the mid-range Raman spectrum into additional sharp lines. The line widths of the lattice bands, even at $78^{\circ}K$ are still somewhat broadened, indicating that some translational disorder is still present.

The most interesting contrast is in the high frequency region. This region contains only hydrogen stretching vibrations of various kinds. Each amino acid molecule contributes 2 C-H stretches, 3 N-H stretches, and 1 O-H stretch for the glycinium ions, none for the zwitterion. These three kinds of hydrogen stretching vibrations lie in slightly different regions but in general we might expect 6 bands from each amino acid molecule for a possible total of 34 in all (deducting 2 O-H stretches for the two zwitterions). Obviously nothing of the kind is observed,   Even allowing for the possibility that the factor group splitting between the two sets of three molecules is likely too

small to observe, 17 bands are expected. In fact only five well defined

bands appear even at 78°K. These are quite likely the C-H stretches

which are not strongly coupled into the hydrogen bond network. The broad

continuum near 3135 cm^{-1} may in fact be the N-H stretches with no

resolvable detail. The extreme broadening implies complete positional

disorder which can be further interpreted as evidence for the free rotation of the NH_3^+

group in all amino acid molecules. Since there is no perceptible change in

this band at the lowest temperature achieved, it may be concluded that the

group is in free rotation at liquid nitrogen temperature. Much lower

temperatures would be required to completely order the structure and produce

sharp spectra.

C. REFERENCES CITED

A.N. Arbatskaya, I.S. Zheludev, U.A. Zirnit, and M.M. Suschinskii (1965)
Low-Frequency vibrational spectra of single crystals of
triglycine sulfate and rochelle salt near phase transitions.
Soviet Phys.-Cryst. 10 270-271.

Henry P. Beerman (1971) Improvement in the pyroelectric infrared radiation
detector. Ferroelectrics 2 123-128.

R. Blinc, S. Detoni, and M. Pintar (1961) Nature of the ferroelectric
transition in triglycine sulfate. Phys. Rev. 124 1036-1038.

R. Blinc, M. Pintar, and I. Zupancic (1967) Deuteron magnetic resonance
study of the O-D--O and ND_3 bonds in ferroelectric triglycine
sulfate. J. Phys. Chem. Solids 28 405-412.

R. Blinc, M. Mali, R. Osredkar, A. Prelesnik, and I. Zupancic (1971) Pulsed
nitrogen-proton double resonance study of the ferroelectric
transition in triglycine sulfate. J. Chem. Phys. 55 4843-4848.

P. Blinc, J. Slak, and J. Stepisnik (1971) ^{9}Be quadrupole perturbed NMR
study of the ferroelectric transition in deuterated triglycine
fluoroberyllate. J. Chem. Phys. 55 4848-4850.

B. Brezina (1966) Concentration dependence of some ferroelectric properties
of solid solutions of TGS with isomorphous substances. Proc.
Internat. Meet. on Ferroelectricity, Prague, Vol. I, pp. 176-181.

B. Brezina and F. Smutny (1966) Some properties of deuterated triglycine
fluoroberyllate single crystals. Proc. Internat. Meet. on
Ferroelectricity, Prague, Vol. I, pp. 182-184.

B. Brezina, M. Safrankova, and J. Kvapil (1966) Ferroelectric properties
of solid solutions of triglycine sulfate and fluoberyllate
crystals. phys. stat. sol. 15 451-456.

B. Brezina and F. Smutny (1968) Preparation of solid solutions of deuterated
triglycine sulfate and concentration dependence of some of their
ferroelectric properties. Czech. J. Phys. B18 393-401.

B. Brezina, E.K. Galanov, N.R. Ivanov, L.D. Kislovskii, and L.A. Shuvalov
(1969) Optical investigations of crystals of solid solutions
of triglycine sulfate with isomorphous compounds. Sov. Phys.-
Cryst. 13 710-712.

B. Brezina (1971) Growth and characterization of solid solutions of ferro-
electric TGS single crystals with isomorphous compounds. Mat.
Res. Bull. 6 401-412.

I.A. Brodskii and E.K. Galanov (1970) Long-wave infrared spectra of ferro-
electric crystals belonging to the triglycine sulfate group in
various phase states. Sov. Phys. Sol. State 11 2005-2008.

**D. Elwell, and B. W. Neate (1971), Mechanisms of Crystal Growth from
Fluxed Melts, J. Mater. Sci. 6, 1499-1519.**

Ryosuke Hoshino (1962) Proton magnetic resonance in $(Glycine)_3 \cdot H_2SO_4$.
J. Phys. Soc. Japan 17 119-123.

Kaxuyuki Itoh and Toshio Mitsui (1971) Refinement of crystal structure of
tri-glycine sulfate. Ferroelectrics 2 225-226.

V.K. Jain (1970) Utilization of space environment for preparing highly
perfect crystals. NASA Tech. Memo. TM X-64564.

F. Jona and G. Shirane (1962) Tri-glycine sulfate and isomorphous crystals.
Chap. II in Ferroelectric Crystals, Pergamon 28-62.

Terumasa Kato and Ryuji Abe (1972) Displacive movement of the radical in
TGS near the Curie point. J. Phys. Soc. Japan 32 717-722.

Kenneth L. Keester and L. Terry Jacobs (1972) Deposition of thin film
ferroelectric triglycine sulfate on silicon. IBM Research
Rpt. RJ 1064, 16 pp.

E.T. Keve, K.L. Bye, P.W. Whipps and A.D. Annis (1971) Structural inhibition
of ferroelectric switching in triglycine sulfate--I. Additives.
Ferroelectrics 3 39-48.

M.F. Koldobskaya, V.A. Meleshina, ∴.S. Rez, Z.A. Mironova, I.V. Gavrilova,
and G.M. Safronov (1967) Change in uniformity of properties
in the body of triglycine sulfate (TGS) crystals depending
on the conditions of growth. Sov. Phys. Cryst. 11 665-671.

V.P. Konstantinova, I.M. Sil'vestrova, and K.S. Aleksandrov (1959) The
preparation of crystals of triglycine sulfate and their physical
properties. Sov. Phys. Cryst. 4 63-67.

V.P. Konstantinova (1963) The application of selective etching to the study
of twin and dislocation structures in triglycine sulfate. Sov.
Phys. Cryst. 7 605-610.

V.P. Konstantinova and G.I. Distler (1970) Defect structure of triglycine
sulfate-TGS. J. PHys. Soc. Japan Suppl. 28 428-429.

V.P. Konstantinova, V.F. Miuskov, and V.M. Maksimov (1972) Defects in
triglycine sulfate crystals. Bull. Acad. Sci. USSR 33 342-346.

R.S. Krishnan (1959) Raman spectrum of crystalline tri-glycine sulphate
$(NH_3CH_2COO)_3H_2SO_4$. Proc. Indian Acad. Sci. 48 138-144.

R. Kunz (1972) Design characteristics of improved capacitive bolometers.
PhD thesis in Solid State Science, The Pennsylvania State University, 137 pp.

P.J. Lock (1971) Doped triglycine sulfate for pyroelectric applications.
Applied Phys. Lett. 19 390-391.

A.G. Lundin, K.S. Aleksandrov, G.M. Mikhailov, and S.P. Gabuda (1960)
Investigation of some ferroelectrics by the method of nuclear
magnetic resonance. Izv. Akad Nauk. SSSR Ser. Fiz. <u>24</u> 1195-
1197.

Z. Malek, F. Moravec, and J. Strajblova (1969) The dielectric properties
of TGS single crystals of improved purity. Czech. J. Phys.
<u>B19</u> 1184-1186.

Zdenek Malek, Frantisek Moravec, Jana Strajblova, and Jan Novotny (1970)
The influence of defects on some dielectric properties of TGS
single crystals. J. Phys. Soc. Japan Suppl. <u>28</u> 430-433.

Z. Malek, M. Polcarova, J. Strajblova, and J. Janta (1972) The effect of
growth rate on the defect structure and dielectric properties
of TGS single crystals. phys. stat. sol. <u>11</u> 195-206.

V.A. Meleshina (1964) Simultaneous selective etching of domains and dislo-
cations and their identification in triglycine sulfate
crystals. Sov. Phys. Cryst. <u>9</u> 304-308.

V.A. Meleshina (1970) Wall motion and nucleation of domains in TGS crystals.
J. Phys. Soc. Japan Suppl. <u>28</u> 357.

V.F. Miuskov, V.P. Konstantinova, and A.I. Gusev (1969) X-ray diffraction
investigation of defects in triglycine sulfate crystals. Sov.
Phys. Cryst. <u>13</u> 791-794.

F. Moravec, Z. Malek, Z. Sulcek, and J. Hrdlicka (1970) The preparation of
pure TGS single crystals and some investigations of their
quality. J. Phys. Soc. Japan Suppl. <u>28</u> 434-436.

F. Moravec and Z. Sulcek (1971) Preparation of pure glycine used for
growing of triglycine sulphate single crystals. Coll. Czech.
Chem. Comm. <u>36</u> 3374-3377.

F. Moravec and J. Novotny (1971) A contribution to the study of the influ-
ence of impurities on the growth and some physical properties
of TGS single crystals. Kristall und Technik <u>6</u> 335-342.

F. Moravets and V.P. Konstantinova (1968) Time variation in the domain width
in triglycine sulfate crystals. Sov. Phys. Cryst. <u>13</u> 221-224.

Terutaro Nakamura and Hanako Nakamura (1962) Domain wall caught in disloca-
tions in ferroelectric glycine sulfate crystals. Jap. J. Appl.
Phys. <u>1</u> 253-259.

R. Nitsche (1958) Growth of ferroelectric crystals of the type $(Glycine)_3H_2AB_4$.
Helv. Phys. Acta <u>31</u> 306-308.

J. Novotny and F. Moravec (1971) Growth of TGS from slightly supersaturated
solutions. J. Cryst. Growth <u>11</u> 329-335.

J. Novotny (1971) A crystallizer for the investigation of conditions of
    growth of single crystals from solutions. Kristall und
    Technik 6 343-352.

J.F. Petroff (1969) Topographic study of 180° domains in triglycine sulfate.
    phys. stat. sol. 31 285-295.

Marguerite Quilichini, Michel Krauzman and Henri Poulet (1969) Spectre de
    Raman du sulfate de glycocolle dans la region des basses
    frequences en fonction de la temperature. Compt. Rend. 269
    774-776.

I. Savatinova and P. Simova (1968) Study of the low frequency Raman spectrum
    of the ferroelectric triclycine sulfate crystal. Opt. and
    Spectros. 24 111-112.

I. Savatinova, P. Simova and M. Markov (1971) Bull. Inst. Phys. and Atomic
    Research 21 251-256.

Akikatsu Sawada and Ryuji Abe (1967) The formation mechanism of domain etch
    patterns in triglycine sulfate crystals. Jap. J. Appl. Phys.
    6 699-707.

J. Stankowska and J. Stankowski (1960) Aging process in triglycine sulfate.
    Proc. Phys. Soc. 75 455-459.

Lucinne Taurel, Claude Delain and Chantal Guerin (1958) Spectre Raman du
    sulfate de glycocolle $(CH_2NH_2CO_2H)_3SO_4H_2$ a temperature ordinaire.
    Compt. Rend. 246 3042-3044.

D.R. Ulrich, A.M. Chung, C.S. Yan and L.R. McCreight (1972) Economic analysis
    of crystal growth in space. General Electric Co. Space Div.
    Final Rpt. on Contract NAS 8-27942, 115 pp.

V. Vand, K. Vedam, and R. Stein (1966) The laser as a light source for
    ultramicroscopy and light scattering by imperfections in crystals.
    Investigation of imperfections in LiF, MgO, and Ruby. J. Appl.
    Phys. 37 2551-2557.

K.L. Bye, P.W. Whipps, and E.T. Keve (1973) High internal bias fields in
TGS(1-alanine). Ferroelectrics (in press).

A.G. Chynoweth and J.L. Abel (1959) Built-in nucleation sites in triglycine
sulfate. J. Appl. Phys. $\underline{30}$ 1615-1617.

I.M. Dion (1959) Monoclinic glycine sulfate: Optical parameters. Acta Cryst.
$\underline{12}$ 259-260.

G.I. Distler, V.P. Konstantinova, Y.M. Gerasimov, and G.A. Tolmacheva (1968)
Interaction of defect and domain structures of triglycine
sulphate crystals in ferroelectric and paraelectric states.
Nature $\underline{218}$ 762-765.

G.I. Distler and V.P. Konstantinova (1969) Electron-microscope study of the
domain structure of triglycine sulfate crystals by the electric-
decoration method. Sov. Phys. Cryst. $\underline{13}$ 536-539.

G.I. Distler and S.A. Kobzareva (1972) Special electrical properties of
regions near domain walls in triglycine sulfate crystals. Sov.
Phys. Solid State $\underline{13}$ 2366-2367.

D.M. Dodd (1959) The infrared absorption characteristics of ferroelectric
triglycine sulfate. Spectrochim. Acta $\underline{15}$ 1072.

D.M. Dodd (1960) Effects of x-irradiation on the near ultraviolet absorption
spectrum of ferroelectric triglycine sulfate. Spectrochim.
Acta $\underline{16}$ 413-418.

Jan Fausek, M. Safrankova and J. Kaczer (1966) A new dew method for revealing
domains. Appl. Phys. Lett. $\underline{8}$ 192-194.

S.R. Fletcher, A.C. Skapski, and E.T. Keve (1971) Crystallographic studies
of irradiation/field treated triglycine sulfate: a new structure
form. J. Phys. C: Solid State Phys. $\underline{4}$ L255-L258.

Yoshio Furuhata (1960) Growth regions in ferroelectric tri-glycine sulfate
crystals. J. Phys. Soc. Japan Suppl. $\underline{28}$ 425-427.

Robert W. Gammon and Herman Z. Cummins (1966) Brillouin-scattering dispersion
in ferroelectric triglycine sulfate. Phys. Rev. Lett. $\underline{17}$ 193-
195.

F. Gilletta (1972) Dielectric relaxation in multi-domain TGS single crystals.
phys. stat. solidi $\underline{12}$ 143-151.

F. Gilletta (1972) Evolution of ferroelectric domains in TGS single crystals.
phys. stat. solidi $\underline{11}$ 721-727.

B. Hilczer (1969) Effect of impurities on polarization switching in triglycine
sulfate crystals. Bull. Acad. Sci. SSSR, Phys. Ser. $\underline{33}$ 1023-1025.

S. Hoshino, Y. Okaya, and R. Pepinsky (1959) Crystal structure of the ferro-
electric phase of $(Glycine)_3 \cdot H_2SO_4$. Phys. Rev. $\underline{115}$ 323-330.

J. Novotny (1971) A crystallizer for the investigation of conditions of growth of single crystals from solutions. Kristall und Technik 6 343-352.

J.F. Petroff (1969) Topographic study of 180° domains in triglycine sulfate. phys. stat. sol. 31 285-295.

Marguerite Quilichini, Michel Krauzman and Henri Poulet (1969) Spectre de Raman du sulfate de glycocolle dans la region des basses frequences en fonction de la temperature. Compt. Rend. 269 774-776.

I. Savatinova and P. Simova (1968) Study of the low frequency Raman spectrum of the ferroelectric triclycine sulfate crystal. Opt. and Spectros. 24 111-112.

I. Savatinova, P. Simova and M. Markov (1971) Bull. Inst. Phys. and Atomic Research 21 251-256.

Akikatsu Sawada and Ryuji Abe (1967) The formation mechanism of domain etch patterns in triglycine sulfate crystals. Jap. J. Appl. Phys. 6 699-707.

J. Stankowska and J. Stankowski (1960) Aging process in triglycine sulfate. Proc. Phys. Soc. 75 455-459.

Lucinne Taurel, Claude Delain and Chantal Guerin (1958) Spectre Raman du sulfate de glycocolle $(CH_2NH_2CO_2H)_3SO_4H_2$ a temperature ordinaire. Compt. Rend. 246 3042-3044.

D.R. Ulrich, A.M. Chung, C.S. Yan and L.R. McCreight (1972) Economic analysis of crystal growth in space. General Electric Co. Space Div. Final Rpt. on Contract NAS 8-27942, 115 pp.

V. Vand, K. Vedam, and R. Stein (1966) The laser as a light source for ultramicroscopy and light scattering by imperfections in crystals. Investigation of imperfections in LiF, MgO, and Ruby. J. Appl. Phys. 37 2551-2557.

V. CRYSTAL GROWTH FROM GLASS SOLVENTS

The growth of high temperature electronic ceramic crystals from solution is one method of crystal preparation which would benefit from the weightlessness of space. Crystal growth from solution is based on the fact that it is possible to dissolve significant amounts of various oxidic compositions in certain molten fluxes. The amount of material in solution increases as the temperature is raised. When such a solution is slowly cooled, the saturation of the solute increases until spontaneous nucleation takes place; the nuclei then grow as material is deposited on them during further cooling. Such crystallization presumably can be continued until the solvent phase has been cooled almost to its solidification point, or freezing temperature.

When growing crystals of electronic ceramic compositions from a molten solution, as opposed to growing from a straight melt, most investigators to-date have used molten salts and simple oxides as the solvents. Potassium fluoride, bismuth oxide, lead oxide, boron oxide and barium chloride are among the materials so used. For space processing, however, various more complex solvents, chiefly silicate glasses, should be more effective. Molten silicate glasses should have much higher viscosity than molten salts, and have less tendency to wet and creep along the walls of the platinum crucible. The glasses would be more stable, chemically, having lower volatility and less tendency to change in composition during the relatively long time allotted to the crystallization procedure. Silicate glass melts show a slow change of viscosity with change in

temperature, in comparison with the abrupt changes experienced with molten salts. The groundmass, being glassy and viscous, would inhibit the formation of spontaneous nuclei during cooling. In addition, the obvious advantage of all the molten solvent systems, that one can prepare a crystal from solution at a convenient temperature well below the melting point of that composition of crystal, must not be overlooked.

In this section the development of glass solvents for the seeded growth of lithium niobate, and potassium sodium niobate and lead germanate crystals is discussed. Crystal growth experiments with lithium niobate and potassium sodium niobate were conducted and the results are presented. The crystal growth of lead germanate from glass solvent was not initiated during this contractual period.

A.   Fused Solvent Development

1.   Considerations in Solvent Selection

It is important to keep several considerations in mind when selecting the solvents for crystal growth. The solvent must be compatible with the crystal phase to be grown. That is, the solvent must be capable of dissolving a significant amount of the desired composition and should yield, during the exsolution or devitrification heat treatment, an adequate quantity of crystalline material consisting essentially of only the anticipated crystal phase. X-ray

diffraction patterns have been taken of the glassy solutions; these patterns indicate that the approved compositions are completely amorphous (non-crystalline) as first made. No crystal phases were detected. After heat treatment, the presence of the desired crystal phase was shown by the new x-ray patterns. If the amount of crystal phase was too small, it was necessary to modify the solvent composition to correct the situation. Finally, it has been found important to control the viscosity of the molten solution of solvent plus solute. In general, the higher the viscosity the more closely can one simulate the growth conditions of space. In other words, the higher the viscosity the smaller are the convection currents in the crucible, characteristic of terrestrial crystal growth.

The viscosity of the molten solution is a function of both the composition and the temperature of the melt. With some compositions, particularly those high in SiO_2, the melt attains a high viscosity gradually during cooling from the molten condition. The viscosity of the melt changes slowly over an appreciable temperature range, and this is a desirable relationship. With other compositions (many fluorides, for example) the viscosity of the melt remains low (that is, the fluidity is high) during cooling until the solidification temperature is reached, when the solution quickly "freezes". This latter is an undesirable condition. The ability to draw continuous glass filaments is considered a good indication that the viscosity range is within the desired limits and that the temperature range is adequately broad since successful drawing of continuous filament and

crystal growth from a molten solvent require similar temperature-viscosity relationship.

In the interest of causing the desired crystal phase to appear from the molten solution, two general principles of crystal chemistry have been followed: (1) the solvent glass is designed to contain to the largest extent possible ions common to those of the desired crystal phase, and (2) the glass-forming ingredients of the solvent consist of atoms whose size does not permit them to fit in the structure of the anticipated crystal phase. The common-ion effect increases the amount of material exsolved and the lack of ion size fit contributes to the purity of the precipitate.

For example, in growing crystals of potassium sodium niobate one uses, for the solvent, potassium sodium silicate. The potassium and sodium provide the common-ion effect, while the size of the Si^{4+} is such that it cannot proxy for Nb^{5+} in the $K_{0.5}Na_{0.5}NbO_3$ crystal. Likewise, in growing lithium niobate the glass solvent is a lithium silicate. Lead germanate $(Pb_5Ge_3O_{11})$ is grown in a lead borate glass. A silicate glass cannot be used here because of the ease with which Si^{4+} can replace Ge^{4+} in the crystal structure. In this instance, the borate atom does not enter the lead germanate crystal. However, in the growth of $Pb_5Ge_2SiO_{11}$ a limited amount of Si can be tolerated in the composition of the solvent.
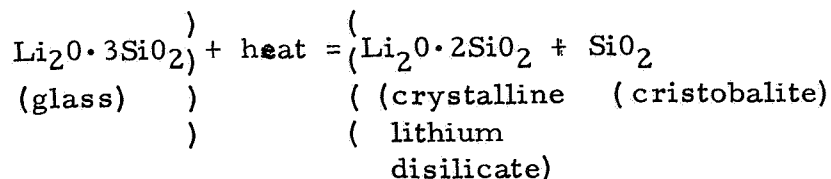
2.   Lithium Niobate

a.   Binary Solvents

The following fused solvents were investigated in connection with the growth of crystals of lithium niobate:

$$Li_2O \cdot 3SiO_2$$

$$Li_2O \cdot 2SiO_2$$

$$Li_2O \cdot 1.5SiO_2$$
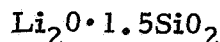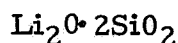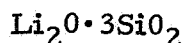
Devitrification studies were made first of lithium disilicate ($Li_2O \cdot 2SiO_2$) and lithium trisilicate ($Li_2O \cdot 3SiO_2$) alone, without lithium niobate. Both glasses were crystallized extensively at $700^\circ C$. In both instances the primary crystallization was of $Li_2O \cdot 2SiO_2$. However, in the trisilicate, excess silica crystallized in the form of cristobaliate:

$$\left. \begin{array}{l} Li_2O \cdot 3SiO_2 \\ \text{(glass)} \end{array} \right) + \text{heat} = \left(\begin{array}{l} Li_2O \cdot 2SiO_2 \quad + \quad SiO_2 \\ \text{((crystalline} \qquad \text{(cristobalite)} \\ \text{(lithium} \\ \qquad \text{disilicate)} \end{array} \right.$$

Four compositions were made up:

FF-60	LiNbO$_3$	40 w/o		FF-62	LiNbO$_3$	30 w/o
	Li$_2$O·3SiO$_2$	60 w/o			Li$_2$O·2SiO$_2$	70 w/o
FF-61	LiNbO$_3$	40 w/o		FF-63	LiNbO$_3$	30 w/o
	Li$_2$O·2SiO$_2$	60 w/o			Li$_2$O·3SiO$_2$	70 w/o

On devitrifying composition FF-61 at 600°C, lithium niobate appeared with a small amount of lithium disilicate. At 700° the amounts of both phases appeared to be greater, but $LiNbO_3$ was still by far the predominant phase. Dielectric constant measurements earlier had indicated that more niobate was precipitated from FF-60 and FF-61 than from FF-62 and FF-63, and that more niobate appeared from the $Li_2O \cdot 2SiO_2$ fused solvent than from the $Li_2O \cdot 3SiO_2$ solvent at the same concentration ratios. Favorable temperature-viscosity relationships were indicated by the fact that it was possible at that time to pull fibers of FF-60 and FF-61 from the melt.

b. **Binary and Ternary Glass Solvent Analysis**

Solvents in the $Li_2O \cdot Al_2O_3 \cdot SiO_2$ ternary system were investigated concurrent with binary $Li_2O \cdot SiO_2$ system solvents. From a crystal chemistry point of view the glass solvent system must meet the following requirements:

1. The solvent stoichiometry must be compatible with the $LiNbO_3$ perovskite structure.

2. The solvent must reduce the lowest fusion or melting temperature of the total composition to less than 1000°C. This is the upper temperature limitation imposed by the M518 furnace.

3. The chemical nature of the glass solvent should be reactive to etchants which are inert relative to $LiNbO_3$.

The stoichiometry of the glass solvent must be favorable for the crystallization of $LiNbO_3$. The network former and network modifier content and ratio must be chosen to prevent reaction of the Li_2O and Nb_2O_5 with the network formers during glass formation[*]. These reactions result in destruction of the octahedral coordination of the perovskite structure in solution and the crystallization of non-stoichiometric phases during recrystallization or seeded crystal growth.

The solvents were studied by the infrared powder spectroscopy and differential thermal analysis of glass. The reaction of Li_2O and Nb_2O_5 with the glass forming oxides can be determined from the fundamental cation-oxygen vibration of the octahedral structural unit and their resultant characteristic absorption bands. Differential thermal analysis (DTA) reveals the exotherms of recrystallization and the associated melting endotherms. The higher temperature endothermic reactions indicate the temperature range for crystal processing; the lower temperature exotherms verify if there has been reaction of the perovskite with the network former(s) since phases other than $LiNbO_3$ and the glass forming compound will crystallize. This will be evident by additional exothermic reactions.

(*) Elements or oxides which seem indispensable to the formation of oxide glasses are referred to as "glass formers" or network formers. They fit into the glass network sites. This can be thought of as being analogous to ions fitting into lattice sites in a crystal structure. Network modifiers are devoid of the glass forming tendency, the designation connotes that such oxides modify the properties of the glass. In making an analogy with crystals, the cation of an oxide modifier would fit into an interstitial position. Network formers include SiO_2, B_2O_3, GeO_2 and P_2O_5; modifiers include Li_2O, K_2O, Na_2O, BaO, MgO and CaO.

Work was conducted on the differential thermal analysis of compositions consisting of by weight 40% $LiNbO_3$ - 60% $Li_2O \cdot 2SiO_2$ (FF-61), 40% $LiNbO_3$ - 60% $Li_2O \cdot 1.5SiO_2$ (FF-64), 70% $LiNbO_3$-30% SiO_2 (LNS-1), and 80% $LiNbO_3$ - 20% $Li_2O \cdot Al_2O_3 \cdot 8SiO_2$ (LNAS-2). The thermograms are shown in Figure 27. The profiles of the binary solvents are similar, showing an annealing endotherm at $530^\circ C$, a recrystallization exotherm at $750^\circ C$, and a melting endotherm at $980^\circ C$. These are in agreement with earlier work reported by Ulrich for the lithium niobate-lithium silicate system [*]. The DTA shows (1) the Li_2O/SiO_2 ratio in the 1.5 to 2.0 range does not reduce the processing temperature from $980^\circ C$; (2) there is no reaction between lithium niobate and the low silica content lithium silicates. However, further refinement of the method is needed to detect a small exothermic reaction in the 530°-$700^\circ C$ range.

The thermograms of the LNAS-2 and LNS-1 glasses are shown in Figure 27. LNAS-2 shows exotherms of crystalliz ation at 625° and $725^\circ C$ and the associated endotherms of melting between 1100°-$1200^\circ C$. LNS-1 shows exothermic reactions at 675° and $960^\circ C$ with endotherms between 1100-1200$^\circ C$. There is only a $50^\circ C$ reduction in the low temperature exotherm by using a ternary solvent as compared to SiO_2. There is a significant reduction in the

[*] Ulrich, D.R., U.S. Patent No. 3,649,353; NASA Working Paper 481, 1966, pp. 55, 56 and 87.

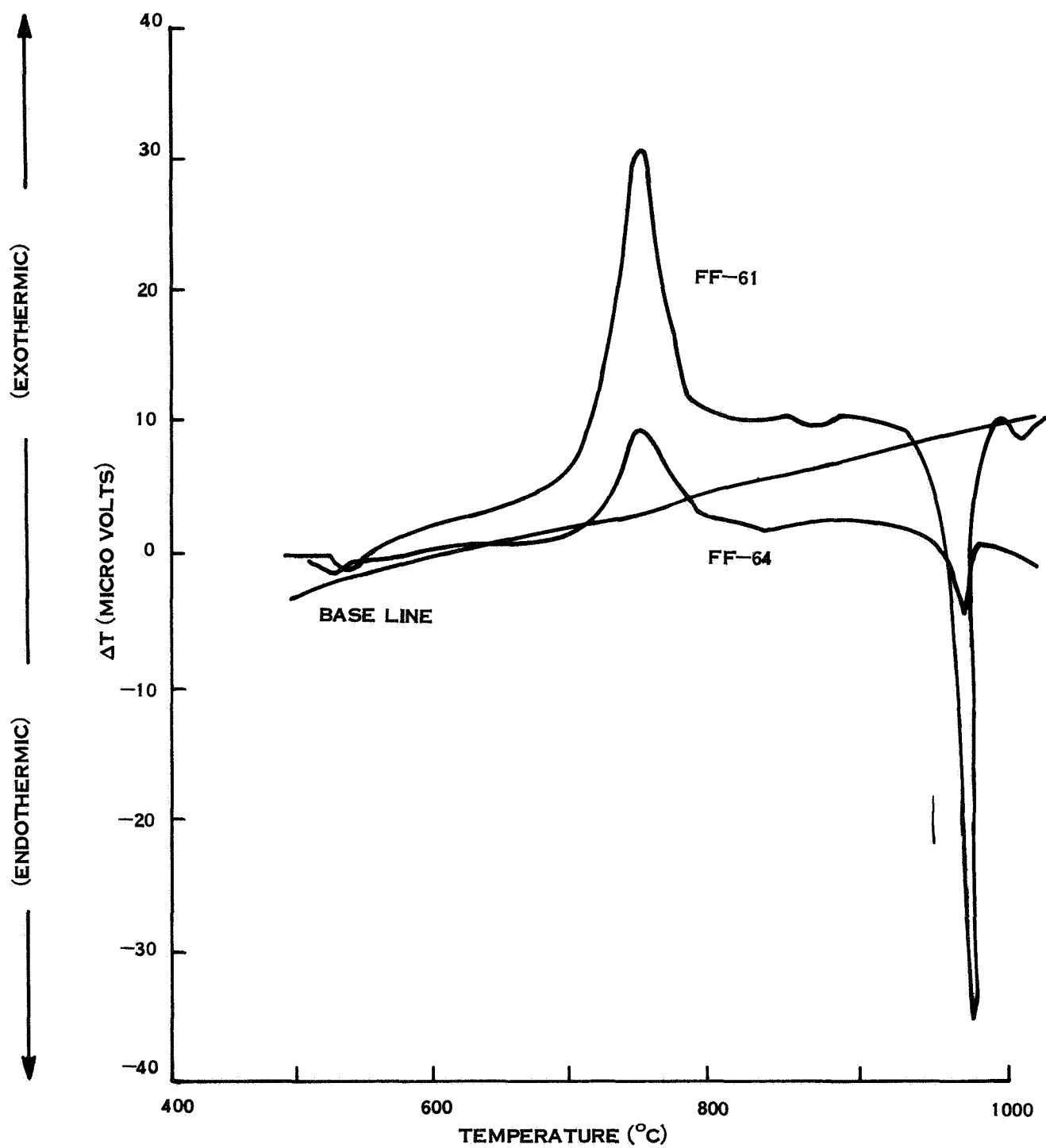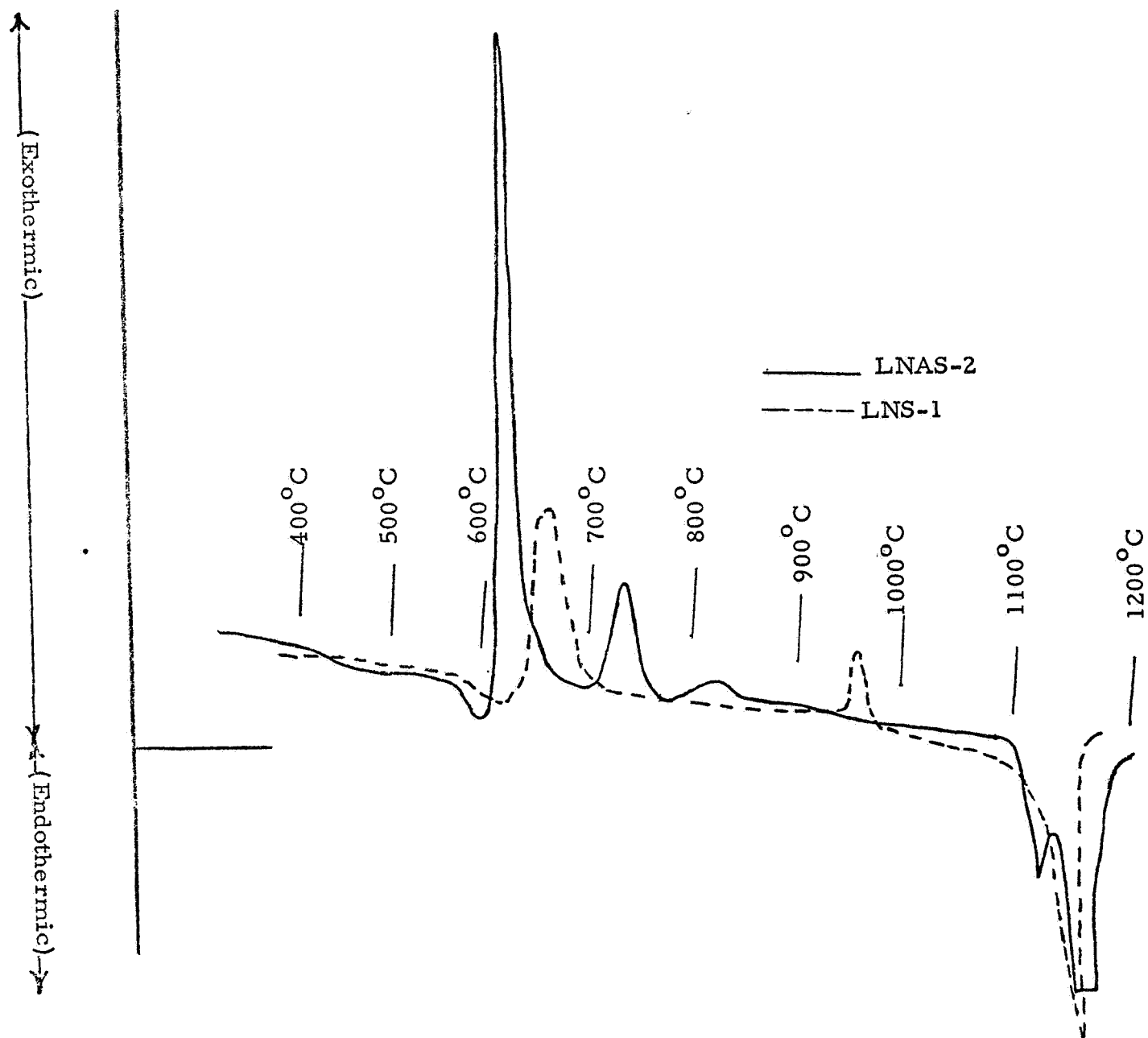Figure 27A. DTA Thermograms of FF-61 and FF-64, LiNbO₃ in Glass Solvents

132

Figure 27B. DTA Thermograms of LNAS-2 and LNS-1
LiNbO$_3$ in Glass Solvents

132A

second exotherm from 960° to 725°. There is no change in the range of the melting endotherms.

These data show that: (1) additional work is required to identify the FF-61 and FF-64 exotherms; and (2) the ternary and SiO_2 solvent system for high content $LiNbO_3$ require processing temperatures exceeding 1000°C.

3. Lead Germanate

a. Solvent Development

Work was directed also toward the preparation and investigation of crystals of lead germanate $(Pb_5Ge_3O_{11})$, grown from the melt and also from fused solvent lead borate $(PbO \cdot 2B_2O_3)$ and alumino-borate $(PbO \cdot 0.5Al_2O_3 \cdot 2B_2O_3)$. Fiberization characteristics of various concentrations of solution were noted, with a view to selecting conditions for growth from the molten solvent. Preliminary DTA (differential thermal analysis) and x-ray diffraction studies were made in this system.

Trigonal lead germanate is of interest because it is a ferroelectric crystal. It has a Curie temperature at 176°C and has an optical rotary power of 5.6° per mm thickness which changes hand (directions) when the polar three-fold axis is inverted [*]. The optical characteristics are sensitive to applied electrical field.

---

[*]   J. P. Dougherty, E. Sawaguchi and L. E. Cross, "Ferroelectric Optical Rotation Domains in Single-Crystal $Pb_5Ge_3O_{11}$," Applied Physics Letters 20 (9) 364 (May 1972).

Low temperature growth of lead germanate crystals having been accomplished at the Space Sciences Laboratory (i.e. see Section VII), work was initiated on the growth of lead germanate crystals from fused glass solvents. Emphasis was placed on the development of solvents that would be chemically compatible, have a high solubility for lead germanate, and have sufficiently high viscosity to offer the possibility of reducing convective effects.

The following compositions were made up from the pure oxides:

PG53	$Pb_5Ge_3O_{11}$	100 w/o		
FF-72	$Pb_5Ge_3O_{11}$	60 w/o,	$PbO \cdot 2B_2O_3$	40 w/o
FF-74	$Pb_5Ge_3O_{11}$	80 w/o,	$PbO \cdot 2B_2O_3$	20 w/o
FF-75	$Pb_5Ge_3O_{11}$	90 w/o,	$PbO \cdot 2B_2O_3$	10 w/o
FF-80	$Pb_5Ge_3O_{11}$	60 w/o,	$PbO \cdot 0.5Al_2O_3 \cdot 2B_2O_3$	40 w/o
FF-81	$Pb_5Ge_3O_{11}$	80 w/o,	$PbO \cdot 0.5Al_2O_3 \cdot 2B_2O_3$	20 w/o

b. Cooling of Melts

It has been reported that small quantities of molten lead germanate, when quenched quite rapidly, will form a glass. In experiments at the Space Sciences Laboratory a 50-gram sample of melt allowed to cool quickly, but not quenched, crystallized readily. Molten solutions (frits) of lead germanate in

134

lead borate glass could be quenched from the melt by passing them through stainless steel rollers and formed clear glass ribbons (composition FF-72, FF-74 and FF-75). In other words, fast cooling resulted in "freezing in" an amorphous (glassy) transparent solution, even with the composition containing only 10 w/o of the fused solvent (FF-75). It was found that composition FF-75 would crystallize readily and become opaque if cooled more slowly or if heated from room temperature to near its softening point. Composition FF-74 was similar in behavior, but crystallized noticeably more slowly than FF-75.

c. Modification of Solvent Phase

It was found that the addition of one-half molecular weight of Al_2O_3 per molecular weight of PbO in the glass significantly improved the viscosity and surface tension relationships (compare compositions FF-80 and FF-81 vs. FF-72 and FF-74). The Al_2O_3 content amounts to 2.8 weight percent of composition FF-81 and 5.6 weight percent of FF-80.

d. Crystallization Studies

In preparation for determination of devitrification behavior, electronic properties, and the like, test disks were poured, annealed, ground polished of compositions FF-72, FF-80 and FF-81.

A disk of FF-75 was poured and annealed. The disk was crushed and passed through a 200-mesh sieve. A differential thermal analysis (DTA) curve of this composition is presented in Figure 28. A 22.66 mg sample of
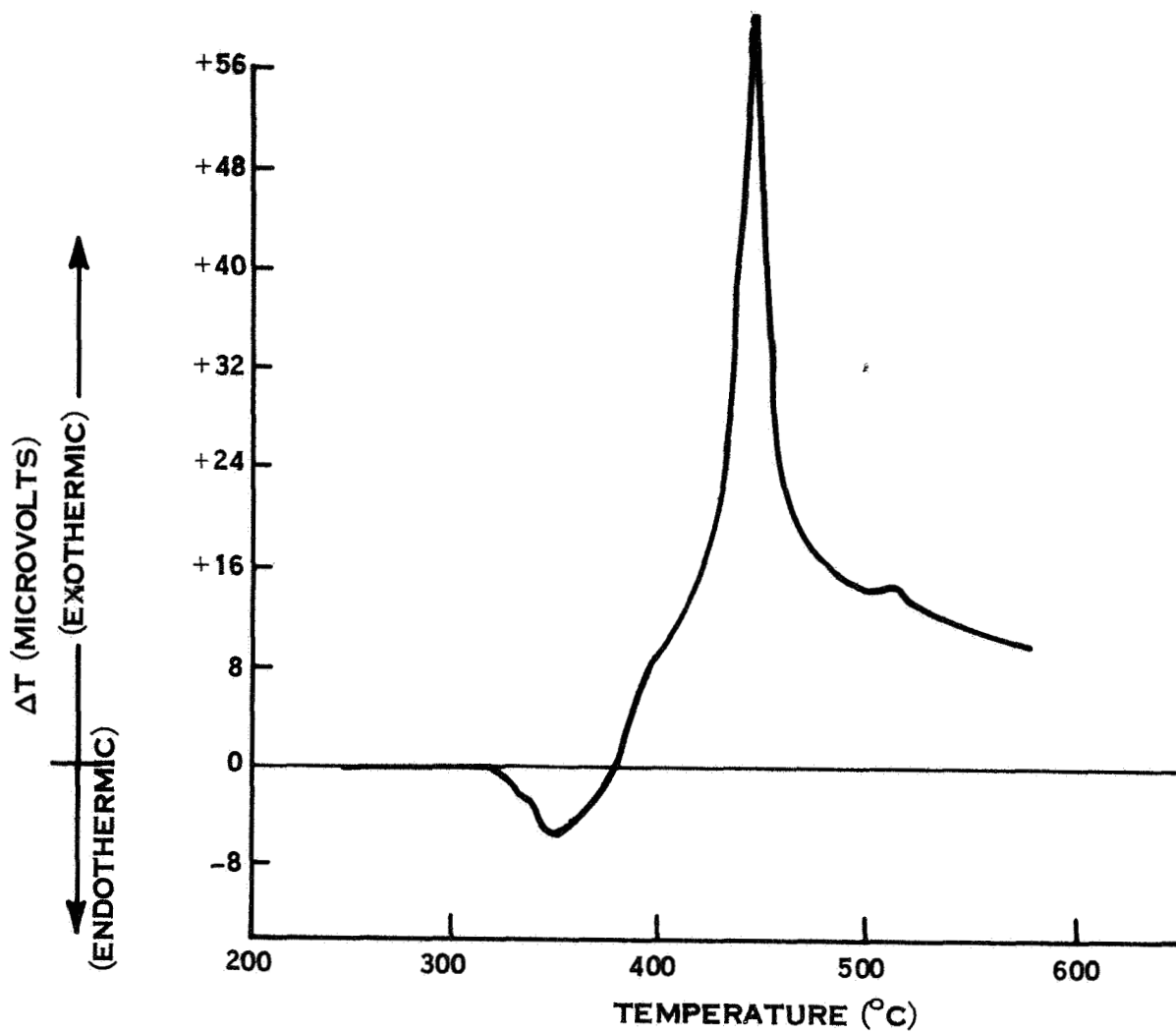
Figure 28.   Differential Thermal Analysis Profile of Composition FF-75.

136

powder was heated at $20^{\circ}C$ per minute. The resulting curve was typical of those generally obtained when a glassy solution is heated from room temperature and a dissolved phase is exsolved (precipitated, or crystallized). In Figure 28 a small endothermic effect was observed starting at about $320^{\circ}C$ and peaking at 345°, while a major exothermic effect began at about 370° and peaked at $445-450^{\circ}$. The effect beginning at 320° was judged to be a relaxation of the rapidly-cooled frit. This effect is characteristic of suddenly-quenched glasses. The effect starting at 370° represented the appearance of a major crystalline phase. The phase was examined by x-ray diffraction analysis. The small effect at 510° is tentatively considered the devitrification of the lead diborate glass.

In order to identify the major crystalline phase that was formed at $370-450^{\circ}$, an x-ray diffraction pattern was taken of a wafer of FF-75 that had been heated at 300° for 3 hours then held at 400° for 2 hours. As seen in Figure 29 the major features of the pattern of FF-75 closely match key peaks of single crystals of $5PbO \cdot 3GeO_2$ ($Pb_5Ge_3O_{11}$) grown from the melt (discussed in Section VII). No additional phase other than that resembling lead germanate was detected in the crystalline material precipitated from the glassy solvent when FF-75 was so heat treated. The fact that no other phase was observed is considered to indicate that the lead diborate glass is a compatible solvent for the lead germanate. A similar x-ray diffraction pattern has not yet been made
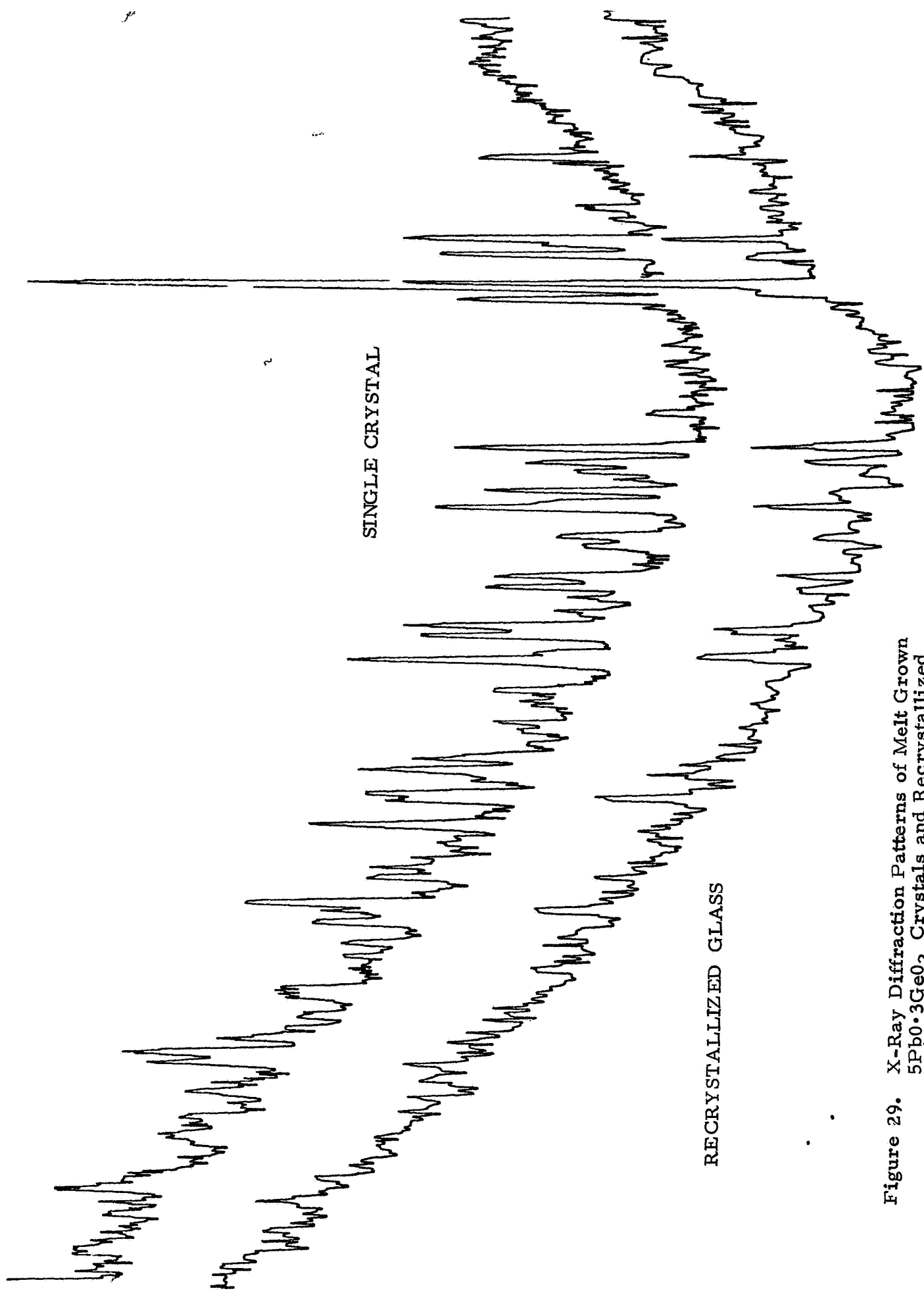
137

SINGLE CRYSTAL

RECRYSTALLIZED GLASS

Figure 29. X-Ray Diffraction Patterns of Melt Grown $5PbO \cdot 3GeO_2$ Crystals and Recrystallized $5PbO \cdot 3GeO_2$ Glass Solvent FF-75.

138

of devitrified FF-80, which would show if $PbO \cdot 0.5Al_2O_3 \cdot 2B_2O_3$ also is an appropriate molten solvent for use in growing lead germanate.

e. Future Work with Fused Solvents

On balance, it appears at present that composition FF-72 would be a promising one from which to grow seeded crystals of lead germanate. There seems to be a strong tendency for composition FF-74 and FF-75 to nucleate rapidly and grow an undesirably large number of small crystals. This possibility should be checked further. Following the same reasoning, FF-80 may prove to be more promising than FF-72. The higher viscosity of melts of FF-80, due to the introduction of Al_2O_3, may help retard the nucleation of numerous small crystals.

The next step in the investigation should be the determination of the temperature at which the first crystals of lead germanate appear when clear melts of compostions FF-72 and FF-80 are cooled slowly. This temperature is not expected to be the same as the temperature at which lead germanate is crystallized when FF-75 is heated from room temperature, because the saturation conditions will be different in the two instances.

B.   Lithium Niobate Crystal Growth Experiments

Based on observations of the devitrification behavior of the aforementioned glass solvents during preparation of the melts, the following work was initiated on the seeded growth of lithium niobate.   Several solvent compositions of lithium silicate glass were investigated.   Of these, $Li_2O \cdot SiO_2$ reached a condition of fluidity at $1150^{\circ}C$.   Lithium niobate was next added to the lithium disilicate solvent and melts formed.   Drops of glass were poured at various temperatures in order to determine the temperatures of spontaneous crystallization and that desirable for seed insertion.   No crystals were seen at temperatures of 1250, 1200, 1150 and $1100^{\circ}C$.   A single crystal was found in the $1050^{\circ}C$ drop.

The growth of lithium niobate crystals from solution in glass solvents was studied from a solution of 40 weight percent lithium niobate and 60 weight percent lithium disilicate.   The procedures used were to insert a seed crystal into the glass solution and then to either cool the solution or hold at a constant temperature for several hours.   Four experiments were completed under the following growth conditions.

Experiment #1 - Seed inserted at $990^{\circ}C$.   Melt slowly cooled to $800^{\circ}C$ at $10^{\circ}C/hr.$, i.e. 19 hours of growth.

Experiment #2 - Seed inserted at $1000^{\circ}C$, melt held at $1000 \pm 5^{\circ}C$ for 64 hours of growth.

Experiment #3 - Seed inserted at $1000^{\circ}C$, melt then cooled rapidly to $960^{\circ}C$ then held at $960 \pm 5^{\circ}C$ for 22 hours of growth.

Experiment #4 - Seed inserted at $1000^{\circ}C$, melt cooled rapidly to $980^{\circ}C$ then held at $980 \pm 5^{\circ}C$ for 112 hours of growth.

The products of these experiments were examined by sectioning through the seed crystal and the surrounding droplet of glass which adheres to the seed when it is removed from the melt. A polished section was prepared across the midplane of the seed so that any growth on the surfaces of the seed or crystallization in the surrounding glass could be observed and measured. Seed crystals were measured and photographed before insertion into the glass solutions.

The results showed that for the experimental conditions reported above there was little growth on the seed crystals even in melts where coarse dendritic structures were formed in the bulk glass surrounding the seed. For example, growth run #4, in which the seed was introduced at 1000°C and the melt then held at 980°C for 112 hours, there was only about 0.1 mm growth on the surfaces of the seed but coarse dendrites (about 0.5 mm long) formed in the adjacent glass. Growth run #1 (seed introduced at 990°C melt cooled to 800°C at 10°C/hr.) showed extensive development of dendrites of $LiNbO_3$ in the surrounding glass, but negligible growth on the seed. However, a seed introduced at 1000°C and held at 1000°C for 64 hours resulted in no growth of the seed and no dendritic growth in the melt. It appears therefore that growth experiments in this system using FF-61 glass (40 w/o $LiNbO_3$ and 60 w/o $Li_2O \cdot 2SiO_2$) should be performed at 990°C but that the rate of growth is very low.

Solvents in the $Li_2O \cdot Al_2O_3 \cdot SiO_2$ system were investigated for lower temperature growth, improved solvent stability to prevent crystallization of the solvent phase, and ease of solvent etching during harvesting of the crystals. $LiNbO_3$ in the amounts of 40 to 70 weight percent were dissolved in solvents with ratios of 1:1:3, 1:1:4 and 1:1:5 ($Li_2O \cdot Al_2O_3 \cdot SiO_2$) and glasses formed. The solvent $Li_2O \cdot 1.5SiO_2$ was also investigated: See Section VI.

C.   Potassium Sodium Niobate Crystal Growth Experiments

Preliminary experiments were performed to study the seeded growth of potassium sodium niobate using a glass solvent consisting of 60 w/o potassium sodium niobate and 40 w/o potassium sodium silicate. PSN crystals were used in earlier studies of the feasibility of zero-g crystal growth[*].

The results obtained were similar to those found with $LiNbO_3$ crystals. Observed growth on seeded melts was very small. Temperature control of the melt was critical. At higher temperatures than optimum the seeds were seen to dissolve whereas at lower temperatures multiple nucleations occurred within the melt leading to complete devitrification. The optimum temperature was higher than desired for the M512 furnace (i.e. over $1000^{\circ}C$ for all melt compositions employed) so that further development of lower melting solvent systems or lower loadings of PSN in the solvents are desirable. These factors are discussed elsewhere in this report.

L. R. McCreight, R. N. Griffin and E. C. Henry, "Investigation of the Preparation of Materials in Space," Final Report, NAS 8-24683, March 1970.

VI. SINGLE-CRYSTAL PLATELET GROWTH OF LiNbO₃

With a view to studying the growth of plate-shaped crystals of lithium niobate, thin films of solution of lithium niobate in lithium disilicate glass were prepared by dipping small wire loops into the molten solution, withdrawing, and cooling rapidly. The films, formed by the surface tension of the melt, were roughly as thick as the wire of which the loops were constructed. The films were completely amorphous (glassy) as made. It was felt that crystals precipitated from solution by heat treatment could growth in length and width (diameter) but would be restricted in thickness by virtue of the geometry of the films.

The investigation was conducted with composition FF-61 which consists of 40 wt. % of LiNbO₃ dissolved in 60 wt. % of $Li_2O \cdot 2SiO_2$ glass. Small loops, varying in diameter from one-quarter to one-half inch, were formed at the ends of three-inch lengths of platinum wires of 10, 20 and 40 mil diameter. The loops were formed perpendicular to the axis of the wire so that the loop could be lowered into the melt parallel to the surface, similar to the technique for measuring surface tension. The end of the wire opposite the loop was bent into a hook so that the wire and glass film could be placed onto a support located inside a furnace.

Results of the film-forming experiment indicated that 20 mil wire was better than the other two sizes used. The 10 mil wire bent too easily and the

40 mil wire tended to gather too much glass. Loop diameters of about one-half inch seemed to be the largest in which good films could be consistently formed. While melt viscosity, as such, was not measured, the temperatures were noted at which (1) the melt was too fluid for film retention on the loop and (2) at which crystals in the melt prevented film retention on the loop. These upper and lower temperatures were 1150 and 980°C respectively. Film formation was less difficult when the loop was placed parallel to the melt surface and lowered into the melt, rather than placing the loop perpendicular to the melt and inserting it from that position.

A. Films Heated in Initially Cold Furnace

Six glass films about one-half inch in diameter and 20 mils or less in thickness were formed by the techniques described above and placed on a support rod in a cold furnace. A platinum crucible containing a solidified melt of FF-61 was also placed in the furnace. The temperature was increased at the rate of 200-250°C/hour until the furnace reached 850°C. From this point on, the temperature was increased more slowly. At a temperature of 900°C, the furnace door was raised and the films on the platinum loops and the glass in the crucible were examined visually. This procedure was repeated at intervals and the following observations were made:

1. At 900°C, both the glass in the crucible and on the platinum loops was slightly opaque and solid.

2. At 950°C, the same results were observed.

3. At 1000°C, the glass in the crucible was becoming fluid and the films had melted and formed a bead on the wire.

4. The glass in the crucible exhibited some opacity at 1030 and 1060°C, but at 1100°C was a clear fluid melt.

To further establish the lowest temperature at which glass films could be consistently formed, platinum wires with a loop in one end were dipped into the molten glass at various decreasing temperatures. Clear, uniform films were formed at temperatures of 1100, 1050, and 1000°C. At 980°C, crystals began to appear at the melt/crucible interface, but a loop dipped into the center of the melt produced a clear film. At 960°C and lower, sufficient crystallization had occurred in the crucible to prevent the formation of clear films.

B. Films Placed in Initially Hot Furnace

Finally, films were formed by dipping loops of 20-mil wire into molten FF-61 and then inserting them directly into a hot furnace. This served both to anneal the glass and to permit the $LiNbO_3$ to crystallize, and avoided the nucleation and crystal growth apparently observed earlier and described above, when the glass films were placed in a cold furnace.

C. Devitrification and Crystal Growth in Films

One film was devitrified by heating for 16 hours at 900°, after which the furnace was turned off and allowed to cool to room temperature. Three films were crystallized at 800° for 16 hours. The films were not further evaluated. As pointed out above, the glassy solution, in film form, became very fluid at

1000° and tended to drain and form a bead on the wire. Single crystals most likely could be formed if loops of smaller diameter were employed, to reduce the span of the film[*]. The sample would have to be held in a temperature range in which the solvent would be viscous (fluid) but not drain from the wire. This temperature probably would be about 960° to 980°, for the composition reported here (FF-61).

In the studies to date, the lithium niobate has tended to exsolve from the solution to form many small crystals, causing the formation of a more or less continuous polycrystalline ceramic structure rather than a few large crystals. A minor problem for consideration is the fact that the thermal expansion of the glass under investigation was different from that of the platinum, which led to a tendency for cracks to form at the interface between the glass and the wire. Roll quenching, as described elsewhere (in Section VI), would seem to be a promising alternative method of forming thin sheets of glassy solution in preparation for crystal growth. Films about 12 mils in thickness have consistently been made of a number of related compositions.

---

[*] J. G. Morley (a) Glass Technology 6 (3) 69-89 (June 1965)
         (b) Contemporary Physics 6 (5) 349 (June 1965)

146

VII. MELT GROWTH OF $Pb_5Ge_3O_{11}$ AND $Bi_{12}GeO_{20}$

Lead germanate ($5PbO \cdot 3GeO_2$) is a new ferroelectric material having large electro-optic, constants and desirable switching properties for electro-optic device applications. Of particular importance is the discovery of switchable optical rotary power. Crystals which are 4 x 4 x 0.4 mm in size are grown by the Czochralski method. However, switching time is strongly dependent due to the crystal inhomogeneities. This crystal was considered to be important enough to warrant consideration for space processing, particularly for a light switch, light modulator, or a second harmonic generator.

Bismuth germanate, $Bi_{12}GeO_{20}$, is the best crystal candidate for surface wave acoustic delay lines and has been identified earlier as a candidate for space processing. With its low velocity of propagation and short wavelength it has a long delay; its velocity is 1.6×10^5 cm/sec as compared to 3.5×10^5 for $LiNbO_3$. However, growth ridges interfere with the propagation of high-frequency surface waves. Because of mechanical damage and imperfections introduced even during grinding and lapping, polished surfaces do not transmit a signal as undistorted as that expected from an equally, large flat natural surface.

Both lead germanate and bismuth germanate can be grown at relatively low temperatures (vicinity of $750^\circ C$) and rates ($1/2^\circ C$ per minute) which were within the capabilities of the M518 Skylab crystal-growth furnace. Because of

147

the emphasis on simple space experiments, the initial work on bismuth germanate and lead germanate was conducted on crystals grown directly from the melt rather than from glass-based solutions: later work (Section V) was directed towards studies of suitable glass solvents for growth of these crystals. The growth of both materials is influenced by, and may be seriously limited by, convection effects in the melt or solution.

A. $Pb_5Ge_3O_{11}$ Crystal Growth from the Melt.

A crystal growth system based on the Czochralski technique was assembled and used to prepare the $Pb_5Ge_3O_{11}$ crystals. The procedure used was similar to that described by Sugii et al[*] with the exception that nucleation was accomplished on the bead of a platinum/rhodium thermocouple for the initial work rather than using seeds. This arrangement enabled the temperature at nucleation and the nucleation exotherm to be conveniently measured and recorded.

The required oxide mixture was prepared from PbO and GeO_2 of 99.99% purity and melted in a pure platinum crucible at about $750^{\circ}C$ in air. The furnace temperature was lowered at about $1/2^{\circ}C$ per minute until a crystal (or crystals) were seen to nucleate on the thermocouple bead immersed about 1 mm beneath the surface of the melt (a corresponding exotherm could usually be detected on the thermocouple read-out). The crucible was positioned in a

---

[*] Sugii, Iwasaki, and Mizazawa, Mat. Res. Bull., **6**, 503-512, 1971.

148

temperature gradient of about $30^{\circ}C$ per cm (cooler at the top) which was maintained constant during growth. When nucleation was observed, the thermocouple was disconnected from the recorder to enable it to be rotated at between 10 and 60 rpm while simultaneously being pulled vertically from the melt at about 0.5 to 2 mm per minute. A top view of the crucible showing nucleation and growth on the thermocouple top is shown in Figure 30.

Initial growths at low rotation speed were multi-crystalline, but a single crystal growth could be induced by pulling at a high rate for a short time to form a "neck" in the growth and then continuing at a slower rate producing a single crystal from the "neck". This is shown in Figure 31. Several small single crystals were prepared by pulling at 0.5 mm per minute with a rotation of 50 rpm: the crystals were up to 10 mm long and 25 mm^2 cross-section. The predominant growth direction was < 100 > and the crystals were light orange in color. X-ray and optical examination of the crystals showed that they closely corresponded to the 5.3 ratio of $PbO \cdot GeO_2$ reported by Sugii, et al. The x-ray identification was very close to the data reported by Sugii et al, indicating that stoichiometry had been maintained in the melt and that other phases reported in this system such as 3:2 or 1:1 had not been formed. (Figure 29).

The x-ray data from the melt-grown crystals was used as the baseline against which to compare materials formed in glass solvents as reported in Section V. The use of glass solvents based on $PbO \cdot B_2O_3$ melts added to the germanate composition is potentially capable of growing crystals at much

Figure 30.   Top View of Crucible Showing Nucleation and Growth
of $Pb_5Ge_3O_{11}$ Crystals.

Figure 31. $Pb_5Ge_3O_{11}$ Boules Grown from the Thermocouple Cooling
Tip.   Note Necked Areas on First and Third Samples.
Point of Contact with Cooling Tip Can be Seen in Center Sample.

lower temperatures than from the pure melt, 738°C. As discussed later, crystals of 5PbO:3GeO$_2$ were identified in glasses devitrified at temperatures below 500°C.

B. $Bi_{12}GeO_{20}$ Crystal Growth from the Melt.

Several specimens of bismuth germanate crystals $Bi_{12}GeO_{20}$ were grown from the melt for evaluation of its potential application to a crystal growth experiment. Growth was induced by: (a) the introduction of a small seed crystal into a melt at a temperature just above the melting point and then slowly cooling the melt; or, (b) the nucleation of a crystal on the bead of a thermocouple immersed in the surface of a melt during slow cooling. The latter method was the most successful and crystals with faces up to 2 cm long were grown, although twinning and multiple nucleations prevented growth of large single crystals.

Growth was accomplished by melting the appropriate oxide mixture in a platinum crucible supported within a vertical tube furnace. The temperature distribution was arranged so that the top of the crucible (and the surface of the melt) was at a slightly lower temperature than the base of the crucible. A platinum/rhodium thermocouple was inserted from the top of the furnace until the bead was in contact with the surface of the melt. The temperature was then lowered at a rate of about 1/2°C per minute until a crystal (or crystals) were observed to nucleate at the thermocouple bead (a corresponding exotherm was observed on the temperature record). Growth was then allowed to proceed at constant furnace temperature while the crystal was slowly pulled vertically

152

from the melt. Crystal growths weighing up to over 20 gms were obtained but were generally multi-crystalline. Single crystal seeds with appropriately controlled orientation would be desirable to nucleate growth in future experiments.

The growth of bismuth germanate is particularly attractive for space processing since the growth temperatures are within the limitations of the M512 furnace. In addition to technological importance, the growth of Bismuth Germanate, especially under microgravity conditions, should provide information of high scientific importance to the Bi_2O_3-GeO_2 system. There is disagreement as to the stability and identification of high bismuth oxide containing compounds within the system. For example, Levin and Roth identify $6 Bi_2O_3 \cdot GeO_2$ with a melting point of $935^{\circ}C$[*] and in later work Speranskaya and Arshakun[*] identify $7 Bi_2O_3 \cdot GeO_2$ with a melting point of $923^{\circ}C$. It is important to surface acoustic applications to identify which crystal formation is stable and piezoelectric.

---

[*] Levin, E.M. and Roth, R.S., J. Research Natl. Bur. Standards, 68A (2) 201 (1964).

Speranskaya, E.I. and Arshakun, A.A., Zh. Neorgan. Khim., 9 (2) 417 (1964).